Industria Textilă

ISSN 1222–5347 (57–112)

2/2011

Revistă **cotată ISI** şi inclusă în **Master Journal List** a Institutului pentru Ştiinţa Informării din Philadelphia – S.U.A., începând cu vol. 58, nr. 1/2007/
***ISI rated** magazine, included in the **ISI Master Journal List** of the Institute of Science Information, Philadelphia, USA, starting with vol. 58, no. 1/2007*

Editată în 6 nr./an, indexată şi recenzată în:/
Edited in 6 issues per year, indexed and abstracted in:
Science Citation Index Expanded (SciSearch®), Materials Science Citation Index®, Journal Citation Reports/Science Edition, World Textile Abstracts, Chemical Abstracts, VINITI

Recunoscută în România, în domeniul ştiinţelor inginereşti, de către **Consiliul Naţional al Cercetării Ştiinţifice din Învăţământul Superior** (C.N.C.S.I.S.), **în grupa A** /
*Aknowledged in Romania, in the engineering sciences domain, by the **National Council of the Scientific Research from the Higher Education** (CNCSIS), **in group A***

Sumar

Contents Inhalt

Capillary rise investigation of core-spun nanofiber yarn

SEYED ABDOLKARIM HOSSEINI RAVANDI

FARZAD DABIRIAN
RAZIEH HASHEMI SANATGAR

REZUMAT – ABSTRACT – INHALTSANGABE

Testarea creşterii capilarităţii la firele din nanofibre filate cu miez

În acest articol este dezvoltată o nouă metodă de acoperire a firelor cu nanofibre. Prin această metodă, direcţia fibrei a fost controlată printr-un sistem convenţional de electrofilare şi prin nanofibrele integrate pe suprafaţa firelor. Acoperirea firelor cu nanofibre ar putea crea proprietăţi speciale. În lucrare, firele filamentare de nailon 66 au fost acoperite cu PVA şi nanofibre de nailon 66. A fost investigat gradul de creştere a capilarităţii. Rezultatele obţinute au demonstrat că modificarea structurii firului prin schimbarea unuia dintre factori are un efect semnificativ asupra coeficientului de capilaritate.

Cuvinte-cheie: nanofibră, electrofilare, acoperire, fir, capilaritate

Capillary rise investigation of core-spun nanofiber yarn

In this article, a new method for yarn coating with nanofiber has been explained. In this method, fiber direction was controlled by manipulating the conventional system of electrospining and embedded nanofibers on yarn surface. Yarn coating with nanofiber could create special properties. In this work nylon66 filament was coated with PVA and nylon 66 nanofiber. The capillary rise rate was investigated. Obtained results were betokened that the change in yarn construction due to the change in each factor has a significant effect on capillary rate coefficient.

Key-words: nanofiber, electrospinning, coat, barrier, yarn, capillary

Teste für das Kapillaritätswachstum bei kerngesponnenen Nanofasergarne

In diesem Artikel wird eine neue Methode für die Beschichtung der Garne mit Nanofaser erklärt. Bei der Methode wurde die Faserrichtung durch Modifizierung des konventionellen Elektrospinnsystems und durch Integration der Nanofaser auf der Garnoberfläche kontrolliert. Die Garnbeschichtung mit Nanofaser kann spezielle Eigenschaften produzieren. In dieser Arbeit wurde ein Nylon 66-Filament mit PVA und Nylon 66-Nanofaser beschichtet. Eu wurde das Kapillaritätswachstum untersucht. Die erhaltenen Ergebnisse beweisen, dass die Modifizierung im Garnaufbau, als Folge der Änderung dieser Faktoren einen wesentlichen Effekt auf dem Kapillaritätskoeffizient hat.

Stichwörter: Nanofaser, Elektrogarnspinnen, Beschichtung, Schranke, Garn, Kapillarität

The behavior of a textile during its contact with the liquid is one of the important properties of textiles [1]. Inter-fiber space in fibrous materials (i.e., yarn) is in the form of capillaries that can be occupied by liquid. Because of this, wetting and wicking are important phenomena in their processing and applications [2].

A spontaneous transport of a liquid driven into a porous system by capillary forces is termed wicking. Wicking is a result of spontaneous wetting in a capillary system [3]. A liquid that does not wet fibers cannot wick into a fabric. Wetting is a complex process complicated further by structure of the fibrous assembly e. g. yarns, woven/nonwoven/knitted fabrics, and pre-forms for composites [4].

Capillary phenomenon occurs when the free energy of the solid-gas interface exceeds the free energy of the solid-liquid interface. Capillary exist in many natural and physiological processes with numerous technological applications [5].

There are several techniques for capillary flow analysis, i.e., spontaneous liquid wicking analysis for yarn structure. These methods measure the time required for a liquid to wick into a certain length of yarn. In this work a method consists of observing and measuring the capillary flow of a colored liquid was used. The yarn is placed perpendicularly to a liquid bath [3, 6, 7].

Various parameters, such as yarn structure, yarn tension, twist, fiber shape, number of fibers in yarns, fiber configuration, finishing, and surfactants, control capillary size and its continuity, influencing wicking of yarns [8, 9, 10].

Sengupta and Murthy [11] reported that the wicking time of open-end spun yarn, for any given vertical wicking height, is less than that of ring-spun yarn. Experiments showed that dye had wicked to a greater height in the core of the open-end yarn than in the surrounding sheath fibers, the same as ring yarns. Open-end yarns have a relatively denser core and less dense skin when compared to ring yarns. Lord [12] reported that open-end yarn wicks faster and more than ring yarn. Chattopadhyay and Chauhan [13] studied the wicking behavior of ring and compact spun yarns. The rate of water rise was very fast at the beginning and slowed down gradually. The equilibrium wicking heights for ring yarns were more than compact yarns and ring yarns wicked faster than compact yarns. The packing coefficient of compact spun yarns is greater than that of corresponding ring yarns, and because of this the average capillary size would be less in compact yarns than ring yarns.

According to Staples and Shaffer [14] smaller capillaries may create sufficient drag to slow down the rise in liquid height. Chattopadhyay and Chauhan [13] reported that there must be an optimum capillary size that will cause fastest entry of water into the yarn pores. Hence, both too small and too large pores are detrimental to quick wicking. The slowing down of height rise with time for any yarn can be ascribed to the gravity action of the water column within the capillary, which acts against the capillary pressure.

Sengupta et al. [15] investigated the wicking behavior of air-jet textured yarns. These yarns have different structures: in addition to the different core, the surface

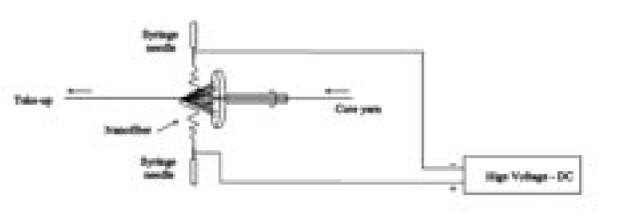

Fig. 1. Schematic of electrospinning setup

of the yarns shows different types of loops of varying shapes and sizes. Both core and surface structure can be affecting the wicking behavior. For the same percentage of floats and arcs, the trilobal filament yarns show better wicking properties, and a higher percentage of floats and arcs tend to increasing equilibrium wicking height. The equilibrium wicking height and wicking rate are higher for air-jet textured yarn than for the corresponding feeder yarn. Ansari and Kish [16] investigated the wicking behavior of polyester spun yarns produced with varying twist levels. Twisted filament yarn shows a lower wicking rate than a yarn without twist. Minor et al. [17] observed similar findings on nylon filament yarns of different twists.

According to Hollies et al. [18] Increasing yarn roughness due to random arrangement of its fibers gives rise to a decrease in the rate of water transport, and this is seen to depend on two factors directly related to water transfer by a capillary process:

- the effective advancing contact angle of water on the yarn is increased as yarn roughness is increased;
- the continuity of capillaries formed by the fibers of the yarn is seen to decrease as the fiber arrangement becomes more random.

This work focuses on capillary rise in a new production in fiber assemblies using electrospinning process to produce coated yarns.

Electrospinning is a known process for forming fibers with nano-scale diameters through the action of electrostatic forces. Any electrospinning equipment consists of four main parts: metallic capillary, high voltage source, pump and a collector. In typical electrospinning process, an electrical potential is being applied to polymeric droplet flow out from the tip of the needle. Droplet charging results the Taylor Cone formation. When the electrical forces (electrostatic and coulomb force) overcome the surface tension of polymer solution, a charged fluid jet is ejected and follows a spiral path. The electrical forces elongate the jet thousands of times and the jet stretches toward the grounded electrode and is collected on it randomly [19, 20].

The great deal of attention has been paid to produce yarns from nanofibers has led to introduce some techniques. Dabirian, et al., employed two needles which were connected to positive and negative voltages separately to produce high bulk nanofiber being collected by a rotating drum slowly [21, 22]. This technique was applied to generate yarn consists of nanofibers too.

In this work, we have succeeded in finding a new innovation in coating on conventional yarns [23]. This method is capable of coating any kind of yarns with nanofibers. Yarn coating has ability to create new properties and application for produced yarns and fabrics. In this article one of the most important properties of coated yarns such as capillary was investigated.

EXPERIMENTAL PART

Materials used

Nylon 66 multifilament (1 260 denier, 7 denier per filament, circular cross-section, and without crimp) has been chosen to coat with different nanofibers such as PVA & nylon 66 for all the wicking experiments. Commercial nylon 66 chips with 2.28–2.34 relative viscosity, RV, in formic acid, was prepared by Zanjan Tire Cord. The usable nylon 66 solvent was 98–100% formic acid from Merck Company. Polymer solution dry chip samples of nylon 66 in formic acid with concentration of 15 wt % was prepared by dissolving and stirring the above mixture with constant speed in room temperature. PVA polymer powder with 72,000 g/mol, molecular weight was used from Merck Company. The 8 wt % solution of PVA in twice-distillation water was prepared at 80^{o}C under constant mixing.

A liquid which was used for the wicking measurements was single-distillation water with 0.2% non-ionic detergent and 0.5% blue basic dye for observing the height of the water wicked. All the wicking measurements were carried out in room conditions.

Electrospinning setup

Nanofiber coating on yarns depending on our new invention was done as following: two nozzles with different charge were positioned opposite each other and electrospun nanofibers with the same charge as their nozzles were produced. Nanofiber with different charge attracted each other and discharged [21, 24]. In this method, a neutral circular plate with a small hole at center was positioned in the middle of electric field. This circular plate was turned anti-clockwise and yarn spindle was positioned behind it. The yarn passed right through the plate center and collect on the rotary collector. Because on the circular plate, surface electrons were dislocated, half of them charged positively and remnant, negatively, the charged jets of polymer solution moved toward the part of circular plate with opposite charge and were gathered on this plate. Collected nanofibers were producing spinning triangle because partly of circular plate with opposite charge attract them. On the other hand, the yarn was positioned at the plate center in nanofiber's way and collected on the rotary collector got involved with them. Circular plate was rotating anti-clockwise, yarn was moved towards rotary collector from plate center. In this way nanofibers were coated on the yarn with *Z*-twist direction. Figure 1 shows the yarn coating mechanism schematically.

To produce coated yarns with nanofiber, the distance between two nozzles was 13 cm and between neutral circular plate and centre of electric field was 3 cm. Plate diameter was 7 cm. The diameter and length of two nozzles was 0.7 mm and, respectively, 3.5 cm. The distance between two nozzles centers and take-up unit was 25 cm. 9 kV voltage was applied. Take-up speed and revolution per minutes of circular plate for coating

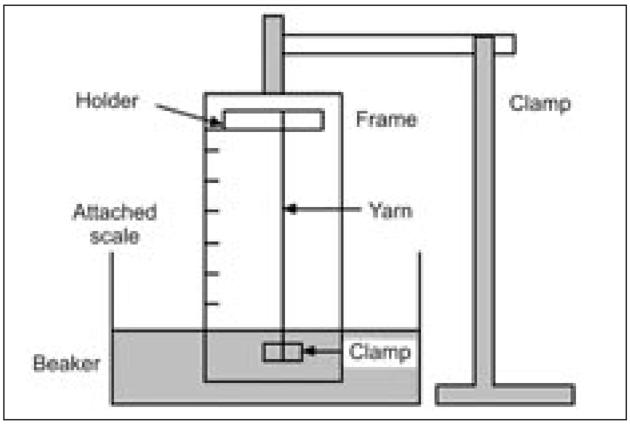

Fig. 2. Schematic of experimental set up for capillary rise measurements

yarn with nanofiber were 6.55 m/hour and, respectively, 21 rpm.

Take up unit

Revolution per minutes of neutral circular plate was controlled by a threephase motor and an inverter for coating the yarn, and the speed of rotating collector was controlled by a stepper motor.

Instrumental used

Figure 2 shows schematically the apparatus designed for capillary height measurement. The yarn is fixed to a holder that comes into contact with the liquid in a beaker.

A Sony digital handy cam (DCR-PC115E) was used to make video films of colored liquid rise in coated filament with nanofibers for capillary flow. Fast-Forward, a digital graphic adapter, was transmitted the video camera to the video signal to the computer. The camera had a resolution of 720 x 576 pixels and magnification of 1X-120X. In order to characterize any liquid flow of the coated yarn with nanofibers, Windows movie maker was applied to make screen capture. Measurement software was used to gain a set of points at given times from the capillary rise of the colored liquid into the coated yarns, *t, h*. The morphology of different nanofibers coating on nylon filament was detected with a Philips scanning electron microscope (XL-30) after gold coating. The SEM images of nylon filament coated with PVA & nylon 66 nanofibers are shown in figure 3.

RESULTS AND DISCUSSIONS

Before doing capillary tests, coated yarns with nanofibers were kept in standard condition: (20 ± 2)°C and 65% relative humidity.

In fibrous structures, the capillary flow follows the equation (1), which provides the variation of the liquid height h as a function of time t in a capillary of radius r_e as follows:

$$\frac{dh}{dt} = \frac{r_e^2}{8\eta h}\left[\frac{2\gamma\cos\theta}{r_e} - \rho g h\right] \quad (1)$$

Liquid rise is determined by the inter-fiber pore structure (equivalent radius of the capillary porous structure, r_e), chemical structure of the fiber surface, and surface properties of the liquid (liquid viscosity η, surface energy γ, contact angle between liquid and fibres θ, and liquid density ρ). According to this fact that the hydrostatic pressure can be almost imperceptible at the early steps of the process (when the height at initial times is very smaller than the height at equilibrium, i.e., $h << h_{eq}$) integration of equation (1) brings about the well-known Lucas-Washburn's equation (2):

$$h^2 = \frac{r_e \gamma \cos\theta}{2\eta} \quad (2)$$

Therefore, the values of h^2 might vary linearly with time as follows equation (3):

$$h^2 = At \quad (3)$$

where:

$$A = \frac{r_e \gamma \cos\theta}{2\eta} \quad (4)$$

which the slope is the capillary rate coefficient [3, 6, 7, 26].

Some researchers have paid attention in capillary rise phenomenon at very last limits as follows:

$$h(t) = h_{ep}\left[1 - \exp\left(-\frac{\rho g r^2}{8\eta h_{eq}} t\right)\right] \quad \text{when } t \to \infty \quad (5)$$

and some of them study the behavior of capillary rise at initial times, i. e., when, $t \to 0$ or where, $h << h_{eq}$, as we proposed in this work.

To apply Washburn's equation to wicking studies numerous researchers established that the wicking height of liquid in a fiber or yarn is proportional to the square root of the time, assuming that gravity is negligible as long as the wicking height is small [3–6; 25–27].

For capillary height measurement, each sample was cut into 18 cm length pieces and yarns were kept at constant tension on a holder (fig. 2), video films were repeated 10 times for each kind of yarn capillary rise. Three samples nylon filament, nylon filament coated with PVA nanofiber, and nylon filament coated with nylon 66 nanofiber were used in this study. The average was obtained by applying Windows movie maker, to make screen capture and measurement software to

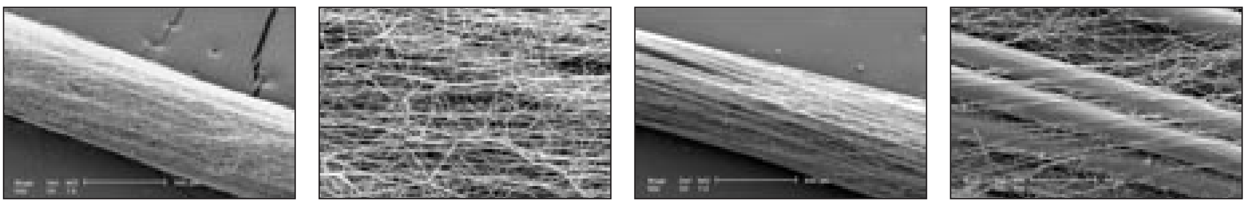

a *b* *c* *d*

Fig. 3: ***a*** and ***b*** – nylon filament coated with PVA nanofiber; ***c*** and ***d*** – nylon filament coated with nylon 66 nanofiber

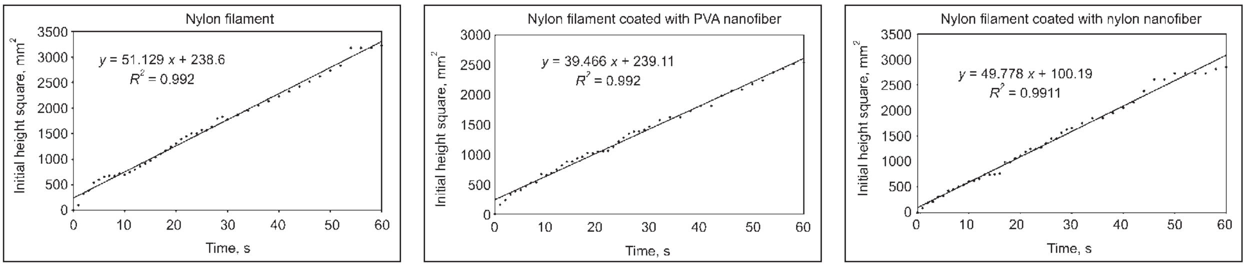

a *b* *c*

Fig. 4. Liquid capillary rise in initial times: ***a*** – nylon filament ***b*** – nylon filament coated with PVA nanofiber; ***c*** – nylon filament coated with nylon 66 nanofiber

measure capillary height. A set of points *t, h* were gained at given times from the capillary rise of the colored liquid to analyze the kinetics of capillary flow in coated yarns with nanofiber.

In experimental values, the curve which obtained from the height square as a function of time at initial times (0–60) is linear. The Lucas-Washburn Equation is valid for the kinetics of capillary flow in yarns if linear regression coefficient is $R^2 > 0.99$ [6, 7].

In this work, as shown by the figure 4, when time is smaller than 60 s, linear regression coefficient R^2 is higher than 0.99 so it could be resulted that the kinetics of capillary flow of colored liquid in coated yarns with nanofiber follows the Lucas-Washburn equation (3). The slope of linear fit of experimental data determined the rate of the liquid capillary rise in initial times. Figure 4 shows the typical variation trend of capillary rise rate by changing yarn samples. The result showed that capillary rate of Nylon filament, nylon filament coated with PVA nanofiber and nylon filament coated with nylon 66 nanofiber is 51 mm^2/s, 39 mm^2/s and, respectively, 49 mm^2/s. As a result, capillary rise rate in yarn coated with nylon 66 nanofiber has no significant difference with nylon filament.

In fact, the change in yarn construction due to the change in each factor has a significant effect on capillary rate coefficient. PVA is one of the polymers that have very good hygroscopic properties. It consists of an OH group at every side of carbon in the chain, so PVA nanofibers can swell rapidly in water. The observed reduction in the capillary rate due to the PVA nanofiber coating could derive from swelling of PVA nanofiber and resultant pore blockage.

CONCLUSIONS

This study has developed a method that allows the yarn coating with nanofibers. This method could be applied for any yarn with different nanofiber coating. Yarn coating with nanofiber could create special properties. In this work the capillary rise of colored liquid along the coated yarns was studied by optical system. In fibrous structures, the capillary flow follows the Lucas-Washburn's equation at the early steps of the process, according to this fact that the hydrostatic pressure can be almost imperceptible. In experimental values, the curve obtained from the height square as a function of time at initial times (0–60) is linear. The Lucas-Washburn Equation is valid for the kinetics of capillary flow in yarns if linear regression coefficient is $R^2 > 0.99$. The kinetics of capillary flow of colored liquid in coated yarns with nanofiber follows the Lucas-Washburn equation. The slope of linear fit of experimental data determines the rate of the liquid capillary rise. In fact, the change in yarn construction due to the change in each factor has a significant effect on capillary rate coefficient. Capillary rise rate in yarn coated with nylon 66 nanofiber has no significant difference with nylon filament. Coating nylon filament with PVA nanofiber could decrease the capillary rate of nylon filament.

BIBLIOGRAPHY

[1] Kamath, Y. K., Hornby, S. B., Weigmann, H. D., Wilde, M. F. *Wicking of spin finishes and related liquids into continuous filament yarns.* In: Textile Research Journal, 1994, vol. 64, issue 1, p. 33

[2] Hsieh, Y. L., Yu, B. *Liquid wetting, transport, and retention properties of fibrous assemblies. Part I: Water wetting properties of woven fabrics and their constituent single fibers.* In: Textile Research Journal, 1992, vol. 62, issue 11, p. 677

[3] Kissa, E. *Wetting and wicking.* In: Textile Research Journal, 1996, vol. 66, p. 660

[4] Miller, B. *In the wearing of fibers, in surface characteristics of fibers and textiles.* Part II. M. J. Schick. Ed.: Marcel Dekker: New York, 1977, p. 417

[5] Kornev, K. G., Neimark, A. V. *Spontaneous penetration of liquids into capillaries and porous membranes revisited.* In: Journal Colloid. Interf. Sci., 2001, vol. 235, p. 101

[6] Perwuelz, A., Casetta, M., Caze, C. *Liquid organization during capillary rise in yarns-influence of yarn torsion.* In: Polym. Test., 2001, vol. 20, p. 553

[7] Perwuelz, A., Mondon, P., Caze, C. *Experimental study of capillary flow in yarns.* In: Textile Research Journal, 2000, vol. 70, p. 333

[8] Patnaik, A., Rengasamy, R. S., Kothari, V. K., Ghosh, A. *Wetting and wicking in fibrous materials.* In: Textile Progress, 2006, vol. 38, issue 1, p. 1

[9] Hollies, N. R. S., Kaessinger, M. M., Watson, B. S., Bogaty, H. *Water transport mechanisms in textile materials. Part II: Capillary-type penetration in yarns and fabrics.* In: Textile Research Journal, 1957, vol. 27, p. 8

[10] Kamath, Y. K., Hornby, S. B., Weigmann, H. D., Wilde, M. F. *Wicking of spin finishes and related liquids into continuous filament yarns.* In: Textile Research Journal, 1994, vol. 64, p. 33

[11] Sengupta, A. K., Murthy, H. V. S. *Wicking in ring-spun vis-a-vis rotor-spun yarns.* In: Indian Journal Textile Research, 1985, vol. 10, issue 4, p. 155

[12] Lord, P. R. *A comparison of the performance of open-end and ring spun yarns in terry toweling.* In: Textile Research Journal, 1974, vol. 44, p. 516
[13] Chattopadhyay, R., Chauhan, A. *Wicking behavior of compact and ring spun yarns and fabrics.* In One Day Seminar on Comfort in Textiles. Dept. of Textile Technology, II T Delhi, New Delhi, India, 2004, October 16, p. 20
[14] Staples, T. L., Shaffer, D. G. *Wicking flow in irregular capillaries.* In: Coll. Surfaces A., 2002, vol. 204, issue 1–3, p. 239
[15] Sengupta, A. K., Kothari, V. K., Rengasamy, R. S. *Wicking behavior of air-jet textured yarns.* In: Indian Journal Fiber Textile Research, 1991, vol. 16, issue 2, p. 123
[16] Ansari, N., Haghighat Kish, M. *The wicking of water in yarns as measured by an electrical resistance technique.* In: Journal Textile Institut, Part I, 2000, vol. 91, issue 3, p. 410
[17] Minor, F. W., Schwartz, A. M., Wulkow, E. A., Buckles, L. C. *The migration of liquids in textile assemblies. Part II: The wicking of liquids in yarns.* In: Textile Research Journal, 1959, vol. 29, issue 12, p. 931
[18] Adamson, A. W. *The solid-liquid interface-contact angle.* In: Physical Chemistry of Surfaces, John Wiley: New York, 1990, p. 379
[19] Doshi, J., Reneker, D. H. *Electrospinning process and applications of electrospun fibers.* In: Journal Electrostatics, 1995, vol. 35, issue 2–3, p. 151
[20] Reneker, D. H., Yarin, A. L., Fong, H., Koombhongse, S. *Bending instability of electrically charged liquid jets of polymer solutions in electrospinning.* In: Journal Appl. Phys., 2000, vol. 87, p. 4 531
[21] Dabirian, F., Hosseini Ravandi, S. A. Patent no. 34894, Iran, 2006
[22] Dabirian, F., Hosseini Ravandi, S. A. *Production and some characteristics of bulk nanofibers layres by manipulation of electrospinning system.* In: I. J. P. S. T., 2008, issue 4, p. 307
[23] Dabirian, F., Hosseini Ravandi, S. A. Patent no. 45555, Iran, 2007
[24] Dabirian, F., Hosseini Ravandi, S. A. *A novel method for nanofiber yarn production using two differently charged nozzles.* In: Fibres & Textiles in Eastern Europe Journal, in press.
[25] Doakhan, S., Hosseini Ravandi, S. A., Gharehaghaji, A., Mortazavi, S. M. *Capillary rise in core-spun yarn.* In: Iranian Polymer Journal, 2007, vol. 16, issue 6, p. 397
[26] Zhong, W., Ding, X., Tang, Z. L. *Modeling and analyzing liquid wetting in fibrous assemblies.* In: Textile Research Journal, 2001, vol. 71, p. 762
[27] Laughlin, R. D., Davies, J. E. *Some aspects of capillary absorption in fibrous textile wicking.* In: Textile Research Journal, 1961, vol. 31, p. 904
[28] Gohl, E. P. G., Vilensky, L. D. *Textile Science.* Second edition, Longman Cheshire: Melbourne, 1983

Authors:

SEYED ABDOLKARIM HOSSEINI RAVANDI
FARZAD DABIRIAN
RAZIEH HASHEMI SANATGAR
Nanotechnology & Advanced Materials Institute
Department of Textile Engineering
Isfahan University of Technology
84156 83111, Isfahan, Iran

Coresponding author:
SEYED ABDOLKARIM HOSSEINI RAVANDI
e-mail: hoseinir@cc.iut.ac.ir

DOCUMENTARE

Aparate de măsură și control

UN NOU SISTEM DE TESTARE A MATERIALELOR

În prezent, testarea eficientă și cu costuri reduse a materialelor este un obiectiv esențial pentru industria textilă și a materialelor plastice.

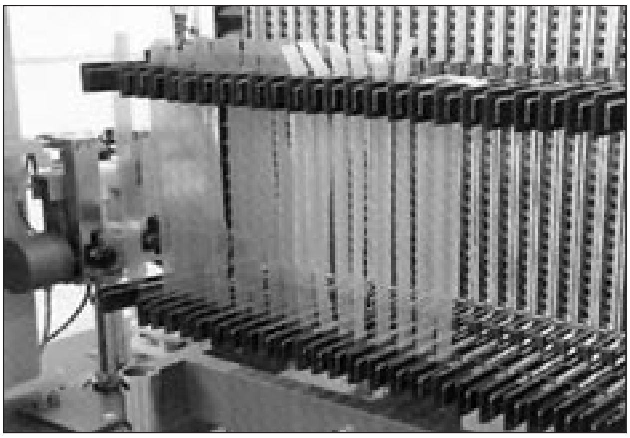

Fig. 1

Sistemul de testare robotizat *„roboTest F“*, elaborat de compania ***Zwick***, oferă o soluție compactă pentru testarea automată a rezistenței la tracțiune pe mostre instabile dimensional (fig. 1). Sistemul de operare este foarte ușor, datorită unei camere speciale cu mostre. Mostrele pentru testarea rezistenței la tracțiune sunt introduse într-o cameră cu o capacitate de până la 200 de articole.

Camera este formată dintr-un suport și un lanț rotativ cu stative paralele, de tip cleme, pe care sunt prinse mostrele. Stativele variază în funcție de tipul și forma mostrei, permițând ca pelicule și materiale textile de diferite dimensiuni să fie testate folosind același sistem.

În plus, acest sistem de testare oferă avantaje privind reducerea pe termen mediu a costurilor și înlăturarea erorilor. Întregul proces de testare este înregistrat de către un software, iar rezultatele testelor sunt transferate într-o bază de date în mod automat și fără erori.

Testele manuale pot fi efectuate, atunci când este necesar, pur și simplu prin deconectarea sistemului de alimentare cu mostre.

Compania ***Zwick*** este specializată în sisteme de testare robotizate, având o experiență de peste 25 de ani.

Sursa: www.zwick.com

Analysis of structure and bending property of spacer fabric composites

DU ZHAOQUN
YU WEIDONG
HAMADA HIROYUKI
YANG YUQIU

REZUMAT – ABSTRACT – INHALTSANGABE

Analiza structurii și proprietăților de încovoiere ale materialelor compozite tridimensionale

În lucrare, sunt prezentate trei tipuri de materiale compozite tridimensionale speciale, având în structura acestora fibre de sticlă. S-a observat morfologia de suprafață a structurilor țesute și tricotate. S-a constatat că se înmagazinează mai multă energie statică la materialele compozite cu porozitate mai mare. În plus, au fost măsurate proprietățile de rezistență la încovoiere pe un aparat Instron și s-au obținut curbele grafice ale rezistenței la încovoiere ale materialului compozit. Curbele grafice tipice au fost calculate atât pentru materiale compozite tridimensionale tricotate din urzeală, cât și pentru materiale compozite țesute.

Cuvinte-cheie: compozite, materiale 3D speciale, rezistență la încovoiere, fibre de sticlă

Analysis of structure and bending property of spacer fabric composites

In the paper, three kinds of special three-dimensional spacer fabrics are presented, having in their structure glass fibers. The surface morphology was observed for both weaving and knitting structure. It exhibited that there would store much static atmosphere within a fabric composite with high porosity. Moreover, the bending properties were measured by Instron tester, where the bending load and deflection curves of the composite were obtained. The typical bending stress and strain curves were calculated both for the spacer warp-knitted fabric composites, and for the spacer woven fabric composites.

Key-words: composites, special three-dimensional fabrics, bending property, glass fibers

Strukturanalyse und Biegungseigenschaften eines Abstandsverbundwerkstoffes

Zweck der Arbeit war der Entwurf dreier Quasi-Abstandsmaterialtypen aus Glasfaser für Strukturanalyse und Biegungsexperimente. Die Oberflächenmorphologie in Vorder-, Drauf- und Seitenansicht wurde sowohl für Gewebe als auch für Gewirke beobachtet, besonders für Garne in der Richtung der Dicke. Es wurde festgestellt, dass die Abstandsmaterialstruktur dank ihrer Porosität mehr Luft speichert. Mehr, es wurden die Biegungseigenschaften mit einem Instron-Tester gemessen, mit Anzeige der Biegkraft- und Deflektionskurven des Verbundwerkstoffes, und es wurden die typischen Biegewiderstands- und Biegedehnungskurven berechnet und untersucht für den schussgewirkten eingelegten Abstandsverbundwerkstoff.

Stichwörter: Quasi-Abstandsmaterial, Biegungseigenschaft, Glassfaser

Energy saving is one of the most important focuses of the twenty-first century, especially for the architecture field. Generally speaking, the buildings are firstly constructed with reinforced steel concrete frame, which is the main load-support structure; while the walls are made by bricks, which are used to separate the indoors and outdoors for protection. So, the walls will be good with the following benefits: the first – have a light mass per cubic meter to lessen the load of the main load-support structure, which is helpful to erect much higher and safer buildings; secondly, have a high bending rigidity to withstand collision from outdoors and indoors and, finally, have a high thermal-resistant property to save energy. Based on the requirements of the walls, sandwich-like walls are designed by three layers. The middle layer is made of thinner and high strength steel nets, while the inner and outer layers are made of the quasi-three-dimensional fabric composites and fabric composites, as two-thirds of the building walls are designed with high porosity, so as to oppose a high thermal resistant property, have a light mass and a high bending strength. Therefore, fiber materials and the whole structure should be required to have low thermal-conductive coefficient, high bending strength and low mass per cubic meter. Glass-fiber spacer fabric composites are effective as architecture walls, considering the above requirements [1] besides low cost.

In the architectural industry, glass fibers are often used as walls for their high thermal-resistant property, and glass-fiber reinforced composites are widely adopted for high strength. Many researchers have been focusing on laminate fabric composites fabricated by resin or linking yarns in the through-thickness direction. The former fixing of the laminate fabric can be easily delaminated, due to the weak shearing-resistant behavior [2–4]. The latter uses the linking yarns in the through-thickness direction; however, the traditional linking yarns are made by general polyester or polyamide yarns with a good flexible property, which causes the strength to be low and the fabric to be easily damaged under high load [5–9]. The three-dimensional spacer-fabric composites by high performance fibers have a high bending strength in the three-dimensional directions [10–11], while the mass per volume is higher and causes the rise in cost. It so needs that the core part between the two faces/layers to be removed, which leads to the fabrication of spacer fabrics with a high porous structure. The spacer fabric decreases the mass per cubic meter and the cost and increases the thermal-resistant ability, while it has low effects on the bending rigidity under small deflection deformation.
Therefore, glass-fiber spacer-fabric composites are effective in saving energy for storing static atmosphere, with a high bending rigidity in through-thickness direction, under slight quake and collision, if applied in architecture. These are largely determined by the bending behavior of the fabric composites in the through-thickness direction [12-13]. The work was to design three kinds of quasi-three-dimensional spacer fabric

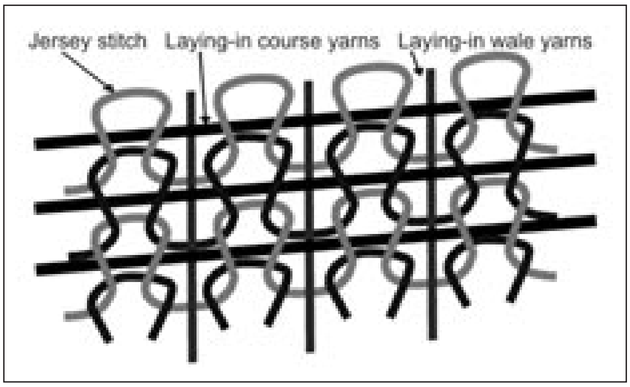

Fig. 1. Upper and bottom surface structure of laying-in weft-knitted spacer fabric

made by glass fibers, to analyze the structure and conduct bending experiments. The yarns at the side edge were continuous to increase the bending strength [14]. The quasi-three-dimensional glass-fiber fabrics consist of weaving or knitting structures for a high porous volume and much static atmosphere within the fabric composite. Then, the aim was to compare the bending properties of the three types of glass-fiber spacer-fabric composites and to provide an effective structure of the spacer-fabric composite to be applied in the architectural field. This is helpful in designing the structure of high performance fiber yarns and in acquiring a high strength of the fabric composites.

STRUCTURAL ANALYSIS OF THE QUASI-THREE-DIMENSIONAL FABRIC PREFORM

The main content dealt with in the paper is to analyze the structure of three kinds of quasi-three-dimensional glass-fiber spacer-fabric preforms by observing the face morphology and comparing the bending properties. The spacer fabric preforms are laying-in weft-knitted spacer-fabric composite (marked sample #1), astrakhan stitch warp-knitted spacer-fabric composite (sample #2) and spacer woven fabric composite (sample #3), respectively, which are all opposing much static atmosphere capability for high porosity.

The first preforms are a biaxial weft-knitted spacer-fabric, whose upper and bottom face structures are two symmetrical jersey stitches (fig. 1), being strengthened by laying-in wale and course yarns. The jersey stitches are located in the outset layer, and the middle layer as laying-in course yarns and the inner layer as laying-in wale yarns. Where the laying-in wale and course yarns are both straight and there is no locking with each other, these are used to increase the utilizing ratio of fiber strength; moreover, both the laying-in yarns are bound by the jersey.

The face structures are linked by *Z*-axis yarns, i.e. through-thickness directional yarns, and the left and right side views are shown in figures 2 and 3. Figures 2 *b* and 3 *b* are the zoom-in pictures of local parts of figures 2 *a* and 3 *d*, and figures 2 *d* and 3 *d* are the structure of the fabric preforms in *Z*-axis direction. It shows that the connecting glass-fiber yarns links the upper and bottom faces, and burdens high strength in through-thickness direction for a high straight line under external applied load. This is also proved by the microscopy picture in figures 2 *c* and 3 *c*, where the pictures are observed by OLYMPUS PME3 microscopy and the samples are polished by REFINE POLISHER (Refine Tec Ltd.) as 400, 800, 1 200 and aluminum powder by 1 and 0.05 μm, respectively. Figures 2 *c* and 3 *c* are used just to prove the yarns structure in the spacer-fabric. Actually, the linking-yarns direction in the spacer-fabric are already proved by the figure 2 *a, b* and figure 3 *a, b*. However, the yarns contour in figures 2 *c* and 3 *c* are not very clear. It shows that the linking yarns will migrate into the three-dimensional shape from the two-dimensional plane, while the pictures captured by OLYMPUS PME3 microscopy, after the samples have been polished by REFINE POLISHER, represent other validating experimental pictures, to present the direction of linking yarns in the spacer fabric. These show the contour of the linking yarns in the *Z*-axis direction, i.e. the through-thickness direction.

The second preform is the astrakhan stitch warp-knitted spacer-fabric, whose faces and linking structures are listed in figure 4. It can be seen from figure 4 *b* and *c* that the upper-face structure is five-thread warp sateen stitch and the bottom surface is open-chain stitch, and

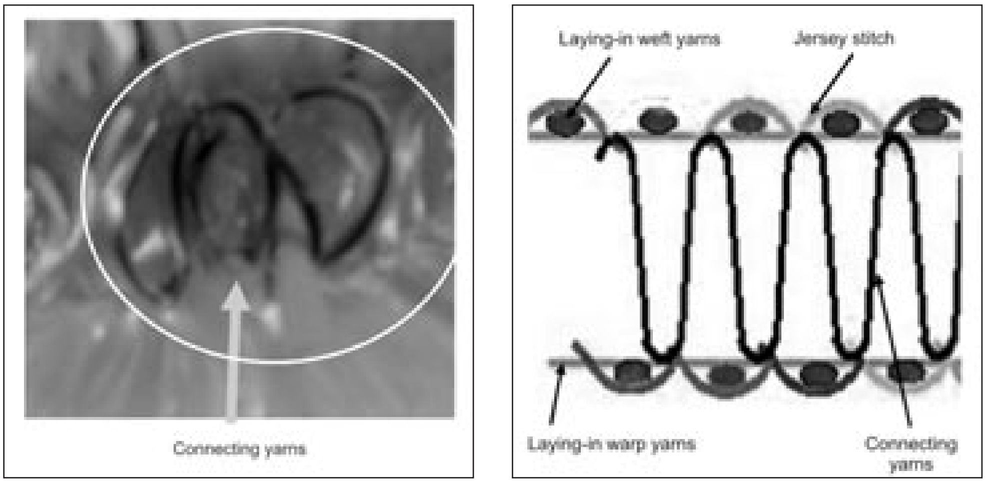

a *b*

Fig. 2. Structure of #1 in thickness direction:
a – morphology of yarns; ***b*** – structure of side view

a

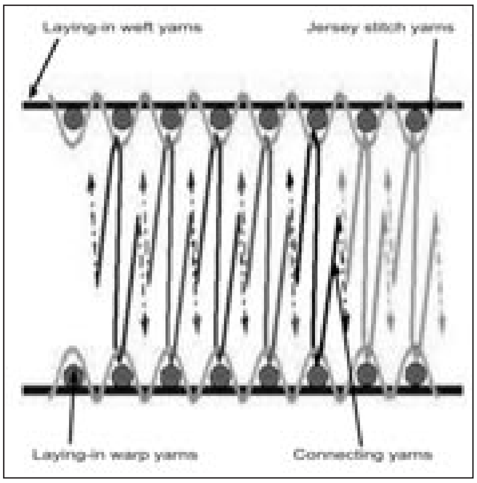

b

Fig. 3. Structure of #2 in thickness direction:
a – morphology of yarns; ***b*** – structure of side view

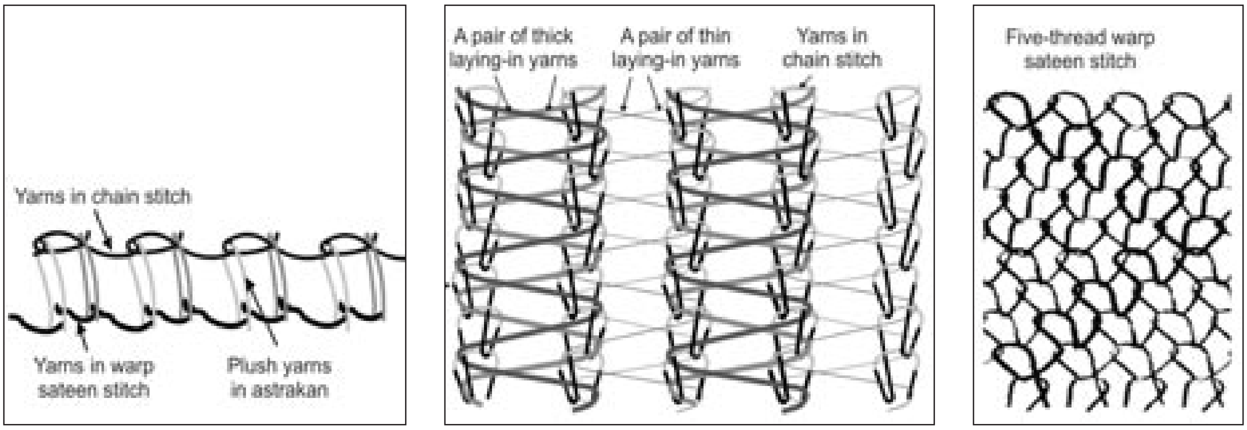

a *b* *c*

Fig. 4. Morphology and structure of astrakhan stitch warp-knitted spacer fabric composite:
a – side view structure; ***b*** – bottom surface structure; ***c*** – upper surface structure

the linking yarns shape is obvious from the side view of the fabric given in figure 4 *a*. The connecting yarns are knitted with the upper face yarns into astrakhan stitch and casting off to interknitting with the chain stitch in the bottom surface, which increases the rigidity in the thickness direction. The chain structures are strengthened by the laying-in yarns in wale direction, and there exists a pair of thick laying-in yarns by two-thread fleecy between neighboring chains, and then a pair of thin laying-in yarns by two-thread fleecy between neighboring chains, as seen in figure 4 *b*.

The schematic morphologies of the third preforms are listed in figure 5 *a*. It is a spacer woven fabric, where the upper and bottom faces' structures are both the same woven structure interwoven by two orthogonal warp and weft yarns, seen in figure 5 *b*. The two symmetrical surfaces are connected by the Z-axis yarns, and the left and right side views are listed in figure 5 *c* and *b*.

FABRIC COMPOSITE PREPARATION AND EXPERIMENT

Composite preparation

Three kinds of spacer fabric preforms with quasi-three-dimensional geometry are selected and made by 1 200 tex glass-fiber bundle, which are laying-in weft-knitted spacer-fabric composite (sample #1), astrakhan stitch warp-knitted spacer-fabric composite (sample #2) and spacer woven fabric composite (sample #3). The fabricated composite preforms are all made as follows:

- we lay one piece of PET membrane (at the bottom), on a platform, and uniformly pour the unsaturated polyester resin on the PET membrane;
- the specimen is cut in sizes of 300 mm x 300 mm for each kind of preform and laid on the unsaturated polyester resin;
- we evenly pour the unsaturated polyester resin again on the specimen and put the second PET membrane (at the top) on the specimen;
- a iron block is laid on the second PET membrane to compress the fabric composite for about 24 hours;
- we put the fabric composite to convection oven at 100^{o}C for 2 hours, and the fabric composites are fabricated, as seen in figure 6.

The spacer-fabrics are impregnated with resin. In order to compare the bending properties of the three kinds of spacer fabrics, the ratio of total fibers mass to composite fabric mass is the same (38%) for the three fabric composites.

Specimens' preparation

Three specimens are cut in sizes of 200 mm x 30 mm for each fabric composite by the cutter for bending

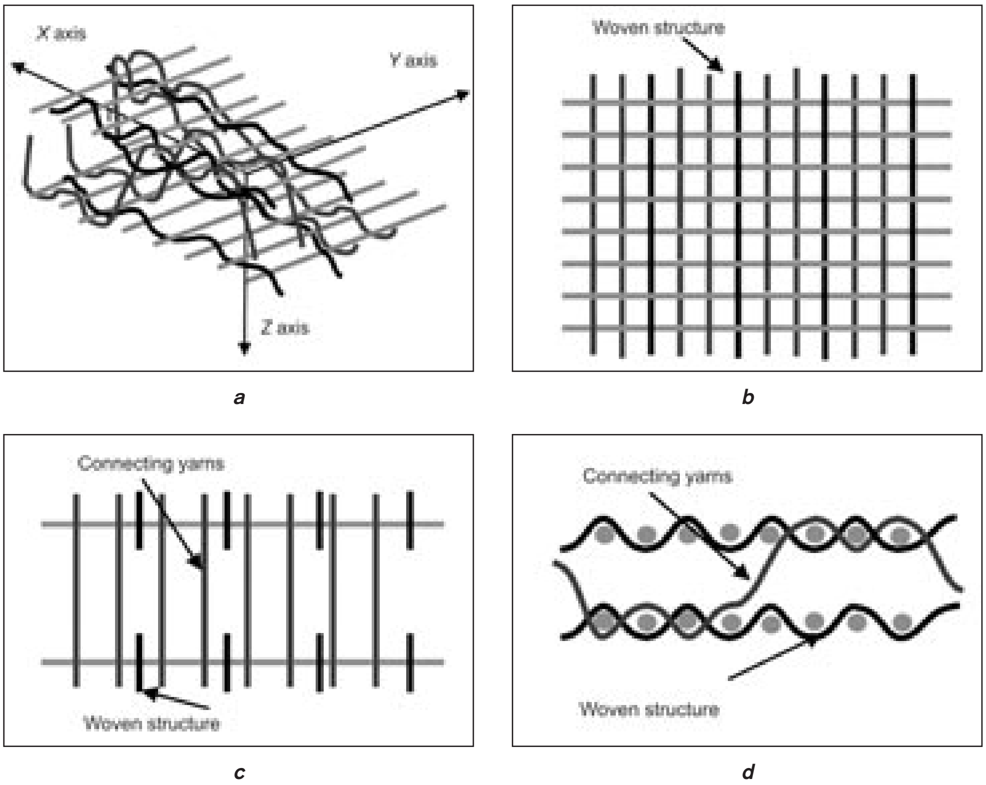

Fig. 5. Morphology and structure of spacer woven fabric:
a – total morphology; ***b*** – surface structure; ***c*** – *Z*–*Y* axis structure; ***d*** – *Z*–*X* axis structure

tests, as seen in figure 7, where only the much stronger direction of the fabric composite is cut just for comparing the increasingly directional strength of the fabric composites, according to measured data.

So, each fabric composite is cut into three specimens, according to requirements, and marked as follows: #1-1, #1-2 and #1-3 (for fabric composite #1); #2-1, #2-2 and #2-3 (for fabric composite #2); #3-1, #3-2 and #3-3 (for fabric composite #3). The thickness of each specimen is measured at three cross sections *A-A´*, *B-B´* and *C-C´*. The average thickness of each specimen is used for the input value of thickness for the bending test, as listed in table 1.

Parameters set for the bending meter

The Instron MODEL 4206 tester is used to conduct the three-points bending experiment for the fabric composites, which is shown in figure 8. The parameters of the

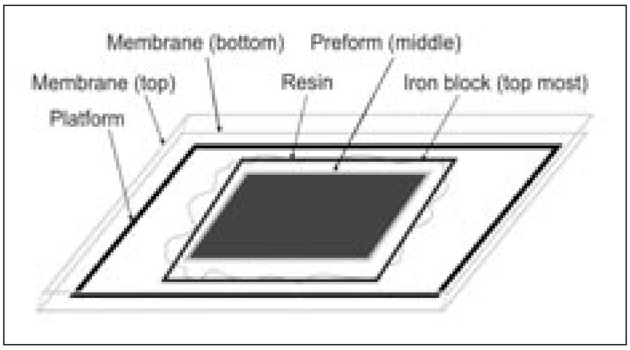

Fig. 6. Fabrication schematic picture of fabric composite

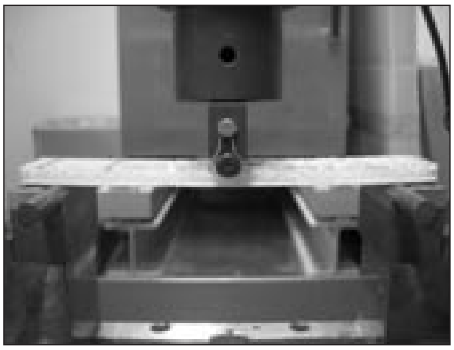

Fig. 7. Schematic diagram of bending testing

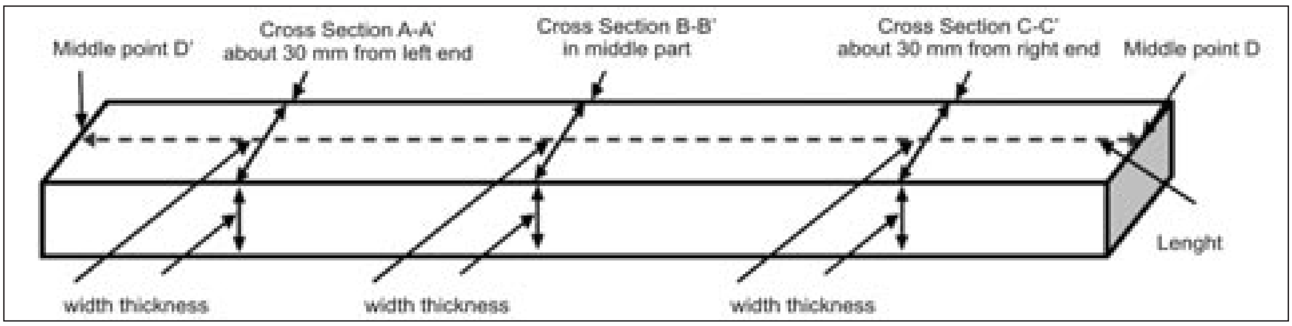

Fig. 8. Three-point bending test specification

Table 1

THICKNESS RESULTS ANALYSIS OF THREE KINDS OF SAMPLES										
Sample no.		#1			#2			#3		
		#1-1	#1-2	#1-3	#2-1	#2-2	#2-3	#3-1	#3-2	#3-3
Thickness	*AVE*, mm	11.33	11.52	11.14	8.51	8.70	8.66	7.65	7.86	7.68
	CV, %	2.1	2.2	2.8	1.13	0.85	0.77	0.87	0.37	2.04

tester are set as follows: sensor volume is selected as 500 kg, bending speed as 5 mm/minute, span length of two supporting points as 160 mm, according to JIS standard K017 (ISO/FDIS 14125: 1997), and the radius of curvature for the three-points bending rods – all at 10 mm.

RESULTS AND DISCUSSIONS

Morphology and structure observation of specimens

The morphology of the upper and bottom surfaces and the left and right side views of the three kinds of spacer-fabric composites are observed by Canon Powershot camera and shown in figures 9–11.

It can be seen in figure 9 that it is a jersey stitch and laying-in weft yarns morphology in the upper and bottom faces and, for the linking yarns in through-thickness direction, there are high parallel relations and orientation. These yarns are almost vertical to the surface if the processing is proper, which will improve the strength in the through-thickness direction. The morphologies of fabric composite #1 are much more obvious in figures 1–3. It also proves in figure 10 that the upper surface structure is warp sateen stitch, where there is much net-like morphology. The surface is rough for the casting-off of the plush in astrakhan stitch, and the bottom surface is clear chain stitch. The connecting yarns in side views are shown to be knitted with the upper surface yarns into astrakhan stitch and cast-off, to be interknitted with the chain stitch in the bottom surface, where the connecting yarns in the through-thickness direction are relatively vertical and parallel and have high orientations in *Z*-axis direction, to improve the burdening capability. The morphology in figure 11 obviously indicates that the upper and bottom

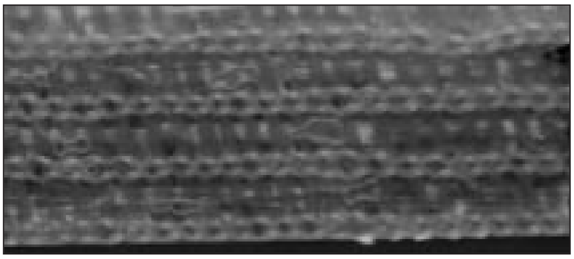

a

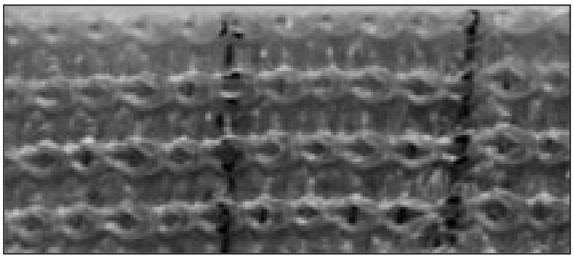

b

Fig. 9. Morphology of fabric composite #1:
a – face up; ***b*** – face bottom

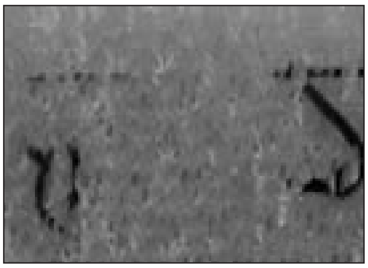

a

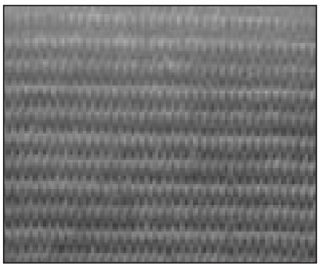

b

Fig. 10. Morphology of fabric composite #2:
a – face up; ***b*** – face bottom

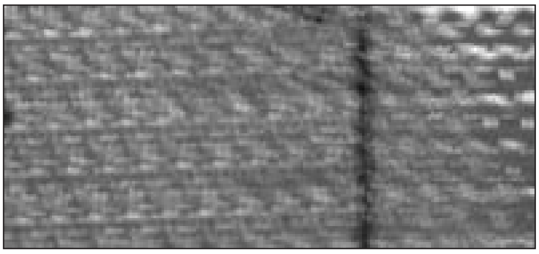

a

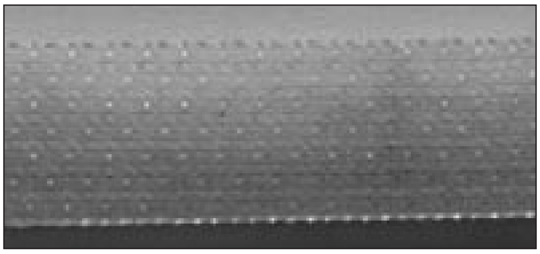

b

Fig. 11. Typical surface and side view morphology of fabric composite #3:
a – face up; ***b*** – face bottom

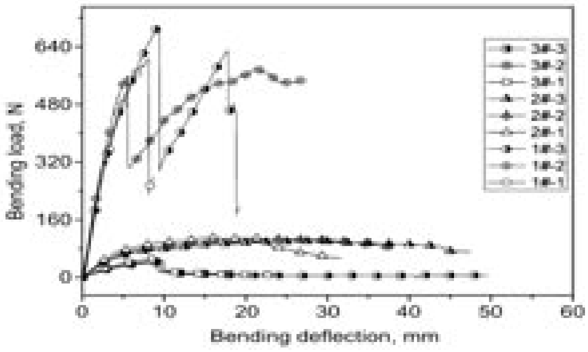

Fig. 12. Bending load and deflection curve

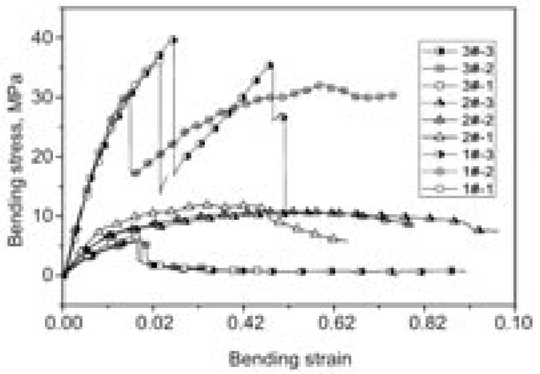

Fig. 13. Bending stress and strain curve

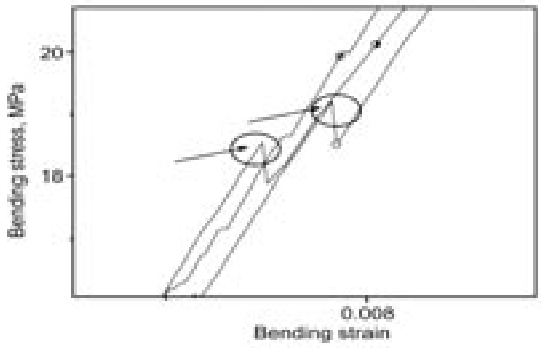

Fig. 14. Local part of bending elastic of #1

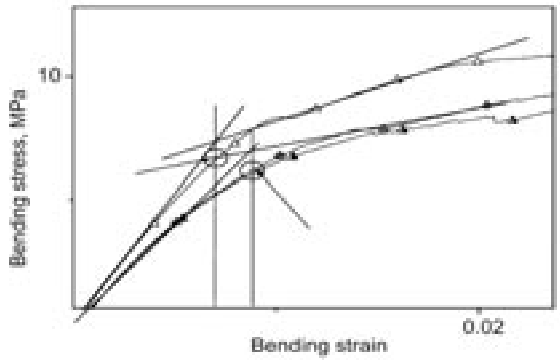

Fig. 15. Local part of bending elastic of #2

surfaces are woven structures, and the connecting yarns in *Z*-axis direction are almost vertical and parallel, having the highest orientation in *Z*-axis directions of the three kinds of spacer-fabric composites, fact useful in storing a high porous ratio of static atmosphere.

Typical bending stress & strain curves

The bending force F(X) is sensed in a whole bending deformation by the force sensor and acquired with the shift distance, *S*, of the bending rod. The typical bending force and deflection curves of each fabric composite achieved by using the Instron tester are shown in figure 12.

In order to compare the bending behavior of the three kinds of spacer fabric composites, the bending stress and bending strain are calculated by the following formulas:

$$\varepsilon = \frac{6Sh}{L^2} \tag{1}$$

$$\sigma = \frac{3FL}{2bh^2} \tag{2}$$

$$E = \frac{L^3}{2bh^2} \cdot \frac{\Delta F}{\Delta S} \tag{3}$$

where:

ε is the bending strain, MPa;

σ – bending stress, MPa;

E – bending modulus, MPa;

L – span length of two supporting points set as 160 mm by Instron tester in the three-point bending principle;

b and h – width (cut as 30 mm) in unit as millimeter and thickness in unit as millimeter of fabric composite;

F and S – the sensed bending load, in N, and the calculated deflection in units as millimeter of middle cross-section of bent fabric composite between the two supporting points measured by Instron tester.

In testing, the shift distance, *S*, is calculated according to the following equations under the moving speed of the bending meter *V* (set as 5 mm/minute) and the sampling frequency of the force sensor *n* (set as 10 points/second) in experiment; the shift distance between two acquiring points is expressed as $S = (V/60)/n$. Then, the bending stress and bending strain of fabric composites are obtained, and the bending stress & strain curves are listed in figure 13.

Analysis of the bending property

The bending indexes of spacer fabric composites include bending modulus *E*, maximum bending stress σ and maximum bending load *F*. The maximum bending load is obtained from the bending load and deflection curve of the spacer-fabric composite, by Instron tester, in three-point bending test in principle, and the maximum bending stress is calculated by equation (2). Then, the bending modulus is obtained from the initial elastic region of the bending stress & strain curve by equations (1) and (2), i.e. to select bending strain range. The starting point of the bending strain is set as zero, and the ending point of the bending strain is set at the point where the bending deformation is elastic (i.e., no energy lost and completely recover deformation). Therefore, the bending strain ranges of the three kinds of spacer-fabric composites are different for a different structure.

The ending point of specimen #1 is set at a local peak where there is a sharp decrease transition point, but not

Table 2

BENDING INDEXES OF FABRIC COMPOSITES				
Fabric composites		Bending indexes		
Preform	No. samples	Max. load, N	Max. stress, MPa	Modulus, GPa
Knitted fabric	#1	620.5	35.6	59.5
	#2	100.9	10.6	45.4
Woven fabric	#3	46.3	6.0	43.0

the peak value of the bending stress & strain curve. The transition peak point may be caused by the yield break deformation of the Z-axis, seen in figure 14, which can be attributed to the de-bindings between the unsaturated polyester resin and the fabric preforms, which causes cracks inside the matrix.

The ending point of specimen #2 is set at the intersecting point of two lines, i.e., the initial elastic line and yield region line, because the pre-peak part is nonlinear and the post-peak part is long extended, seen in figure 15.

The ending point of specimen #3 is also set at the intersecting point of two lines, i.e., the initial elastic line and yield region line, because the pre-peak part is nonlinear and the post-peak part decreases sharply showing broken deformation, seen in figure 16.

The bending indexes of the spacer-fabric composites are calculated and listed in table 2, which could be used to characterize and compare the bending properties of the three kinds of spacer-fabric composites. The typical whole bending force and deflection curves of each fabric composite determined by using the Instron tester are nonlinear, while they should be linear in the initial bending region. However, the initial region is also nonlinear for normal noise disturbance, and the correlation coefficient of the linear fitting arrives as high as over 0.95. Moreover, modulus was the slope at any point in the bending stress & strain curve, according to equation (3), by the differential algorithm. So, the slope of the linear fitting line to the initial bending region is used as the ratio of differential force, ΔF, to differential shift distance, ΔS, in equation (3). As about the maximum broken bending-load, the broken region is located in the nonlinear region. The cross-section changed a little, so we assume the cross-section is not varied in the bending process and we adopt the bending stress to compare the bending property of different cross-sections of spacer-fabric samples, which are just to neglect the effect of the cross-section area.

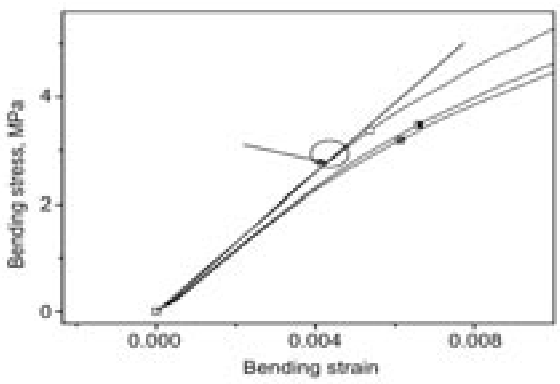

Fig. 16. Local part of bending elastic of #3

It can be seen from table 2 that the maximum bending load, stress and modulus of spacer fabric composite #1 are the largest, followed by spacer fabric composites #2 and #3. The bending stress trend can be attributed to the yarns orientation in the fabric composite. Yarns in *Z*-axis direction fabric composite #1 provide supporting for both upper and bottom surfaces, where the weft-&-warp laying-in parallel yarns are linear and with no crimp. Yarns in *Z*-axis direction of fabric composites #2 is a knitted fabric and have warp laying-in-yarns with larger radius of curvature and lower crimp ratio than those of fabric composite 3#. It means that the bending stress of the fabric composite is largely determined by yarns in *Z*-axis direction of the fabric preforms, whose supporting actions for connecting upper and bottom layers play an important role under bending deformation.

It is also obvious from figure 12 that there are bending cracks in fabric composites #1 and #3, for the double layers, and the post-peak parts followed are different. The former increased gradually after a short fast descending and could support large strength to some extent, while the latter kept very gentle and could support low strength. In addition, the bending trend of fabric composite #2 is general, as a normal single-layer fabric composite. The small differences of maximum bending stress and modulus between fabric composites #2 and #3 show that the double-layer woven fabric preforms (i.e., sample #2) have the contiguous action with single-layer knitted fabric preforms (sample #3), which indicates that the former have just one-layer supporting action in the bending property with the latter and also implied that the *Z*-axis yarns do not play a significant role. As far as fabric composite #1 is concerned, the *Z*-axis yarns can support the upper and bottom faces layers, and help to let the two layers simultaneously respond to anti-bending response. Moreover, the straightly parallel yarns also provide the highest bending strength.

The bending modulus trend can be attributed to the yarns orientation in the fabric composite surface. Yarns in upper and bottom surfaces of fabric composite #1 are linear and with no crimp. Surface of fabric composites #2 has warp laying-in-yarns with continuous connection in fabric surface, while the surface of fabric composite #3 has only interweaving yarns and no significantly strengthening yarns. It can be concluded that the linking yarns of the fabric preforms largely affect the bending modulus of the fabric composite.

CONCLUSIONS

The work and paper studied the structure and bending behavior of the quasi-three-dimensional spacer-fabric composite by high performance glass fibers, and the conclusions are as follows:

- By structural and morphological analysis, the three kinds of spacer-fabric preforms are double-layer knitted fabric marked as #1, single-layer knitted fabric #2 and double-layer woven fabric #3. The first preform is laying-in weft-knitted spacer-fabric, which consists of two symmetrical surfaces that are connected by *Z*-axis yarns. Each surface is wale-&-course laying-in weft-knitted fabric composed of glass fiber yarns. The second preform is single-layer warp-knitted fabric with laying-in warp yarns, and the substrate layer is warp laying-in knitted fabric, and one loop is long, so as to be knitted with adjacent loop, which is also useful for tightening the laying-in warp yarns. The third preform is double-layer woven fabric, and the fabric consists of two symmetrical surfaces, which are connected by *Z*-axis yarns. Each surface is a woven fabric composed of glass fiber yarns.
- By three-point bending tests based on Instron meter, the maximum bending stress and modulus of fabric composite #1 are the largest, followed by fabric composites #2 and #3. The bending stress and modulus trend can be attributed to the *Z*-axis and surface yarns orientation in the fabric composite, which significantly determine the bending crack behavior of the fabric composite in application. Therefore, the linking yarns structure in the spacer-fabric preforms largely affect the bending modulus of the fabric composite.

Acknowledgements

The authors express their sincere gratitude for the financial support to “Chen Guang” project supported by Shanghai Municipal Education Commission and Shanghai Education Development Foundation, supported by Chinese Universities Scientific Fund and wish to thank professor NAKAI and team members of Advanced Fibro Science in Kyoto Institute of Technology for help, and to the Venture laboratory of Kyoto Institute of Technology for the financial support.

BIBLIOGRAPHY

[1] Mouritz, A. P., Banister, M. K., Falzon, P. J., Leong, K. H. *Review of applications for advanced three-dimensional fiber textile composites.* Composites Part A. In: Applied Science and Manufacturing, 1999, vol. 30, issue 12, p. 1 445
[2] Ramesh, T. *Stiffness properties of composite laminates with matrix cracking and interior delamination.* In: Engineering Fracture Mechanics, 1986, vol. 25, issue 5–6, p. 751
[3] Huang, Gu. *Tensile and bending behaviors of laminates with various fabric orientations.* In: Materials and Design, 2006, vol. 27, issue 10, p. 1 086
[4] Bigaud, D., Szotkiewica, C., Harlock, C. S. *Tearing analysis for textile reinforced soft composites under mono-axial and biaxial tensile stresses.* In: Composite Structures, 2003, vol. 62, issue 2, p.129
[5] Xu, D. S., Ganesan, R., Suong, V. H. *Buckling analysis of tri-axial woven fabric composite structures subjected to biaxial loading.* In: Composite Structures, 2007, 78(1), p. 140
[6] Yu, W. M., Yeung, K. W., Harlock, S. C., Leaf, G. A.V. *Predicting energy requirements for molding flexible polyurethane foam sheets.* In: Textile Research Journal, 1998, vol. 68, issue 4, p. 289
[7] Machova, K., Klug, P., Waldmann, M. *Determining of the bending strength of knitted spacer fabric.* In: Melliand Textiberichte, 2006, vol. 87, issue 6, p. 93
[8] Lehmann, W. *Elastic molded spaced fabric.* In: Kettenwirk Praxis, 1994, issue 3, p. 19
[9] Joanne, Y., Sunpui, N. G. *Study of three-dimensional spacer fabrics: Physical and mechanical properties.* In: Journal of Materials Processing Technology, 2008, vol. 206, issue 1–3, p. 359
[10] Shen, C., Chen, H. C., and Chen, H. E. *Effect of weave structure on mechanical fracture behavior of three-dimensional carbon fiber fabric reinforced expoxy resin composites.* In: Composites Science and Technology, 1992, vol. 45, issue 1, p. 23
[11] Wang, X., Hu, B., Feng, Y., Liang, f, Mo, J., Xiong, J., and Qiu, Y. *Low velocity impact properties of 3D woven basalt aramid hybrid composites.* In: Composites Science and Technology, 2008, vol. 68, issue 2, p. 444
[12] Liu, Y., Lv, L., Sun, B., Hu, H., Gu, B. *Dynamic response of 3D biaxial spacer weft-knitted composite under transverse impact.* In: Journal of Reinforced Plastics and Composites, 2006, vol. 25, issue 15, p. 1 629
[13] Wang, F., Hu, H. *Properties of biaxial reinforced weft-knitted spaced fabric.* In: Knitting Industries, 2006, issue 4, p. 9
[14] Hamada, H., Nakatani, T., Nakai, A., and Kameo, K. *The crushing performance of a braided I-beam.* In: Composites Science and Technology, 1999, vol. 59, issue 12, p. 1 881

Authors:

DU ZHAOQUN
Key Laboratory of Textile Science & Technology
Ministry of Education
College of Textiles, Donghua University
Shanghai, 201620, China

YU WEIDONG
College of Clothing and Art Design
Jiaxing University, Jiaxing, Zhejiang 314001, China

HAMADA HIROYUKI
YANG YUQUI
Advanced Fibro Science
Kyoto Institute of Technology
Kyoto. 606-8585, Japan

Coresponding author:
DU ZHAOQUN
e-mail: duzq@dhu.edu.cn

Investigating dyeing properties of regenerated bamboo material dyed with reactive and direct dyes

B. YEŞIM BÜYÜKAKINCI
NIHAL SÖKMEN

ERHAN ÖNER

REZUMAT – ABSTRACT – INHALTSANGABE

Studierea proprietăţilor tinctoriale ale materialelor din bambus regenerat, vopsite cu coloranţi reactivi şi coloranţi direcţi

Datorită proprietăţilor antibacteriene şi tinctoriale, a tuşeului moale şi a altor proprietăţi superioare, comparativ cu cele deţinute de alte tipuri de fibre celulozice regenerate, fibrele regenerate din bambus sunt tot mai mult utilizate în industria textilă. În cadrul experimentului, au fost utilizate mostre de materiale din bambus regenerat 100%. Materialele au fost pretratate enzimatic, albite şi vopsite cu coloranţi reactivi (Albastru – C.I. Reactive Blue 19, Roşu – C.I. Reactive Red 239 şi Galben – C.I. Reactive Yellow 186), pentru a investiga efectul pretratării asupra proprietăţilor fizice şi tinctoriale ale materialelor. De asemenea, în condiţii de climatizare date, au fost studiate proprietăţile de absorbţie a coloranţilor direcţi şi a celor reactiv (Albastru – C.I. Direct Blue 90, Rosu – C.I. Direct Red 83:1 şi Galben – C.I. Direct Yellow 98). În plus, au fost realizate vopsiri cu coloranţi reactivi în câmp de ultrasunete, proprietăţile acestor materiale fiind comparate cu cele ale materialelor vopsite în mod convenţional.

Cuvinte-cheie: material din bambus, vopsire prin epuizare, coloranţi reactivi, coloranţi direcţi, imagini SEM, rezistenţa culorii, vopsire în câmp de ultrasunete

Investigating dyeing properties of regenerated bamboo materials dyed with reactive and direct dyes

Because of its inherent antibacterial property, soft handle, easy dyeability and many other better properties over the other regenerated cellulosic fibers, the use of regenerated bamboo fiber is increasing in the textile industry. In this research, 100% regenerated bamboo fabric samples were used throughout. The fabrics were enzymatically pretreated, bleached and dyed with reactive dyes (C.I. Reactive Blue 19, C.I. Reactive Red 239 and C.I. Reactive Yellow 186) to investigate the effect of the pretreatment on the physical and dyeing properties of the materials. In another part of this research, the dye uptake properties of reactive and direct dyes (C.I. Direct Blue 90, C.I. Direct Red 83:1 and C.I. Direct Yellow 98) were studied under atmospheric conditions. In addition, the microwave heat dyeings were carried out with the reactive dyes, and the properties of the dyed materials were compared with those of the conventionally dyed materials.

Key-words: bamboo fabric, exhaust dyeing, reactive dyes, direct dyes, SEM image, color fastness, microwave heat dyeing

Untersuchung der Farbeigenschaften der regenerierten Bamboomaterialien gefärbt mit reaktiven und direkten Farbstoffe

Dank ihrer innerlichen antibakteriellen Eigenschaft, weichen Griff, leichte Färbung und viele andere gute Eigenschaften gegenüber anderer regenerierten Zellulosefaser, gewinnt die Anwendung der regenerierten Bamboofaser in der Textilindustrie an Bedeutung. Bei dieser Untersuchung wurden 100% regenerierte Bamboofaser-Muster verwendet. Die Materialien wurden enzymatisch vorbehandelt, gebleicht und mit Reaktivfarbstoffen gefärbt (C.I. Reactive Blue 19, C.I. Reactive Red 239 und C.I. Reactive Yellow 186) um den Vorbehandlungseffekt auf den physischen und färblichen Eigenschaften der Materialien zu untersuchen. In einem anderen Teil der Analyse wurden die Farbpenetrationseigenschaften der reaktiven und direkten Farbstoffe in atmosphärischen Bedingungen untersucht (C.I. Direct Blue 90, C.I. Direct Red 83:1 und C.I. Direct Yellow 98). Mehr, die Mikrowellenwärmefarbstoffe wurden mit Reaktivfarbstoffen behandelt, und die Eigenschaften der gefärbten Materialien wurden mit den konventionellen Farbstoffen verglichen.

Stichwörter: Bamboo-Materialien, Reduzierfärben, Reaktivfarbstoffe, Direkte Farbstoffe, SEM-Bilder, Farbechtheit, Mikrowellenwärmefärbung

The regenerated bamboo fiber, one of the latest discoveries in the rapidly developing textile sector is considered to be the fiber of the 21st century. It is being more widely used in the textile industry due to its features, such as the inherent antibacterial property, easy dyeability, absorbency, breathability and having a smooth texture [1–9]. Even after fifty washing cycles, the bamboo fabric still possesses an excellent antibacterial function, bacteriostasis [1]. The bamboo fiber is also the only 100% biodegradable textile material, which does not cause any environmental pollution, naturally recycling itself. In this sense, it is a new environmentally friendly textile material. However, the research on the dyeing properties of the bamboo fiber is very limited in the technical literature. Therefore, in this work, 100% regenerated bamboo fabrics were dyed with the reactive and direct dyes, and the dyeing properties of these materials as well as the fastness of the dyed materials were investigated. The mechanical properties and SEM images of the dyed materials were also provided.

EXPERIMENTAL PART

Materials and methods

100% regenerated bamboo fabric was used throughout the experimental work. The fabric was single jersey knit and the fabric weight was 130 g/m^2. The samples were scoured, bleached and dyed with reactive dyes, in order to investigate the effect of the pretreatment on the dyeing and the physical properties of the regenerated bamboo fabrics.

Scouring was carried out with 0.5% o.w.f. Scourzyme L (Nova Nordisk) at 55°C for 20 minutes, with a liquor ratio of 40:1 and *p*H range was kept at 8.0–8.5. After the enzymatic scouring process, the materials were kept in distilled water at 80°C for 10 minutes, in order to remove the enzyme by decomposition.

The bleaching of the scoured bamboo materials was carried out in a bath containing 8 mL/L H_2O_2 (50%), 1 g/L NaOH, 0.2 mL/L wetting agent (Uniwett HGA – Alfa Kimya) and 2 g/L organic stabilizer (Prestogen P – BASF) at 80°C for 45 minutes, with a liquor ratio 40:1. The samples were rinsed twice at 70°C in warm water, neutralized with CH3COOH and later soaped with a nonionic detergent (Perlavin NIC – Dr. Petry) at the boil. The samples were eventually rinsed twice at 70°C in warm water and overflow rinsed in cold water. Each process lasted 10 minutes, the total process being 60 minutes.

The dyeing of the non-pretreated, scoured and bleached samples was carried out with the reactive dyes

Table 1

DYES USED IN THIS WORK		
Color index generic name/ Commercial name	Chemical class	Reactive groups
C.I. Reactive Blue 19 (Remazol Brilliant Blue R)	Anthraquinone	Vinyl sulfone (VS)
C.I. Reactive Red 239 (Remazol Brilliant Red 3BS)	Monoazo	Monochlorotriazinyl/VS
C.I. Reactive Yellow 186 (Remazol Brilliant Yellow 3GL)	Monoazo	Vinyl sulfone (VS)
C.I. Direct Yellow 98 (Indosol Yellow SF GL 160)	Azo	–
C.I. Direct Blue 90 (Indosol Blue SF2G 400)	–	–
C.I. Direct Red 83:1 (Indosol Rubin SF RGN)	Disazo	–

listed in table 1, under the atmospheric conditions, in accordance with the diagram shown in figure 1. The color strength was 1%, with a liquor ratio 40:1, for all dyeing. Samples dyeing was carried out in an atmospheric dyeing machine (Roaches 16-tube dyeing machine) and initiated at 30°C with a bath containing 30 g/L Na_2SO_4. The temperature was gradually increased to 60°C and 5 g/L Na_2CO_3 was added to the bath. At this temperature, the dyeing lasted 45 minutes. The reactive dyed materials were rinsed twice at 70°C in warm water, neutralized with CH^3COOH, and soaped with a nonionic surfactant (Perlavin NIC) at the boil for 10 minutes. Eventually, the materials were rinsed with cold water. The effects of the pretreatment on the dyeing, morphological and tensile properties of the bamboo materials were investigated.

In addition to this study, the dye uptakes of the non-pretreated materials were also carried out with the reactive and direct dyes listed in table 1. Dyeing with direct dyes was performed under the atmospheric conditions, in accordance with the diagram shown in figure 2. The dyeing was initiated at 40°C. 10 g/L Na_2SO4 was portion-wise added to the bath. The direct dyed samples were later rinsed twice at 30°C for 20 minutes each, and later treated with a cationic fixing agent (Indosol E-50 POW – Clariant), and finally were rinsed with cold water.

Eventually, microwave heat dyeing with reactive dyes was carried out with 100% regenerated bamboo materials, in order to investigate the effect of MW heating, and the results were compared with the conventionally

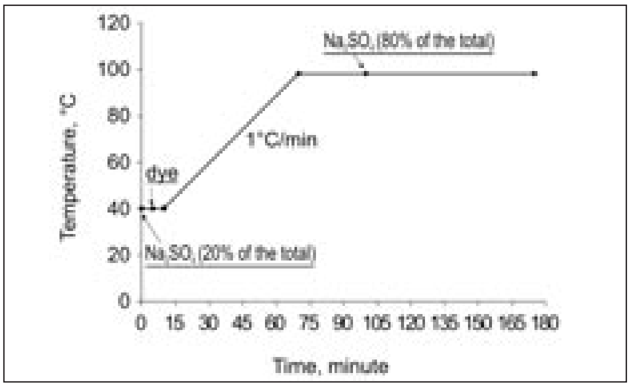

Fig. 2. Exhaust dyeing of the samples with direct dyes

dyed samples. Microwave (MW) heat dyeing was carried out in a microwave oven (White Westinghouse, Model KM06VF2W with a maximum output power of 700 W, operating at 2,450 MHz), in accordance with the time-temperature diagram given in figure 3. Each dye-bath in a 400 mL glass beaker was placed into the microwave oven at 30°C and microwave oven's energy level was adjusted to 120 W (Low Level: L), and the temperature rose up to 80°C in 4 minutes. The microwave oven's energy level was later immediately shifted to 460 W (Medium level: M), and the dye bath was kept at this temperature for 6 minutes. The dye bath was finally taken out from the microwave oven and cooled down. The dyed samples were washed out with warm and cold water as described above.

All the experiments were performed in triplicates. The color measurements of the materials were carried out by Datacolor SF600+ spectrophotometer (Illuminant D65, specular reflection included mode, 10° Standard Observer and 6.6 mm measuring plate). The color strengths (K/S values) of the samples were calculated from the reflectance values by the Kubelka-Munk equation (equation 1) at the maximum wavelength of absorption (λ_{max}) of each dye.

$$K/S = (I - R)^2 / 2R \tag{1}$$

The dye uptake values (% E) were calculated by the use of a UV-Visible spectrophotometer (Shimadzu UV-1200), measuring the absorbance at the wavelength of maximum absorption (λ_{max}) of each dye, in accordance with equation 2.

$$\%E = 100\left[(C_o - C_t)/C_o\right] \tag{2}$$

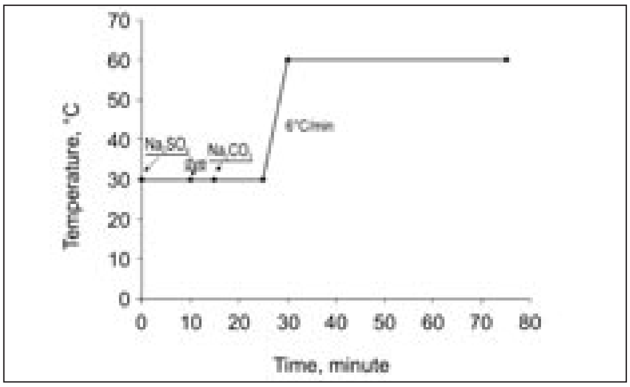

Fig. 1. Exhaust dyeing of the samples with reactive dyes

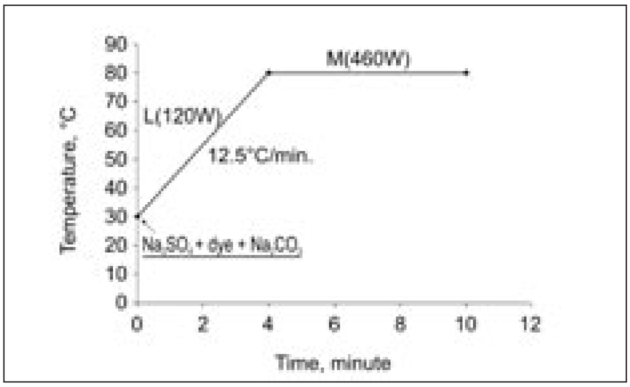

Fig. 3. MW heat dyeing process of the samples with reactive dyes

Table 2

THE WHITENESS INDEX VALUES OF BAMBOO MATERIALS	
Material	**CIE whiteness index**
Un-pretreated	25.70
Scoured	31.30
Bleached	57.00

In equation 2, C_o and C_t indicate the concentrations of the dye initially used in the dyebath and the residual amount of dye at time *t* (minutes) during dyeing, which were calculated from the absorbance values measured at λ_{max} of the dye. The changes on the surface of the processed bamboo materials were examined by using a scanning electron microscope (JEOL JSM-5910 LV, high-resolution 20,000 X magnification). All samples were coated with gold before SEM testing. The fastnesses of the dyeings to washing and to wet and dry rubbings were determined in accordance with the ISO 105-C06 method (A1S) and ISO 105-X12. The bursting strength of the bamboo fabrics was also tested by SDL Atlas M229, in accordance with EN ISO 13938-1, and abrasion resistance tests were conducted by Nu-Martindale Model 103, in accordance with EN ISO 12947-2.

RESULTS AND DISCUSSIONS

The whiteness index values of the untreated, scoured and bleached un-dyed materials are given in table 2. The CIELab values of the samples, which were un-pretreated, scoured, bleached and dyed with reactive and direct dyes, are presented in table 3.

The scouring process had a very little effect on the whiteness of the materials; however, a reasonable whiteness was achieved after bleaching.

The *K/S* values are given in figure 3. The scouring process slightly improved the *K/S* values, but it is also possible to dye the material without any pretreatment, since very close *K/S* values were obtained with the un-pretreated materials, compared with those of the scoured and bleached materials. Since almost similar *K/S* values and materials with good dyeing properties were obtained in a very short processing time, microwave heat dyeing proved to be a successful technique.

The dye uptake properties of un-pretreated regenerated bamboo materials were also studied with reactive and

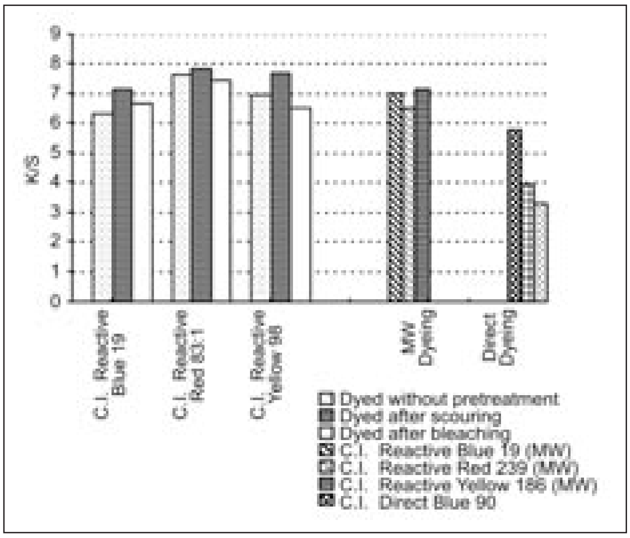

Fig. 4. Maximum *K/S* values of the dyed materials

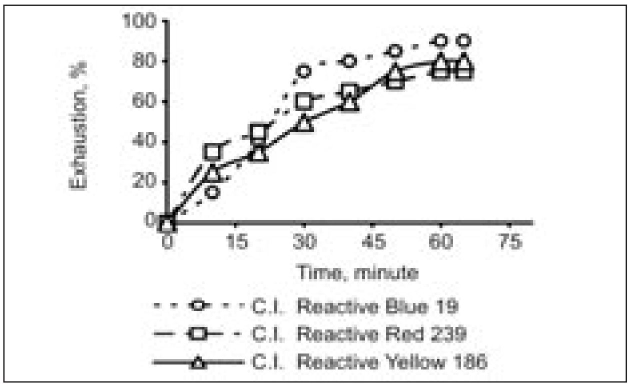

Fig. 5. Exhaust dyeing of the samples with direct dyes

Table 3

CIELAB VALUES OF THE SAMPLES DYED WITH THE REACTIVE AND DIRECT DYES								
	Dyestuff		***L****	***a****	***b****	***C****	***h***	***K/S* max.***
Remazol	C.I. Reactive Blue 19	Untreated	46.44	–3.85	–39.19	39.38	264.39	6.33
		Scoured	45.85	–3.69	–41.15	41.32	264.88	7.12
		Bleached	46.56	–2.91	–41.72	41.82	266.01	6.67
	C.I. Reactive Red 239	Untreated	49.80	58.10	–6.29	58.44	353.83	7.61
		Scoured	49.58	58.45	–6.60	58.82	353.56	7.84
		Bleached	50.03	58.38	–7.50	58.86	353.68	7.45
	C.I. Reactive Yellow 186	Untreated	86.90	–5.76	75.78	75.99	94.35	6.94
		Scoured	86.35	–5.67	77.06	77.27	94.21	7.66
		Bleached	88.77	–6.64	78.26	78.54	94.85	6.49
Remazol (MW dyeing)	C.I. Reactive Blue 19		45.87	–2.47	–41.93	42.00	266.62	6.98
	C.I. Reactive Red 239		49.59	54.29	–8.45	54.94	351.16	6.50
	C.I. Reactive Yellow 186		85.99	–6.69	75.73	76.02	95.05	7.12
Indosol	C.I. Direct Blue 90		44.30	–10.88	–16.63	19.87	236.80	5.77
	C.I. Direct Red 83:1		48.03	31.89	–8.16	32.92	345.64	3.90
	C.I. Direct Yellow 98		83.28	–2.49	32.74	32.83	94.35	3.30

* *K/S values at 600 nm for C.I. Reactive Blue 19. at 430 nm for C.I. Reactive Yellow 186, at 550 nm for C.I. Reactive Red 239, at 630 nm for C.I. Direct Blue 90, at 530 bm for C.I. Direct Red 83:1 and at 410 nm for C.I. Direct Yellow 98*

Table 4

COLOR FASTNESS VALUES OF MATERIALS DYED								
Dye	Dyeing method	Color change	Staining					
			CA	*C*	*P*	*PES*	*P*	*W*
C.I. Reactive Yellow 186	MW	4–5	5	5	4–5	5	5	5
	Conventional	4–5	5	5	4–5	5	5	5
C.I. Reactive Red 239	MW	4–5	5	5	4–5	5	5	5
	Conventional	4–5	5	5	5	5	5	5
C.I. Reactive Blue 19	MW	4–5	5	5	4–5	5	5	5
	Conventional	4–5	5	5	5	5	5	5
C.I. Direct Yellow 98		3–4	5	5	4–5	4–5	4–5	4–5
C.I. Direct Red 83:1		2–3	5	5	4–5	4–5	4–5	4–5
C.I. Direct Blue 90		3	4–5	4–5	4–5	4–5	4–5	3–4

* *CA – cellulose acetate; Co – cottone; PA – polyamide;*
PE – polyester; PAN – acrylic; Wo – wool

Table 5

THE BURSTING STRENGTH AND ABRASION RESISTANCE VALUES OF BAMBOO FABRIC					
Applied process		Bursting strength, kPa		Abrasion resistance, cycle	
Un-dyed	Un-pretreated	351.0		102,000	
	Scoured	330.3	(↓ 6%)	99,00	(↓ 3%)
	Bleached	291.2	(↓ 17%)	93,000	(↓ 9%)
Reactive dyed	Un-pretreated	311.5		81,000	
	Scoured	303.6	(↓ 3%)	75,000	(↓ 7%)
	Bleached	288.7	(↓ 7%)	75,000	(↓ 7%)
Direct dyed		282.5		80,000	

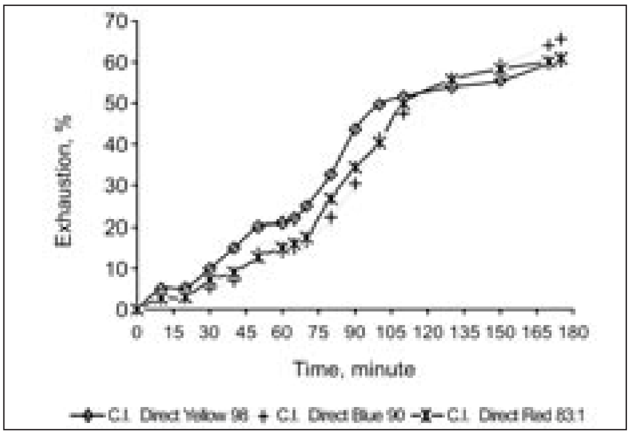

Fig. 6. The direct dye uptakes by bamboo fabrics

direct dyes under atmospheric conditions, and the exhaustion curves are given in figures 4 and 5. The maximum exhaustion values of the C.I. Reactive Blue 19, C.I. Reactive Yellow 186 and C.I. Reactive Red 239 were 90%, 80% and 75% and, with the direct dyes, maximum exhaustion values of 66%, 61% and 60% were achieved for C.I. Direct Blue 90, C.I. Direct Red 83:1 and C.I. Direct Yellow 98 (figure 6).
The color fastnesses to washing and staining of the dyed samples are given in table 4. For all dyed materials, the fastness test results are quite good. The wet and dry rubbing fastness values for all MW and conventional dyed materials are also 5. Table 5 shows the bursting strength and the abrasion resistance results.

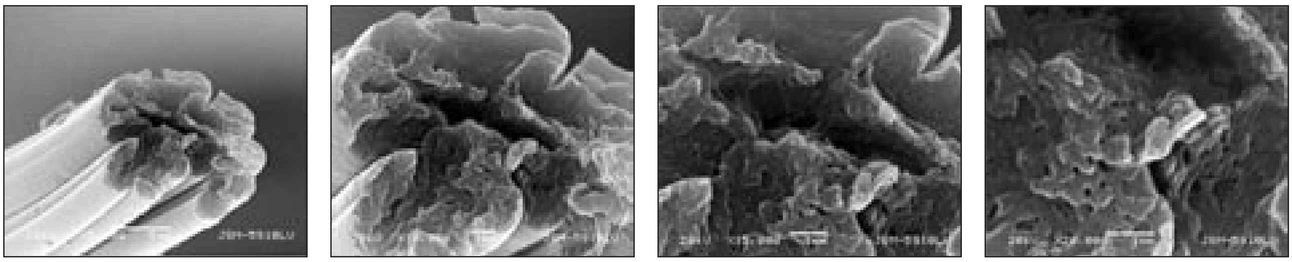
Fig. 7. The cross-sectional SEM images of the un-dyed bamboo fiber. Magnification 5 000 x – 10 000 x – 15 000 x and 20 000 x

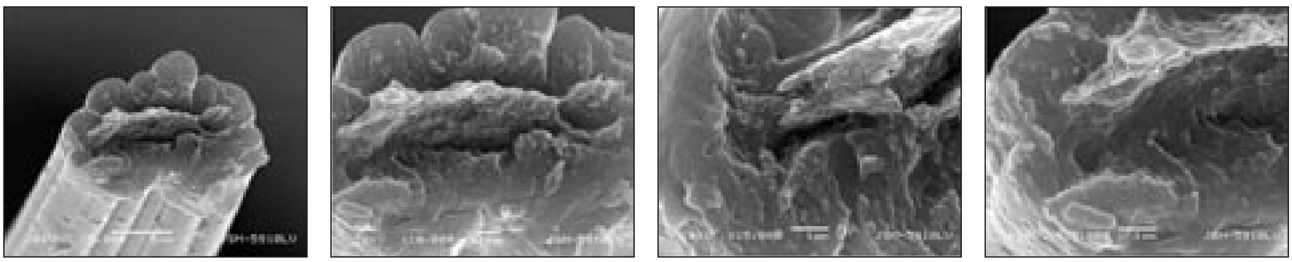
Fig. 8. The cross-sectional SEM images of the dyed bamboo fiber. Magnification 5 000 x – 10 000 x – 15 000 x and 20 000 x

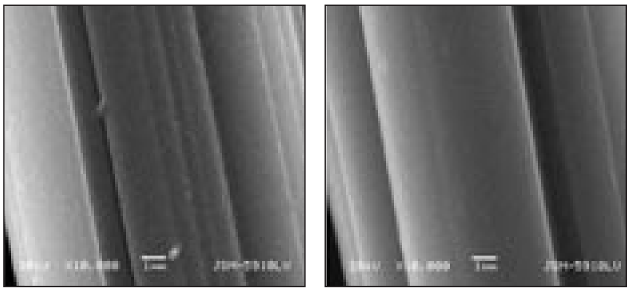

Fig. 9. SEM images of un-dyed and dyed bamboo fibers. Magnification 10 000 x

The SEM images regarding the cross-sectional view of the un-dyed bamboo fibers are given in figures from 7 to 9, compared in terms of magnification levels ranging from 5,000 to 20,000. By observing the SEM images in figure 7 of the 100% bamboo fibers, it was noticed that the cross-section of the bamboo fiber was not circular and filled up with various micro-grooves. The SEM images regarding the longitudinal view of un-dyed and dyed bamboo fibers are given in figure 9. So, it was observed in figure 9 that the surfaces of all the samples were very smooth, no difference being observed between the surfaces of the un-dyed and dyed bamboo fiber samples.

The 'bursting strength test' and the 'abrasion resistance test' results are given in table 5. The percentages in the parentheses indicate the decrease in values of the bursting strength and abrasion resistance, compared to the values of the un-pretreated ones. The abrasion resistance values were slightly decreased after pretreatment and dyeing and slight changes were also observed in the bursting strength of the materials.

CONCLUSIONS

The pretreatment of the regenerated bamboo materials improves the whiteness of the fabric to some degree, but it only slightly enhances the color yield and dye exhaustion. In addition, the un-pretreated materials have better mechanical and fastness properties than the pretreated ones. The exhaustions of reactive dyes are quite good, and the fastness properties of the dyed materials are excellent. However, dyeing with direct dyes, even when a fixing agent is used, needs to be improved, since less color yields and dye exhaustions were achieved, with limited fastnesses. The MW heat dyeing process of the materials is promising, since the materials with good color yields, excellent color fastness and level dyeing are achieved in very short processing times. SEM results show that the fine structure of the material is quite different from the cotton or other regenerated cellulosic, and the good handle and absorbency properties of the regenerated bamboo materials are probably due to the micro-grooves within the fiber.

Acknowledgements

We would like to thank Bilkont A.S. for supplying 100% regenerated bamboo materials; Mr. M. Ilhan for the technical help in taking the SEM photographs of the regenerated bamboo fibers.

BIBLIOGRAPHY

[1] Waite, M. *Sustainable textiles: The role of bamboo and a comparison of bamboo textile properties.* In: Journal of Textile and Apparel, Technology and Management, 2009, vol. 6, issue 2, p. 1

[2] Wang, Y., Gao, X. *The performance of fabric from bamboo fibre.* In: Textile Asia, 2005, vol. 36, issue 6, p. 35

[3] Shen, Q., Liu, D., Gao, Y., Chen, Y. *Surface properties of bamboo fiber and a comparison with cotton linter fibers.* In: Colloids and Surfaces B: Biointerfaces, 2004, vol. 35, p. 193

[4] Büyükakinci, B. Y. *Investigation of the properties of bamboo fibers.* PhD Thesis, Marmara University, Istanbul, 2009

[5] Büyükakinci, B. Y. *Investigation of the internal structure of regenerated bamboo fiber.* In: Tekstil ve Konfeksiyon, 2010, issue 4, p. 277

[6] Xiangyu, X., Yueping W., Xiaodan Z., Guangyin J., Dapeng Y., Shouguo W. *Effects on surface properties of natural bamboo fibers treated with atmospheric pressure argon plasma.* In: Surface and Interface Analysis, 2006, vol. 38, p. 1 211

[7] Yueping, W., Ge, W., Haitao, C., Genlin, T., Zheng, L., Feng, X. Q., Xiangqi, Z., Xiaojun, H., Xushan, G. *Structure of bamboo fiber for textiles.* In: Textile Research Journal, 2010, vol. 80, issue 4, p. 334

[8] Yanping, L., Hong, H. *X-ray diffraction study of bamboo fibers treated with NaOH.* In: Fibers and Polymers, 2008, vol. 9, no. 6, p. 735

Authors:

B. YEŞIM BÜYÜKAKINCI
NIHAL SÖKMEN
ERHAN ÖNER
Marmara University – Faculty of Technical Education
Department of Textile Education
Göztepe, Istanbul – Turkey

Coresponding author:
ERHAN ÖNER
e-mail: eoner@marmara.edu.tr

Dezvoltarea durabilă – formă de creștere economică. Partea a III-a. Proiectarea și simularea standurilor pneumatice destinate testării elementelor textile filtrante*

ANCA BUCUREȘTEANU

DAN PRODAN
DANIELA BUCUR

ABSTRACT – INHALTSANGABE

Sustainable development – form of economic growth. Part III. Design and simulation of the pneumatic stands meant for testing the filtering textile elements

In the paper, the research activity results achieved within the project entitled "Sustainable development enabled by the manufacture and testing of woven textile technical articles meant for clean industrial processes" are presented. For a good functioning of the pneumatic apparatuses, we need the industrial air used to have a certain purity degree. According to the "sustainable development" concept, after the completion of the technological cycle, the pneumatic work medium discharge into the surrounding environment under the form of residual/wasted air represents a highly actual problem. The industrial air filtering should be conducted so that to meet both the requirements needed for a good functioning of the system employed, and the needs resulting from the sustainable development type of conditions. The paper presents the designing concept for a stand meant for testing the textile air filters. So as to check the solutions addressed, simulation methods specific to the pneumatic driven systems and elements were used in the designing stage.

Key-words: sustainable development, textile filters, test stand, pneumatic stand

Nachhaltige Entwicklung – eine Form des Wirtschaftswachstums. III Teil. Pneumatische Ständer für die Prüfung von Textilfiltrierelemente – Entwurf und Simulation

Im Artikel werden die Ergebnisse der Forschungsaktivität in Rahmen des Projektes „Nachhaltige Entwicklung durch Fertigung und Prüfung von gewebten technischen Textilartikeln für reine Industrieprozesse" vorgestellt. Für die gute Arbeitsweise der pneumatischen Apparatur ist es nötig, dass die verwendete Industrieluft einen bestimmten Reinheitsgrad hat. Entsprechend dem Konzept der „Nachhaltigen Entwicklung", hat die Abführung des pneumatischen Mittels als Luft in die Umwelt, nach der Durchführung des technologischen Produktionszyklus, eine besondere aktuelle Bedeutung. Die Filtrierung der Industrieluft muss sowohl den Bedingungen für eine gute Arbeitsweise als auch den Bedingungen für eine nachhaltige Entwicklung entsprechen. Die Arbeit stellt das Fertigungskonzept eines Ständers dar, bestimmt für die Prüfung von Textilluftfiltern. Für die Untersuchung der Lösungen, welche in der Entwurfsphase angesprochen wurden, wurden spezifische Simulationsmethoden für pneumatische Antriebselemente und -systeme angewendet.

Stichwörter: Nachhaltige Entwicklung, Textilfilter, Prüfungsständer, Pneumatisches Ständer

IMPURIFICAREA MEDIULUI PNEUMATIC

Mediul pneumatic utilizat în instalațiile de acționare pneumatice este aerul industrial. Impurificarea aerului are următoarele cauze:

- poluarea aerului atmosferic aspirat de compresoare și folosit în instalații;
- prezența în conductele rețelei de distribuție a aerului industrial și a conductelor de alimentare a unor particule poluante – apă, vopseluri, șpan etc.;
- uzura pieselor aflate în mișcare relativă, mai ales a celor din compresor și din alte elemente ale instalațiilor de acționare pneumatică (distribuitoare, cilindri pneumatici, elemente logice etc.);
- prezența umezelii în agentul pneumatic, care provoacă corodarea chimică a suprafețelor active și care, la temperaturi scăzute, determină înghețul și blocarea pieselor aflate în mișcare.

Aerul industrial din mediul ambiant normal al uzinelor conține în jur de 50 mg/m^3 sau 10^6–10^8 particule/minut; în cazul încăperilor curate acest număr ajunge la 10^5–10^6 particule/minut; ponderea poate crește până la 200 mg/m^3 sau 10^8–10^{10} particule/minut, în atelierele de turnătorie.

În ceea ce privește umezeala, aceasta depinde de umiditatea relativă și de temperatura mediului ambiant. Capacitatea aerului de a absorbi umezeala se mărește odată cu creșterea temperaturii și scade odată cu creșterea presiunii. Iată câteva semnificative: în 10 m^3 aer saturat se află 0,2 dm^3 de apă la 4°C, 0,35 dm^3 de apă la 40°C și circa 4,5 dm^3 de apă la 70°C [1].

ELEMENTE FILTRANTE PENTRU AERUL INDUSTRIAL

Filtrarea aerului constituie o condiție de funcționare nu numai a instalațiilor pneumatice, dar și a celor în care aerul nu este doar un mediu fluid al instalațiilor de acționare pneumatică, ci și un agent de răcire a altor tipuri de instalații. Filtrele pneumatice pot fi clasificate în: filtre uscate, filtre umede și filtre separatoare.

Filtrele uscate sunt alcătuite din hârtie filtrantă pliată. Uneori, această hârtie poate avea un suport alcătuit dintr-o sită metalică și o manta de protecție.

Filtrele umede se bazează pe o structură de sită sau celulară cu pori relativ mari, impregnați în ulei. Efectul de filtrare se produce atât prin reținerea contaminanților, datorită dimensiunii porilor, cât și prin aderența lor la particulele de ulei. Elementul filtrant poate fi alcătuit din hârtie filtrantă, împletituri textile (fibroase) sau materiale plastice pluricelulare.

Separatoarele pneumatice funcționează pe principiul separării inerțiale a particulelor solide și lichide. Acestea se folosesc, de obicei, ca primă treaptă de filtrare pentru reținerea particulelor mari [2].

ÎMPLETITURI FIBROASE

Aceste împletituri, care acționează pe baza mecanismului filtrării „în profunzime", sunt formate din mai multe

* Part III. Part I has been published in Industria Textilă magazine, 2008, vol. 59, issue no. 2, p. 69.
Part II has been published in Industria Textilă magazine, 2009, vol. 60, issue no. 5, p. 279

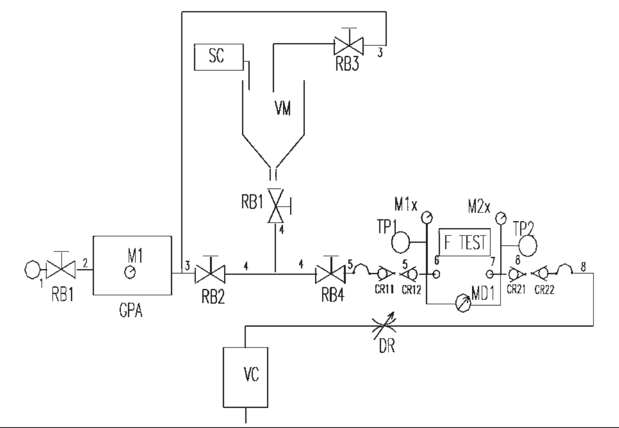

Fig. 1. *1* – sursa pneumatică; *RB1, RB2, RB3, RB4* – robinete; *GPA* – grup preparare aer; *M1, M1x, M2x* – manometre; *SC* – sistem de colmatare; *CR11, CR12, CR21, CR22* – cuple rapide; *DR* – drosel; *VC* – vas de recuperare; *TP1, TP2* – traductoare de presiune; *MD1* – manometru diferențial; *VM* – vas de amestec; *F TEST* – filtru testat

fibre fine, având diametrul cuprins între 0,5 și 30 μm, în funcție de materialul din care sunt alcătuite. Așezate aleatoriu, aceste fibre formează pori, prin care trece fluidul impur. Fibrele care alcătuiesc materialul filtrant pot fi: celulozice, din bumbac, din microfibre de sticlă sau sintetice (din relon, polipropilenă etc.).

Finețea de filtrare este în funcție de diametrul fibrelor. Cu cât diametrul este mai mic, împletitura este mai compactă, porii sunt mai mici și, prin urmare, se realizează o finețe de filtrare mai bună. De exemplu, microfibrele de sticlă asigură o finețe de filtrare mai mică decât fibrele celulozice. Aceste medii filtrante permit realizarea unui material filtrant cu grosimea cuprinsă între 0,25 și 2 mm. Pentru a îmbunătăți rezistența mecanică redusă a acestor medii filtrante, acestea se impregnează cu rășini fenolice, epoxidice sau acrilice.

Deșeurile de bumbac, lână sau fibre sintetice (nylon, polietilenă, polipropilenă, acrili, poliesteri etc.) pot fi folosite pentru realizarea unor filtre „în profunzime“.

Filtrele din împletituri fibroase prezintă o serie de avantaje, și anume posibilitatea realizării unei fineți de filtrare scăzute (5–10 μm) și a unor costuri reduse. Există, însă, și unele dezavantaje, cum ar fi: rezistența mecanică redusă, permeabilitatea scăzută, imposibilitatea de a fi spălate sau regenerate [3].

STAND DE TESTARE A ELEMENTELOR FILTRANTE TEXTILE PENTRU GAZE

Testarea filtrelor cuprinde totalitatea probelor care se realizează asupra elementelor filtrante, aceste probe fiind reglementate prin norme internaționale aplicabile și în țara noastră.

Schema unui stand de încercare a filtrelor pentru gaze este prezentată în figura 1. Având în vedere tipurile de filtre pentru gaze utilizate în mod frecvent, s-au stabilit următoarele caracteristici tehnice pentru acest stand:

- presiunea maximă de lucru – 7 bari;
- mediul de lucru – aer (sursa – un compresor independent sau o rețea de aer comprimat).

La proiectarea standului s-au utilizat tipurile de aparatură, comercializată de diverse firme [4].

Determinările specifice care se pot efectua pe acest stand sunt: căderea de presiune la debitul sursei și determinarea gradului și a fineții de filtrare.

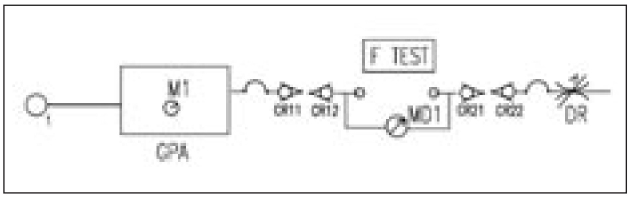

Fig. 2. *1* – sursa pneumatică; *GPA* – grup preparare aer; *M1* – manometru; *MD1* – manometru diferențial; *CR11, CR12, CR21, CR22* – cuple rapide; *DR* – drosel; *F TEST* – filtru testat

Modul de lucru cuprinde următoarele etape:

- se deschide robinetul de alimentare RB1;
- se închid complet robinetele RB2 și RB3;
- se comută regulatorul grupului de preparare GPA la presiunea maximă de lucru, valoarea acestei presiuni putând fi vizualizată pe manometrul M1;
- se închide robinetul RB1.

Determinarea caracteristicii debit-cădere de presiune se realizează în următoarea succesiune:

- se montează filtrul de testat (F.TEST) cu ajutorul cuplelor rapide CR11, CR12, CR21 și CR22;
- se deschid robinetele RB2 și RB4;
- droselul DR permite reglarea debitului de tranzit.

Presiunea la intrarea în filtrul testat se vizualizează pe manometrul M1x și pe traductorul TP1. Presiunea la ieșirea din filtru se vizualizează pe manometrul M2x și pe traductorul TP2. Manometrul diferențial MD1 permite citirea directă a căderii de presiune pe filtrul testat. Aerul, la presiunea reglată, trece prin filtrul F.TEST, având debitul reglat cu droselul DR și este evacuat în atmosferă prin vasul de recuperare VC.

Determinarea gradului și a fineții de filtrare se realizează prin închiderea robinetului RB2, deschiderea robinetelor RB1, RB3 și RB4 și încărcarea sistemului de contaminare, aerul contaminat din vasul VM trecând prin filtrul testat. Se poate verifica eficiența filtrului prin determinarea randamentului filtrului.

SIMULAREA FUNCȚIONĂRII STANDULUI DE ÎNCERCARE A FILTRELOR PNEUMATICE. DETERMINAREA CĂDERII DE PRESIUNE

O fază importantă înainte de realizarea prototipului o constituie simularea instalației proiectate. Cu această ocazie, pot fi efectuate corecțiile necesare în ceea ce privește caracteristicile aparaturii folosite. Pentru simularea funcționării standului s-a recurs la pachetul de programe AUTOMATION STUDIO. Programul permite reconstrucția schemei din figura 1, păstrându-se numai elementele active, care influențează caracteristicile sistemului. În aceste condiții, schema utilizată pentru simulări, păstrând notațiile din figura 1, este prezentată în figura 2 [5].

Urmează apoi simularea colmatării filtrului testat, cu determinarea căderii de presiune pe acesta, folosind manometrul diferențial MD1. Manometrul M1 indică presiunea la sursa pneumatică. Sursa pneumatică *1* poate fi un compresor sau o rețea de aer industrial. Se consideră că această sursă furnizează aer la o presiune constantă de 8 bari. Regulatorul din grupul de preparare a aerului GPA se reglează la 6 bari.

Pentru început, filtrul se consideră ca fiind nou. În aceste condiții se obțin caracteristicile de presiune prezentate în figura 3.

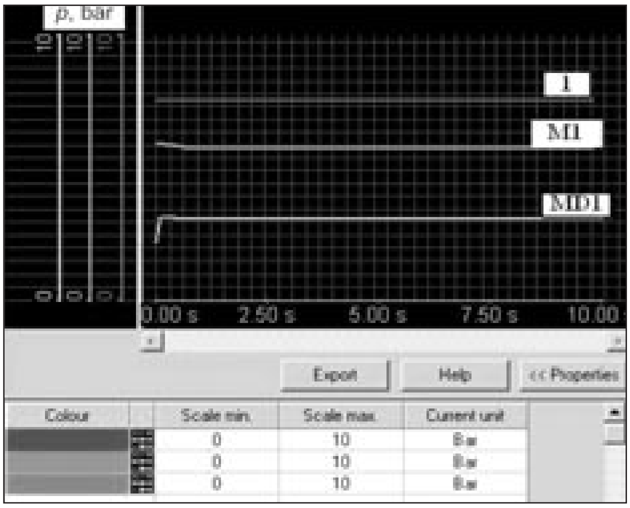

Fig. 3

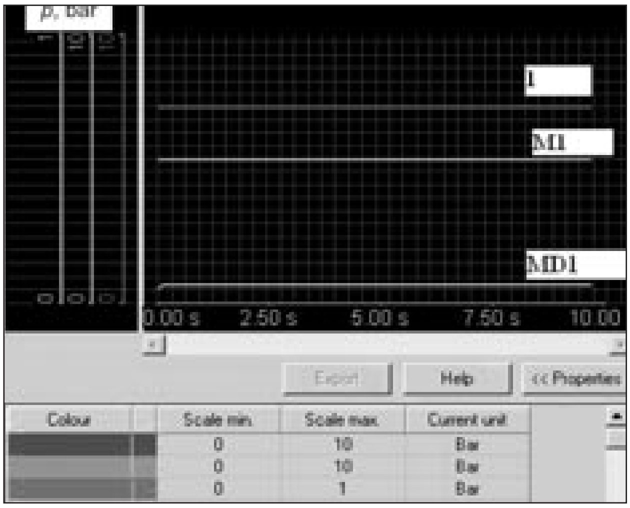

Fig. 4

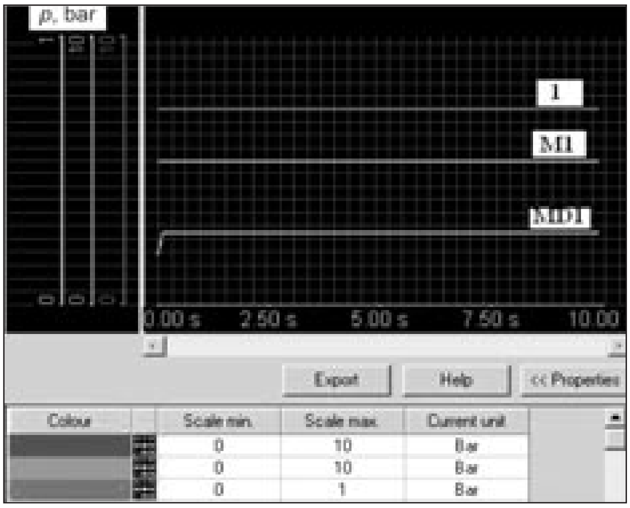

Fig. 5

Căderea de presiune pe filtru este nesemnificativă, având valoarea de aproximativ 1/20 bari. Dacă se simulează o colmatare de aproximativ 50% din valoarea acceptabilă, se obțin caracteristicile prezentate în figura 4. Căderea de presiune pe filtrul testat este de 5/20 bari, în condițiile în care s-au folosit aceleași surse și același reglaj la regulatorul de presiune. Dacă se continuă colmatarea filtrului la 80%, apropiindu-ne de compromiterea acestuia, se observă o creștere considerabilă a căderii de presiune (fig. 5). Căderea de presiune este, în acest caz, de 3 bari. În cazul colmatării filtrului, căderea de presiune crește, existând riscul distrugerii elementului filtrant sau chiar obturarea circuitului.

CONCLUZII

Cunoașterea și rezolvarea problemelor impuse de procesele de filtrare a aerului industrial sau rezultat din procesele industriale, dar și de protejarea mediului, presupun elucidarea a numeroase aspecte de natură teoretică și practică legate de producerea aerului industrial, de tipurile de elemente filtrante și de modul de utilizare a acestora [6].

Filtrele realizate din materiale textile sunt utilizate în combinații cu alte tipuri de elemente filtrante. Pentru determinarea caracteristicilor acestor elemente filtrante sunt necesare standuri care să permită realizarea unui număr cât mai mare de măsurători. Standurile de acest tip conțin elemente pneumatice moderne, produse de firme specializate [7].

În ultimii zece ani, proiectarea clasică, la planșetă, a fost înlocuită cu proiectarea asistată de calculator. Din păcate, sunt foarte multe cazuri în care conceptul de proiectare asistată este greșit înțeles. Astfel, se consideră că desenarea și realizarea unor baze de date cuprinzând informații privind caracteristicile componentelor, prețurile, furnizorii etc. reprezintă „proiectare asistată“. Nici chiar realizarea unor programe de animație, de altfel foarte spectaculoase, nu se poate considera a fi „proiectare asistată“.

Etapele mai sus menționate fac parte din „proiectarea asistată“, dar acestea trebuie completate cu încă două, și anume modelarea și simularea.

Modelarea reprezintă o serie de ecuații sau sisteme de ecuații, algebrice sau diferențiale, liniare sau nu, care descriu funcționarea elementului sau sistemului studiat. În aceste modele trebuie definite foarte clar care sunt mărimile de intrare – presupuse ca fiind cunoscute, și cele de ieșire – ce urmează a fi determinate.

Proiectarea asistată nu se poate realiza numai în fața calculatorului. O serie de factori și coeficienți necesari proiectantului nu sunt furnizați nici de către producătorul de aparate pneumatice și nici chiar în literatura de specialitate. Aceștia trebuie să fie determinați experimental, în laboratoare dotate cu aparatură specializată.

După stabilirea schemelor de acționare prin simulare, se pot determina elementele reale, cu ajutorul cărora se pot realiza obiectivele propuse.

BIBLIOGRAFIE

[1] Tureac, I. ș. a. *Dezvoltarea durabilă a produselor în construcția de mașini.* Editura Universității Transilvania, București, 2006
[2] Bucureșteanu, A., Isar (Bucur), D. *Elemente și sisteme pneumatice. Aplicații industriale.* Editura Certex, București, 2007, ISBN 978-973-1716-06-0
[3] Medar, S., Ionescu, F. *Filtre pentru acționări hidraulice și pneumatice.* Editura Tehnică, 1986, București, C.Z 66.067.3

[4] Prodan, D. *Mașini-unelte. Modelarea și simularea elementelor și sistemelor hidrostatice.* Printech Publishing House, 2006, ISBN 973-718-572-2
[5] Bucureșteanu, A., Isar (Bucur), D. *Dezvoltarea durabilă - formă de creștere economică. P. I. Concepte și principii de dezvoltare durabilă.* În: Industria Textilă, 2008, vol. 59, nr. 2, p. 69
[6] Prodan, D., Bucureșteanu, A., Bucur, D. *The sustainable development – a form of economic improvement. Part II. Design and simulation of stands meant for testing the textile filter elements.* În: Industria Textilă, 2009, vol. 60, nr. 5, p. 279

Autori:

Dr. ing. ANCA BUCUREȘTEANU
Dr. ing. DAN PRODAN
Universitatea Politehnica București
Splaiul Independenței nr. 313
060042 București
e-mail: ancab66@yahoo. com

Cerc. șt. gr. II drd. ing. DANIELA BUCUR
Institutul Național de Cercetare-Dezvoltare
pentru Textile și Pielărie
Str. Lucrețiu Pătrășcanu nr. 16
030508 București
e-mail: certex@ns.certex.ro

VA AVEA LOC...

TECHTEXTIL 2011

Târgul Comercial Internațional pentru Textile și Nețesute Tehnice, care va avea loc la Frankfurt am Main, în perioada 24–26 mai 2011, se va concentra asupra utilizării eficiente a energiei, materialelor și resurselor – o temă majoră în producția de utilaje textile.

În acest an, furnizorii de tehnologii vor expune la Techtextil un număr mare de soluții privind eficiența energetică și sustenabilitatea producției.

Oerlikon Textile oferă soluții universale în domeniul utilajelor textile și al instalațiilor, stabilind, prin inovațiile lor, noi standarde ale producției globale de textile. Cercetarea-dezvoltarea sunt domenii prioritare, în care, timp de ani de zile, s-a investit peste 7% din profit. Unul dintre rezultate obținute îl constituie programul pentru eficiență energetică „e-save“, ce se evidențiază printr-o economie de excepție a resurselor în timpul proceselor de producție.

Oerlikon Neumag oferă cel mai mare portofoliu mondial de tehnologii în domeniul producerii de nețesute. Recent, *Oerlikon Neumag* – din Austria, a construit numeroase plăcuțe cu ace, pe baza rezultatelor obținute cu ajutorul noului software implementat, cu care poate fi simulată geometria de penetrare a acelor și, astfel, pot fi optimizate modelele de imprimare pentru ace. În acest fel, se pot controla rigiditatea și elasticitatea materialului nețesut.

J. Zimmer Maschinenbau GmbH, din Klagenfurt/Austria, specializată în mașini de peliculizat ce utilizează materii fluide, sub formă de pastă și spumă, va expune o mașină de peliculizat multifuncțională, pentru paste pe bază de apă, dar și pentru tipuri de spumă stabilă și instabilă.

Compania *Karl Mayer* din Obertshausen, cu sucursala *Karl Mayer Malimo,* este un renumit actor global, ce produce utilaje flexibile, de înaltă eficiență, pentru realizarea de textile funcționale și, în același timp, creează noi posibilități de aplicare și noi piețe pentru produsele tricotate. Un nou tip de mașină Rașel, cu magazin de alimentare inclus, produce structuri tip plasă și materiale tricotate plane, din fire de înaltă performanță, cu o greutate mică, pentru a fi utilizate, în principal, în domeniul publicității imprimate.

În domeniul materialelor compozite, noua generație de mașini *Malitronic Multiaxial* oferă atât o îmbunătățire a parametrilor ce determină performanța, cât și o creștere a gradului de eficiență și de flexibilitate. Straturile liate duroplastic și termoplastic sunt deja utilizate pentru consolidarea caroseriilor auto și a componentelor de avion, paletelor de rotor ale unor echipamente de generare a energiei eoliene, echipamentelor sport și componentelor mobile ale unor mașini, dar și în industria construcțiilor, ca înveliș de consolidare a betonului ranforsat cu textile.

Problematica legată de acest domeniu va fi abordată în cadrul ***Simpozionului Techtextil***, ce va avea loc în paralel cu târgul. Prezentarea *„Cerințe ale unei producții reproductibile de materiale 3D țesute, destinate materialelor compozite, prin utilizarea de fire hibride din fibre de sticlă și termoplastice“,* susținută de Universitatea Tehnică din Dresda, abordează tematica dezvoltării unui lanț de procese, prin care noul tip de materiale 3D să poată fi țesut, prin utilizarea de fire hibride, din fibre de sticlă și polipropilenă, laminate, tăiate conform unor preformate, amortizate și presate termic în formă. Pentru aceasta, a fost proiectat și brevetat cu succes un nou dispozitiv de laminare, tăiere și depunere a materialelor 3D cu structură tip plasă pătrată.

De asemenea, va fi prezentată o nouă tehnologie, creată pentru a „revoluționa producția de frânghii“. Spre deosebire de metodele tradiționale de producție, noua tehnologie *MultiSphere* oferă producătorilor de țesături tip bandă îngustă oportunitatea lărgirii gamei de produse, iar producătorilor de frânghii niveluri crescute ale producției, la costuri mai mici.

Techtextil și Texprocess

În acest an, ***Texprocess*** – târgul comercial internațional de top în domeniul prelucrării textilelor și a materialelor flexibile, va fi organizat, pentru prima dată, în același timp cu ***Techtextil***. În timp ce, la *Techtextil,* furnizorii de tehnologii de producție și prelucrare, destinate textilelor tehnice din grupul „Tehnologie, Procese, Accesorii“, sunt cei care își vor prezenta produsele și serviciile, la *Texprocess* cei care vor expune vor fi furnizorii de tehnologii de producție pentru industria de îmbrăcăminte.

În paralel cu Techtextil, va avea loc ***Material Vision*** – conferință și expoziție având ca tematică materialele destinate dezvoltării, proiectării și arhitecturii produselor.

Cele trei târguri comerciale, de importanță majoră pentru sectorul textil, care au loc în același timp și în același loc, oferă sinergii semnificative și prezintă un mare interes atât pentru expozanți, cât și pentru vizitatori, din perspectiva unor considerente precum costul și timpul.

Comunicat de presă. Messefrankfurt, Techtextil, februarie 2011

Predicting the tensile strength of polyester/viscose blended open-end rotor spun yarns using artificial neural network and statistical models

ERDEM KOÇ OGÜZ DEMIR YÜREK

REZUMAT – ABSTRACT – INHALTSANGABE

Estimarea rezistenței la tracțiune a firelor filate cu rotor și capăt liber, din poliester-viscoză, prin utilizarea rețelei neuronale artificiale și a modelelor statistice

În acest studiu au fost dezvoltate o rețea neuronală artificială (ANN) și un model statistic, pentru a determina rezistența la tracțiune a firelor filate cu rotor cu capăt liber, realizate dintr-un amestec de poliester/viscoză. Au fost produse șapte benzi din poliester-viscoză, cu diferite raporturi ale amestecului. Aceste benzi au fost realizate la patru valori diferite ale vitezei rotorului și ale fineții firelor. Pentru determinarea proprietăților de tracțiune ale acestor fire, au fost dezvoltate o rețea perceptron multistrat de propagare inversă și un model de regresie încrucișată a procesului de amestecare, având două raporturi ale amestecului din poliester-viscoză și două variabile ale procesului de realizare - finețea firului și viteza rotorului. În concluzie, atât ANN, cât și modelul statistic au oferit rezultate satisfăcătoare, mai fiabile fiind, totuși, predicțiile ANN. Deși capacitatea de predicție a modelelor statistice este la un nivel satisfăcător, datorită simplității utilizării, acestea pot fi folosite pentru estimarea rezistenței firelor.

Cuvinte-cheie: filare cu rotor și capăt liber, poliester, viscoză, amestec, rezistență la tracțiune, design tip rețea simplex, rețea neuronală artificială

Predicting the tensile strength of polyester/viscose blended open-end rotor spun yarns using the artificial neural network and statistical models

In this study, an Artificial Neural Network (ANN) and a statistical model were developed to predict the tensile strength of polyester/viscose blended open-end rotor spun yarns. Seven different blend ratios of polyester/viscose slivers were produced and these slivers are manufactured with four different rotor speed and four different yarn counts in the rotor spinning machine. A Back Propagation Multi Layer Perceptron (MLP) network and a mixture process crossed regression model with two mixture components (polyester and viscose blend ratios) and two process variables (yarn count and rotor speed) were developed to predict the tensile properties of polyester/viscose blended open-end rotor spun yarns. In conclusion, both ANN, and the statistical model have given satisfactory predictions; however, the predictions of ANN gave relatively more reliable results than those of the statistical models. Since the prediction capacity of statistical models is also obtained as satisfactory, it can also be used for the strength prediction of yarns, because of its simplicity and non-complex structure.

Key-words: OE-rotor spinning, polyester, viscose, blend, tensile strength, simplex lattice design, artificial neural network

Schätzung des Zugwiderstandes der Polyester-Viskose Offenendspinngarne durch Anwendung künstlicher Neuronalnetze und statistischer Modelle

In dieser Untersuchung wurde ein *künstliches Neuronalnetz (ANN) entwickelt sowie ein statistisches Modell für die Bestimmung des Zugwiderstandes der Polyester-Viskose Mischungsgarne, produziert auf Offenendspinnmaschinen. Es wurden sieben Polyester-Viskose Bänder mit unterschiedlichen Mischungsverhältnissen gefertigt. Diese Bänder wurden bei vier unterschiedlichen Rotorgeschwindigkeiten und Garnfeinheiten produziert. Für die Bestimmung der Zugeigenschaften dieser Garne, wurde ein Multi Layer Perceptron (MLP) – Netz und ein gekreuztes Regressionsmodell, mit den beiden Kreuzkomponenten (Polyester und Viskose Mischungsverhältnisse) und zwei Prozessvariablen (Granfeinheit und Rotorgeschwindigkeit) entwickelt. Schlussfolgernd resultierten zufriedenstellende Prädiktionsergebnisse sowohl vom ANN als auch vom statistischen Modell. Weil die erhaltene Prädiktionskapazität der statistischen Modelle auch zufriedenstellend ist, kann sie auch für die Zugfestigkeitprädiktion der Garne angewendet werden, dank ihrer Einfachheit und nicht-komplexer Struktur.*

Stichwörter: Offenendspinnen, Polyester, Viskose, Mischung, Zugwiderstand, Simplex Netzstruktur, künstliches Neuronalnezwerk

Two or more different types of fibres can be blended at different percentages in order to improve the appearance, performance, quality, comfort and of the fabric and the performance of the yarns produced, such as: tensile strength, elongation, hairiness, yarn imperfections, unevenness etc. Tensile strength is one of the most important parameter of yarns, which directly affects the fabric features and the performance of the processes such as winding, weaving, and knitting. The strength and elongation properties of yarns produced can be predicted, by different prediction methods, by means of the blend ratio of fibres and production parameters of the yarn spinning machines.

There are various studies carried out on the prediction of the mechanical properties of yarns by theoretical, statistical, mathematical and artificial neural network models. Because of the nonlinearity and having better capacity of prediction performance, generally, ANN gave more reliable results than other models in these studies.

Cheng & Adams [1] developed an ANN for predicting the strength of cotton yarns. The HVI test results were used for training the network, and the yarn strength prediction was carried out by the cotton fibre properties. Ramesh, Rajamanickam & Jayaraman [2] also developed an ANN model by introducing the yarn count, blend and front-and-back nozzle pressures on an air jet spinning machine as input parameters, in order to predict the tensile properties (strength and elongation). The prediction errors of this model were small compared to the standard deviation of experimentation.

Majumdar & Majumdar [3] presented a comparative study of three modelling methodologies (mathematical, statistical and artificial neural network models) for predicting the breaking elongation of ring-spun cotton yarns. Constituent cotton fibre properties and yarn counts are determined as input parameters to those systems, and the breaking elongation is taken as an output parameter. The prediction capability of those systems is compared and it is found that ANN gives the best results, compared to the mathematical and statistical models.

Cheng & Lam [4] also investigated and compared the physical properties of spliced yarns by regression and

Table 1

THE PROPERTIES OF POLYESTER AND VISCOSE FIBRES				
Fibre	Length, mm	Fineness, dtex	Strength, cN/tex	Elongation, %
Polyester	38	1.6	55.42	22.21
Viscose	40	1.7	30.18	26.49

ANN techniques. Strength, bending, abrasion and appearance properties of the spliced yarns are modelled by both those techniques and, in conclusion, ANN results gave a precise and accurate prediction, compared to the regression models.

The tensile strength and yarn count properties of melt spun fibres are predicted by an ANN model [5] where extruder screw speed, gear pump and gear speed were introduced as input parameters, and the strength and yarn count were determined as output parameters. The ANN results gave a satisfactory prediction for these parameters.

A comparison is carried out of the linear regression models and ANN, for the prediction of tensile properties of the 100% cotton ring-spun yarn [6]. The prediction of hairiness and unevenness is also investigated in the second part of this study [7]. The results indicated that ANN is a more powerful tool than the linear regression models.

Different models were used [8], such as linear and linearised regression, non-linear multiple regression models, as well as ADALINE and two layer perceptron (*MLP*) artificial neural networks for predicting the polyester/cotton blended open-end rotor-spun yarn parameters, such as tenacity, irregularity of yarn's mass hairiness, number of yarn faults. It was shown that MLP networks gave the best results among these models.

A back-propagation artificial neural network was used [9] to develop a model relating to cotton fibre properties and micro-spun yarn lea CSP. Fibre properties, such as span length, bundle strength, fineness, breaking elongation, uniformity ratio and percentage of mature fibres have been studied and it was observed that the predictions of ANN were more accurate than those obtained from the regression models.

The capability of the artificial neural networks and multiple linear regression methods to model the tensile properties of cotton-covered nylon core yarns based on process parameters was investigated [10]. The developed models were assessed by verifying the mean square error (*MSE*) and the correlation coefficient (*R*-value) for the test data prediction. The results indicated that the artificial neural network algorithm has better performance, in comparison with multiple linear regressions.

A statistical model for the strength and elongation properties of cotton/polyester blended open-end rotor-spun yarns was introduced [11] and this model gave a reliable prediction on the related yarn properties.

A statistical model was developed [12] to predict the important yarn quality characteristics derived from the cotton fibre properties that were measured by means of an HVI system. Linear multiple regression methods were used for the estimation of yarn quality characteristics. Yarn count, twist and roving properties – all had considerable effects on the yarn properties and therefore these parameters were selected as predictors. In conclusion, the regression equations derived from the analysis of variance were significant at the alpha = 0.01 significance level.

A statistical and ANN models were developed [13] for assessing and predicting the unevenness of polyester/viscose blended open-end rotor-spun yarn, of which the statistical model developed gave more reliable results than those of ANN. The mechanism and/or prediction of the breaking elongation of polyester/viscose blended open-end rotor-spun yarns was performed in another study [14] by using the statistical and ANN models and it was concluded that ANN results are more reliable than those of the statistical models.

Using the ANN method in textiles, especially for the prediction of yarn tensile properties, has been reported in journals since 1993 and there are various studies comparing ANN and the statistical models. It is generally found that ANN has better prediction performance in comparison to the statistical models in these studies. Moreover, it is observed that the regression estimations of the statistical models in these studies were as of the linear and/or multiple regression models. However, the prediction capacity of the linear regression equations could be low, since obtaining low correlation coefficient (R), R^2 and adjusted – R^2 values, which are very important parameters for determining the regression equation, as well as for the prediction performance of the statistical models, as expected.

In this study, an ANN model and a statistical model are developed, in order to predict the tensile strength of polyester/viscose blended OE-rotor spun yarns. The blend ratio, yarn count and the rotor speed are selected as input parameters, and the tensile strength of the yarns is determined as output parameter for the back propagation feed forward ANN model. Also, a simplex mixture process crossed-regression model with two mixture components (polyester and viscose blend ratios) and two process variables (yarn count and rotor speed) is also developed to predict the tensile strength of polyester/viscose blended open-end rotor-spun yarns. It is concluded that ANN gave relatively more reliable results in comparison to the statistical models. However, since the prediction capacity of the statistical models is also obtained as satisfactory, statistical models can also be used for yarn strength prediction, because of its non-complex structure.

EXPERIMENTAL STUDY

Sliver production

Polyester and viscose fibres are selected for the blending components of sliver produced. The length, fineness, tensile strength (cN/tex) and tensile elongation (%) properties of polyester and viscose fibres are indicated in table 1. The strength tests of these fibres were carried out in Instron-4301 and the results indicated in the table are the average of 15 experiments. Seven different polyester/viscose blended slivers were produced in different proportions. The fibres are opened and blended in specific machines. Then, the blended fibres are carded and two-passage drawing is applied. The blend proportion and count of slivers produced are listed in table 2. All slivers are produced as

Table 2

THE PROPERTIES OF POLYESTER AND VISCOSE FIBRES				
Sliver no.	Blend proportion, %		Sliver count	
	Polyester	Viscose	Ne	tex
1	0	100	0.150	3933.3
2	20	80	0.150	3933.3
3	35	65	0.150	3933.3
4	50	50	0.150	3933.3
5	65	35	0.150	3933.3
6	80	20	0.150	3933.3
7	100	0	0.150	3933.3

Ne 0.150 and the corresponding direct counts are determined as 3933.3 tex.

Yarn production

Schlafhorst Autocoro rotor-spinning machine is used in different rotor speeds by feeding seven types of slivers produced, simultaneously. Table 3 shows the open-end yarn production plan. Yarns are produced at four different rotor speeds and four different yarn counts in indirect yarn counts (Ne); however, it is also evaluated in terms of the direct count system (tex), as seen in the table. Two replications are made in order to reduce the error in production. The seven different blend ratios of slivers are fed into the rotor-spinning machine simultaneously for one production parameter. The total number of bobbins produced can be calculated by taking into consideration the number of slivers (*7*), the number of yarn counts (*4*), the number of rotor speeds (*4*), as follows: 7 x 4 x 4 x 2 = 224. However, there are 112 different types of bobbins because of the replication. Rotor speed and yarn count are determined as variables, whereas opener type and speed, rotor diameter, navel type and twist factor are taken as constant parameters. The features of the constant parameters are shown in table 4.

The tensile strength tests of polyester/viscose blended yarns produced were carried out in Uster Tensorapid 3, in standard atmospheric conditions (20 ± 2°C temperature and 65% ± 2 relative humidity). The replication results of bobbins tensile properties are used in the statistical model, while the average of the tensile properties of these replicated bobbins are evaluated for the ANN model to be developed.

MODELS DEVELOPED

The artificial neural network model

In this study, back propagation feed-forward Multi-Layer Perceptron (MLP) network was used. Since the network weights are initialized to random values, it is unlikely that reasonable outputs will result before training. The weights are adjusted to reduce the error by

Table 3

OPEN-END ROTOR YARN PRODUCTION PLAN			
Count		Rotor speed, rpm	Replication
Ne	tex		
16	37	50.000	2
20	30	60.000	2
24	25	70.000	2
28	21	80.000	2

Table 4

THE PROPERTIES OF CONSTANT PARAMETERS	
Parameter	Value
Opener speed	8 000 rpm
Opener type	OS21
Twist factor, a_e	3.8
Rotor diameter	33 mm
Rotor type	TI33
Navel	KN4

propagating the output error backward through the network. This process is where the back propagation neural network gets its name from and is known as the backward pass. The training set is repeatedly presented to the network and the weight values are adjusted until the overall error is below a predetermined value. Since the Delta rule follows the path of greatest decent along the error surface, local minima can impede training. The momentum term compensates for this problem to some degree [15].

One of the most crucial aims of the Back Propagation Network (BPN) is to minimise the error function by using the gradient steepest descent method. The error function is:

$$E = \frac{1}{2}\sum_{k}\left(Y_{dk} - Y_k\right)^2 \qquad (1)$$

where:

Y_{dk} is the desired output;

Y_k – the calculated output value of the output layer.

The weights updated themselves by using the error function as:

$$\Delta w_{ij} = -\eta \frac{\partial E}{\partial w_{ij}} \qquad (2)$$

Here η is the learning rate (momentum used in this study) and it determines the performance of the learning capability of the network [5].

Sigmoid function was used as activation function in this study. Sigmoid function is equation (3), as follows:

$$f(x) = \frac{1}{1 + e^{-x}} \qquad (3)$$

The average in the tensile strength properties of the replicated bobbins is evaluated (total 112) and divided into two groups, namely learning and testing. 75 percent of total data is selected randomly and determined as learning data (84 samples) and the residual 25 percent of total data is determined as testing data (28 samples). In this study, a three-layered network structure was used, which is composed of the input, hidden and output layers. The number of the hidden layer node is determined as 40, the learning rate and momentum were optimised at 0.01 and 0.2, respectively, for the tensile strength (cN/tex). The model built in this study can be seen in figure 1, schematically.

Statistical model

Since the factors are the components of the mixture (blend) ingredients, the statistical analysis is carried out by considering the simplex lattice design. However, there are two process variables independent from this

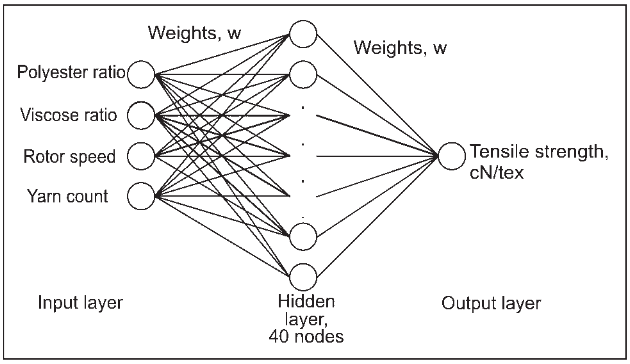

Fig. 1. The ANN model for the tensile strength of the yarns produced

blend (yarn count and rotor speed). Thus, the mixture process crossed-regression model with two mixture components (polyester and viscose blend ratios) and two process variables (yarn count and rotor speed) is developed to predict the tensile strength of polyester/viscose blended open-end rotor-spun yarns. Simplex designs are used to study the effects of the mixture components on the response variable [16].

Design Expert software was used in this study for statistical purposes. The test results of the tensile strength of polyester/viscose blended OE rotor-spun yarns were introduced to the software to analyse the mixture process crossed-design. The software has given suggestions for the tensile strength of yarns, in the lack of fit tests and residual analysis. The regression equation was found by determining the [mixture]*process model as [Linear]*Quadratic. Hence, the regression equation (4) of this model was found as:

$$\begin{gathered}\text{Strength} = +9.48586{*}P + 2.26749{*}V + \\ + 0.10254{*}P{*}YC + 2.81154E-004{*}P{*} + \\ + 0.47016{*}V{*}\,YC + 1.72888E-006{*}V{*}R - \\ - 1.59231E-003{*}P{*}YC^2 - 2.60654E - \\ - 009{*}P{*}R^2 - 6.07106E-003{*}V{*}YC^2 + \\ + 1.30948E-010{*}V{*}R^2 + \\ + 2.04622E-006{*}P{*}YC{*}\,R - 1.63372E - \\ - 007{*}V{*}YC{*}\,R\end{gathered} \qquad (4)$$

where:

P and *V* are the proportions of polyester and viscose in the blend;

YC – the yarn count;

R – the rotor speed.

Note that, since the model is selected as being [Linear]*Quadratic, the blend components are linear, while the process parameters are quadratic (second-order) in the regression equation. The Analysis of Variance (ANOVA) table of this model is also given in table 5. Here, *p*-values lower than 0.05 are expected to be significant. ANOVA table also indicates that there is significant interaction between the blend parameters:

A – coded proportion of polyester;

B – coded proportion of viscose and the process variables;

C – coded yarn count;

D – coded rotor speed.

The significant cases of the corresponding parameters in the table show that the interaction of the process parameters and blend variables for the tensile strength of the yarns produced are meaningful.

RESULTS AND DISCUSSIONS

In this study, seven different blend ratios of polyester/viscose slivers were produced and these slivers were manufactured with four different rotor speed and four different yarn counts in a rotor-spinning machine. Then, a back propagation feed forward multi-layer perceptron ANN and mixture process crossed-regression model (simplex lattice design) were developed by introducing the blend ratio, yarn count and rotor speed as input variables, and the tensile strength as output variable. The predictions were carried out by those models, and the best models were selected and introduced in this paper.

The selected regression curves generated by the regression equation are demonstrated in figure 3. In this figure, the design points indicate the experimental result obtained, and the curve is fitted by the regression equation. In addition, changing the blend ratio of actual polyester and viscose fibres in the blend from 0.0 to 1.0 can also be seen in the figures. In figure 2, the yarn count is fixed at 25 tex and the rotor speeds are determined as 50 000 rpm (*a*) and 70 000 rpm (*b*). It can be inferred from these figures that increasing the

Table 5

ANOVA FOR THE [LINEAR]*QUADRATIC REGRESSION MODEL

Source	Sum of squares	Mean square	*F* value	*p*-value	Significance
Model	2857.523	259.7748	512.043	<0.0001	significant
Linear mixture	2724.398	2724.398	5370.07	<0.0001	significant
AC	47.58045	47.58045	93.78599	<0.0001	significant
AD	0.021285	0.021285	0.041955	0.8379	
BC	26.4221	26.4221	52.08069	<0.0001	significant
BD	1.545408	1.545408	3.046158	0.0824	
AC^2	0.131153	0.131153	0.258515	0.6117	
AD^2	4.384554	4.384554	8.64241	0.0037	significant
BC^2	1.905898	1.905898	3.756722	0.0539	
BD^2	0.011122	0.011122	0.021923	0.8824	
ACD	1.213838	1.213838	2.3926	0.1234	
BCD	0.007545	0.007545	0.014872	0.9031	
Residual	106.032	0.50733			
Pure error	30.53487	0.27759			
Cor total	2963.555				

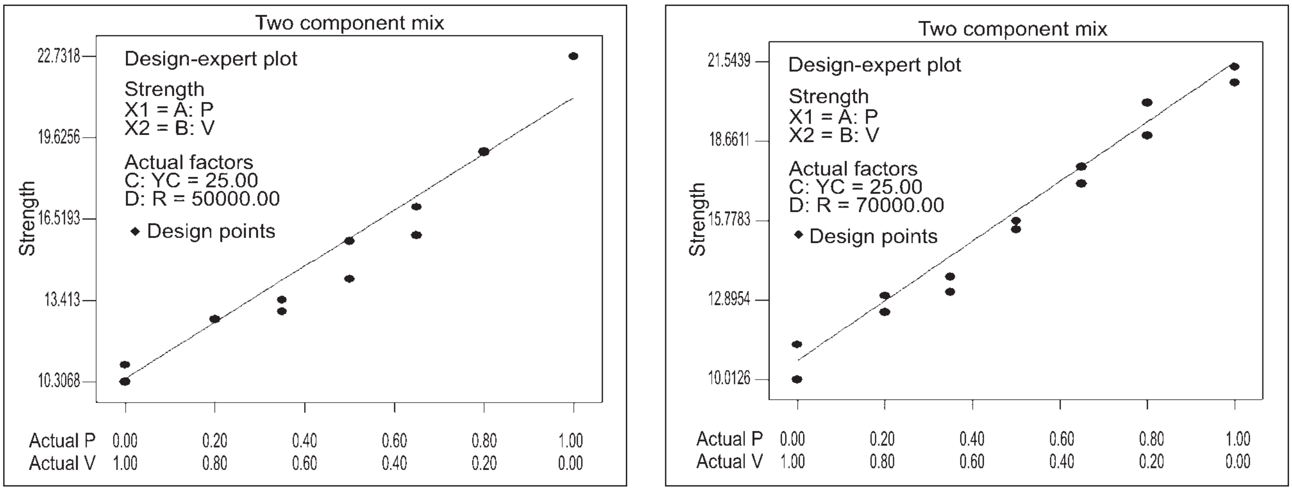

a *b*

Fig. 2. Variation between the blend ratio and tensile strength at different production parameters

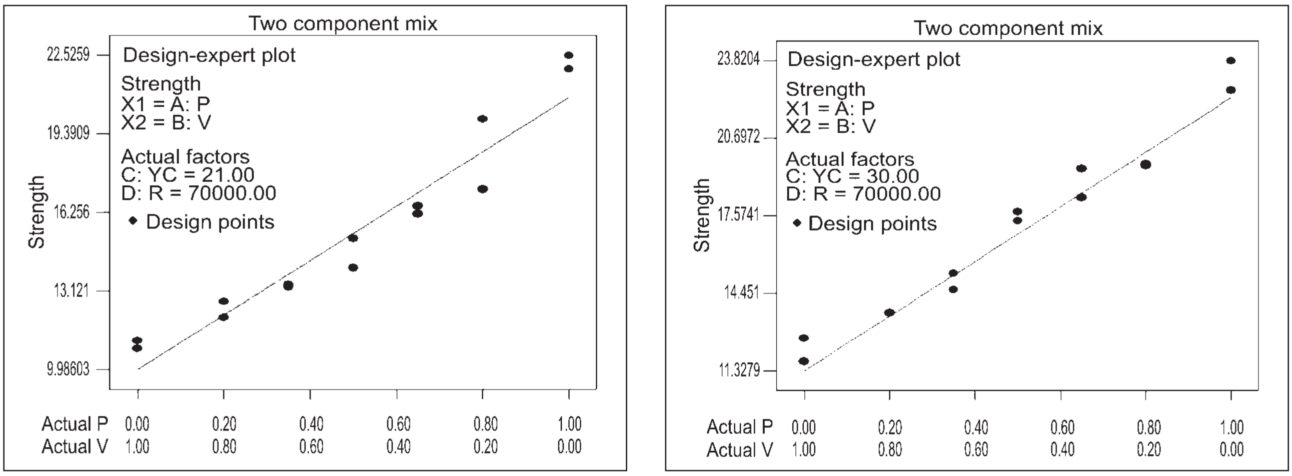

a *b*

Fig. 3. Variation between the blend ratio and tensile strength at different production parameters

polyester proportion in the yarn blend increases the tensile strength value, since the strength of polyester fibres are greater than that of the viscose fibres (table 1). Increasing the presence of polyester fibre in the yarn structure increases the yarn strength, as expected. Strength values of the yarns are not changed significantly by increasing the rotor speed from 50 000 rpm to 70 000 rpm. The effect of yarn count on the strength value can also be seen more clearly in figure 3. Here, the rotor speed is fixed at 70 000 rpm and the yarn counts are determined as 21 tex (*a*) and 30 tex (*b*). It can also be seen in these figures that increasing the polyester proportion in the blend increases the strength value. In addition, increasing the yarn count also increases the strength value of the yarns, as expected. Some of the values of actual tensile strength (28 samples) are selected randomly and determined, in order to test the prediction confidence of these models. In table 6, actual values of the tensile strength of these testing samples are obtained from the real blend parameters and production parameters; and the predictions made by those models are shown as well. In addition, in order to see the prediction capability of the models, Absolute Percent Errors (*APE*) of the ANN (*ANN-APE*) and the Statistical models (*Stats.-APE*) are also given in the table. *APE* shows the absolute error of the prediction for the models, with respect to the real tensile strength value. For instance, selecting the sample No:20, polyester rate and viscose rate in the blend is 0% and 100%, respectively; yarn count is 37 tex, rotor speed is 50000 rpm and the actual tensile strength result for these real production parameters is obtained as 12.02301. The ANN prediction and Statistical prediction are as 11.81661 and 11.46, respectively, by the models developed. The prediction errors (*APE*) of ANN and Statistical model are evaluated as 1.716724% and, respectively, 4.682804%. Hence, the ANN prediction for this specific sample is more reliable than the statistical model.

The overall prediction performances of the ANN and statistical model are summarised and given in table 7. Here, the correlation coefficient of the ANN model is slightly greater than for the statistical model, whereas the Mean Square Error (*MSE*) of ANN is lower than that of the statistical model. The Mean Absolute Percentage Error (M*APE*), which is an important parameter in assessing the prediction performance of the models, is also calculated.

The *MAPE* values of ANN and Statistical models are obtained as 2.33916% and, respectively, 3.2539%.

Table 6

PREDICTIONS MADE BY ANN AND STATISTICAL MODELS AND THEIR PREDICTION CONFIDENCE									
No.	PES rate, %	Viscose, rate, %	Yarn count, tex	Rotor speed, rpm	Actual strength, cN/tex	ANN predictions	Statistical predictions	ANN-APE	Statistical APE
1	65	35	37	50000	18.19143	18.5886	18.59	2.183283	2.190985
2	20	80	25	50000	12.68006	12.61996	12.58	0.473989	0.789137
3	80	20	21	70000	18.5837	18.17457	18.68	2.20544	0.518215
4	65	35	25	80000	16.00453	17.43506	17.43	8.938233	8.906636
5	35	65	25	80000	14.31778	14.42165	14.4	0.725414	0.574237
6	65	35	37	70000	18.72099	19.34798	19.24	3.349139	2.772341
7	100	0	37	60000	23.18304	23.10469	23.13	0.337973	0.228783
8	65	35	21	70000	16.35758	16.43699	17.05	0.485466	4.23305
9	50	50	25	70000	15.61227	15.79053	16.12	1.141844	3.252145
10	100	0	21	60000	21.80029	21.17877	21	2.850984	3.671024
11	65	35	25	70000	17.42651	17.30262	17.75	0.710909	1.856334
12	50	50	37	80000	17.37747	18.05044	17.41	3.872648	0.187183
13	35	65	37	50000	14.74928	15.15086	15.3	2.722729	3.7339
14	80	20	25	60000	18.77983	19.05798	19.4	1.481103	3.302317
15	100	0	37	50000	22.27102	22.9976	22.43	3.262474	0.713862
16	0	100	30	70000	12.17011	11.24955	11.33	7.564132	6.903096
17	50	50	21	60000	14.9356	14.88641	15.42	0.329345	3.243229
18	80	20	30	80000	20.14296	20.1173	19.78	0.127412	1.801929
19	20	80	25	70000	12.75852	12.73141	12.87	0.212455	0.873795
20	0	100	37	50000	12.02301	11.81661	11.46	1.716724	4.682804
21	100	0	21	80000	21.09421	20.73053	20.19	1.724071	4.286539
22	50	50	25	80000	16.66158	15.9477	15.92	4.284585	4.450857
23	65	35	30	60000	17.84819	18.07935	18.41	1.295118	3.147691
24	0	100	21	70000	10.9835	10.47737	9.99	4.608125	9.045419
25	50	50	21	70000	14.6316	15.00582	15.42	2.557612	5.388364
26	80	20	37	50000	20.45678	20.60692	20.23	0.733933	1.108563
27	100	0	30	70000	23.16343	22.53071	22.33	2.731545	3.598023
28	50	50	25	50000	14.95522	15.38498	15.8	2.873687	5.648748
MAPE, %								**2.33916**	**3.2539**

Table 7

COMPARISON OF THE PREDICTION PERFORMANCE OF ANN AND STATISTICAL MODELS		
Parameter	ANN	Statistical model
Correlation coefficient, *R*	0.989	0.981
Mean square error, *MSE*	0.25133	0.27759
Mean absolute error, *MAE*	0.38639	0.5442
Mean absolute percent error – *MAPE*, %	2.33916	3.2539
Cases with more than, 5% error	2	5
Cases with more than, 3% error	7	16

Moreover, the number of the prediction errors (*APE*) of both models is no greater than 10%. There are 2 cases for ANN and 5 case for Statistical model with more than 5% error.

In addition, there are 7 cases of ANN and 16 cases of statistical model for more than 3% error for the prediction of the tensile strength. In conclusion, both models gave satisfactory results, but the ANN is more reliable than the statistical model. In statistical models, increasing the number of experiments results into a more reliable regression equation.

The prediction performance of ANN is also increased by increasing the number of experiments; however, training of the model can be limited by increasing the number of experiments, which is one of the disadvantages of ANN. In addition, in artificial neural networks, there is not an optimum prediction performance, but the best. Here, in this study, a number of trials were carried out and the best and acceptable ANN model is presented, however there should be always a better model in ANN and obtaining the best ANN model requires time. However, the statistical model is practical, easy and has a non-complex structure, in comparison to ANN. In this study, both the two models gave reliable and satisfactory results, but the predictions of ANN model are more accurate, than that of the statistical model.

In conclusion, although ANN gave more reliable results than the statistical model, the statistical model could also be used for the strength prediction of polyester/viscose blended open-end rotor yarn.

CONCLUSIONS

As a result of the experimental study, ANN and the statistical investigation into the prediction of the tensile strength value of polyester/viscose blended open-end rotor-spun yarns, the following conclusions can be drawn:

- Strength in blended yarns depended mainly on the strength of fibres, number of fibres and fibre location or positioning in the yarn cross-section, yarn count, blend ratio and working performance of the yarn-spinning machine.
- Since the strength of the polyester fibre is greater than that of viscose, increasing the polyester ratio in the blend increases the yarn strength, as expected.
- The predictions on the tensile strength value of these two models are compared, in order to see the

prediction confidence. Considering the overall performances of the models (correlation coefficients, *MSE, MAPE*, errors with more than 5% and 3%), it was concluded that both models gave satisfactory results; however, the ANN model gave more reliable predictions than the statistical model.

- Although the ANN model gave more reliable results, the statistical model can also be used for predicting the tensile strength of polyester/viscose blended open-end rotor-spun yarns, because of having a non-complex structure and because of its simplicity.
- Here, in this study, a number of trials were carried out and the best and acceptable model was presented; however, there should be always a better model in ANN.
- Both the two models are practical and useful for OE-yarn spinners, in order to predict the tensile strength value of any polyester/viscose blended yarns before the yarn production.

BIBLIOGRAPHY

[1] Cheng, L., Adams, D. L. *Yarn strength prediction using neural networks.* P. I. *Fiber properties and yarn strength relationship.* In: Textile Research Journal, 1995, vol. 65, issue 9, p. 495

[2] Ramesh, M. C., Rajamanickam, R., Jayaraman, S. *The prediction of yarn tensile properties by using artificial neural networks.* In: Journal of The Textile Institute, 1995, vol. 86, issue 3, p. 459

[3] Majumdar, P. K., Majumdar, A. *Predicting the breaking elongation of ring spun cotton yarns using mathematical statistical and artificial neural network models.* In: Textile Research Journal, 2004, vol. 74, issue 7, p. 652

[4] Cheng, K. P. S., Lam, H. L. I. *Evaluating and comparing the physical properties of spiced yarns by regression and neural network techniques.* In: Textile Research Journal, 2003, vol. 73, issue 2, p. 161

[5] Kuo, C. F. J., Hsiao, K. I., Wu, Y. S. *Using neural network theory to predict the properties of melt spun fibres.* In: Textile Research Journal, 2004, vol. 74, issue 9, p. 840

[6] Üreyen, M. E., Gürkan, P. *Comparison of artificial neural network and linear regression models for prediction of ring spun yarn properties. P. I. Prediction of yarn tensile properties.* In: Fibers and Polymers, 2008, vol. 9, issue 1, p. 87

[7] Üreyen, M. E., Gürkan, P. *Comparison of artificial neural network and linear regression models for prediction of ring spun yarn properties. P. I. Prediction of yarn hairiness and unevenness.* In: Fibers and Polymers, 2008, vol. 9, issue 1, p. 92

[8] Strumillo, L. J., Cyniak, D., Czelkalkski, J., Jackowski, D. *Quality of cotton yarns spun using ring-, compact- and rotor-spinning machines as a function of selected spinning process parameters.* In: Fibres and Textiles in Eastern Europe, 2007, vol. 15, issue 1, p. 24

[9] Shanmugam, N., Chattopahyay, S. K., Vivekanandan, M. V., Sreenivasamurthy, H. V. *Prediction of micro-spun yarn lea csp using artificial neural networks.* In: Indian Journal of Fibre & Textile Research, 2001, vol. 26, issue 4, p. 372

[10] Gharehaghaji, A. A., Shanbeh, M., Palhang, M. *Analysis of two modelling methodologies for predicting the tensile properties of cotton covered nylon yarns.* In: Textile Research Journal, 2007, vol. 77, issue 8, p. 565

[11] Duru Baykal, P., Babaarslan, O., Erol, R. *Prediction of strength and elongation properties of cotton/polyester-blended OE rotor yarns.* In: Fibres and Textiles in Eastern Europe, 2006, vol. 14, issue 1, p. 18

[12] Üreyen, M. E., Kadoõlu, H. *Regressional estimation of ring cotton yarn properties from hvi fiber properties.* In: Textile Research Journal, 2006, vol. 76, issue 5, p. 360

[13] Demiryürek, O., Koç, E. *Predicting the unevenness of polyester/viscose blended open-end rotor spun yarns using artificial neural network and statistical models.* In: Fibers and Polymers, 2009, vol. 10, issue 2, p. 237

[14] Demiryürek, O., Koç, E. *The mechanism and/or prediction of the breaking elongation of polyester/viscose blended open-end rotor spun yarns.* In: Fibers and Polymers, 2009, vol. 10, issue 5, p. 694

[15] Shihab, K. *A back propagation neural network for computer network security.* In: Journal of Computer Science, 2006, vol. 2, issue 9, p. 710

[16] Montgomery, D. C. *Design and analysis of experiments.* John Wiley & Sons, Inc., USA, 2001

Authors:

ERDEM KOÇ
University of Ondokuz Mayis
Department of Mechanical Engineering
55139 Samsun – Turkey
e-mail: erdemkoc@omu.edu.tr

OĞUZ DEMIR YÜREK
University of Erciyes
Department of Textile Engineering
38039 Kayseri – Turkey
e-mail: demiryurek@erciyes.edu.tr

PRIMA ANCHETĂ ANTROPOMETRICĂ A COPIILOR DIN ROMÂNIA

Institutul Național de Cercetare-Dezvoltare pentru Textile și Pielărie, cu sprijinul Ministerului Educației, Cercetării, Tineretului și Sportului efectuează prima ***Anchetă antropometrică a copiilor cu vârsta cuprinsă între 6 și 19 ani.***

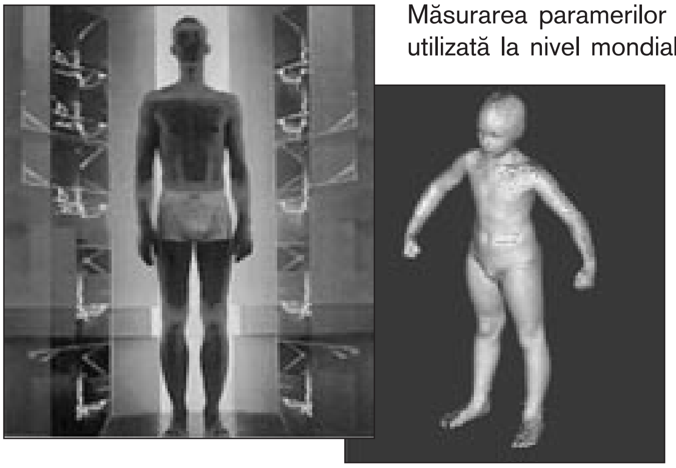

Măsurarea paramerilor antropometrici se face prin cea mai nouă tehnologie utilizată la nivel mondial, și anume prin scanarea corpului cu laser optic, 3D VITUS Smart XXL-ANTHROSCAN Pro.

Obiectivul acestei acțiuni îl constituie obținerea unor date antropometrice 3D, atât în scopul elaborării de normative naționale, necesare sectorului de confecții îmbrăcăminte, și al proiectării tehnologice a produselor destinate copiilor – jucării, echipamente pentru sport, dispozitive medicale, mobilier etc., cât și al evaluării stării de sănătate – *greutatea în raport cu vârsta, greutatea în raport cu înălțimea, indicele de masă corporală, circumferința medie a brațului etc.*

Redacția

Study on the measured error of thermal conductivity of fibrous porous materials. Part II. Improved calculating formula*

PENG CUI

FUMEI WANG
ZHIYONG LIANG

REZUMAT – ABSTRACT – INHALTSANGABE

Studiul erorii măsurate a conductivității termice la materialele fibroase poroase. Partea a-II-a. Formulă de calcul îmbunătățită

În lucrare au fost analizați factorii de influență asupra erorii măsurate a conductivității termice a materialelor fibroase poroase, prin rezolvarea ecuațiilor privind transferul integral, conductiv și prin convecție, de căldură. A fost simulat transferul de căldură prin corpul materialelor fibroase poroase, folosind metoda volumului finit. Prin intermediul simulării, s-a constatat că fluxul total de căldură ce trece prin corpul materialelor fibroase poroase reprezintă o funcție liniară a conductivității termice, atunci când aceasta este măsurată cu ajutorul plăcii de uscare cu protecție, și că unele constante ale funcției liniare sunt legate de grosimea și de coeficientul de permeabilitate al mostrei. Datele simulate sunt utilizate pentru ajustarea curbelor de variație a fluxului total de căldură în funcție de grosime, conductivitatea termică și coeficientul de permeabilitate. Formula îmbunătățită de calcul al conductivității termice a materialelor fibroase poroase a fost stabilită pe baza estimării ajustării. S-a demonstrat pe cale experimentală că formula îmbunătățită de calcul este mai precisă decât cea originală, acest lucru bazându-se pe analiza unui material alcătuit dintr-o singură componentă continuă și cu un transfer de căldură unidimensional.

Cuvinte-cheie: conductivitate termică, formulă de calcul îmbunătățită, materiale fibroase poroase, placă de uscare cu protecție

Study on the measured error of thermal conductivity of the fibrous porous materials. Part II. Improved calculating formula

In the paper, the effect factors on the measured error of thermal conductivity of fibrous porous materials were analyzed by solving the integral convective and conductive heat transfer equations. In this paper the heat transfer through the body of fibrous porous materials was simulated with finite volume method. By the simulation, it is found that the total heat flux through the body of fibrous porous materials is a linear function of the thermal conductivity when it is measured by the guarded plate, and some constants in the linear function are related with the thickness and permeability coefficient of the sample. The simulated data are employed to fitting the variation curves of the total heat flux with thermal conductivity, thickness and permeability coefficient. The improved calculating formula of thermal conductivity for fibrous porous materials was established based on the fitting estimation. Through the experimental, it is demonstrated that the improved calculating formula is more accurate than the original one, which is based on the assumptions of single component continuum material and one dimensional heat transfer.

Key-words: thermal conductivity, improved calculation formula, fibrous porous materials, guarded hot plate

Untersuchung des gemessenen Fehlers der thermischen Konduktiviät bei porösen Fasermaterialien. II Teil: Verbesserte Berechnungsformel

In diesem Artikel wurden die Effektfaktoren auf das gemessene Fehler der thermischen Konduktivität bei porösen Fasermaterialien analysiert, durch Lösung der Integralgleichungen des konvektiven und konduktiven Wärmetransfers. In der vorliegenden Arbeit wurde das Wärmetransfer durch den porösen Fasermaterial aufgrund der Methode des Finiten Elementes simuliert. Als Folge der Simulation wurde festgestellt, dass bei der Messung mit Protektionsplatte der Gesamtwärmefluss durch den Inneren des Fasermaterials eine lineare Funktion der thermischen Konduktivität darstellt, und dass einige Konstanten der Linearfunktion von der Dicke und dem Permeabilitätskoeffizient der Probe/des Musters abhängig sind. Die simulierten Daten benutzt man für die Anpassung der Variationskurven des Gesamtwärmeflusses mit der Dicke, der thermischen Konduktivität und dem Permeabilitätskoeffizient. Es wurde somit eine verbesserte Berechnungsformel der thermischen Konduktivität bei porösen Fasermaterialien aufgrund der Anpassungsschätzung festgestellt. Durch die experimentelle Komponente wird die Tatsache bewiesen, dass die verbesserte Berechnungsformel eine grössere Genauigkeit als die Ursprüngliche aufweist, wobei ein gleichförmiges Material aus einer einzigen Komponente und ein uni-dimensionelles Wärmetransfer vorausgesetzt werden.

Stichwörter: Thermische Konduktivität, verbesserte Berechnungsformel, poröse Fasermaterialien, Trocknungs-Protektionsplatte

The guarded hot plate is a universally used testing method for the thermal conductivity. Yet, for the convective heat transfer, the heat leakage on the verges of a test specimen and other reasons lead to measuring errors existing in the test [1–2]. Taking effort for reducing these errors and for enhancing the measuring accuracy, most researchers worked on simulating the ideal temperature field in the body of the fibrous porous materials [3–6]. Then, through the analysis of the temperature field, they tried to modify the size of the test specimen and restrict the applicable scope of the physical parameters of the materials, thus conform to one-dimensional supposition, based on which the thermal conductivity is calculated. In spite of these, till now, all the efforts had been only based on the assumptions of single component continuum materials [7], not suitable to the fibrous porous materials, case complicated with the fiber and air inside. That is to say, the size and the physical parameters of fibrous porous materials cannot be approximated previously, even controlled, like in the case of single component continuum materials. Until now, there had been no report about a testing method of thermal conductivity, precisely under the original size of fibrous porous materials.

In this paper, the integral convective, conductive and radiative heat transfer equation is established to simulating the total heat flux through the body of fibrous porous materials. Solving with FVM method, the variation of total heat flux is obtained with thermal conductivity, permeability coefficient and thickness. Based on the regression relations of heat flux with thermal conductivity, permeability coefficient and thickness, respectively, the improved calculating formula of thermal conductivity is evolved. This way, it is not only out of the restriction of the size and physical parameters of the samples, but also out of the presumption of one-dimensional heat transfer, substituted with a three-dimensional heat transfer, which is considered on the actual temperature field in the body.

* Part II. Part I has was published in Industria Textilă, 2010, issue 6, p. 276

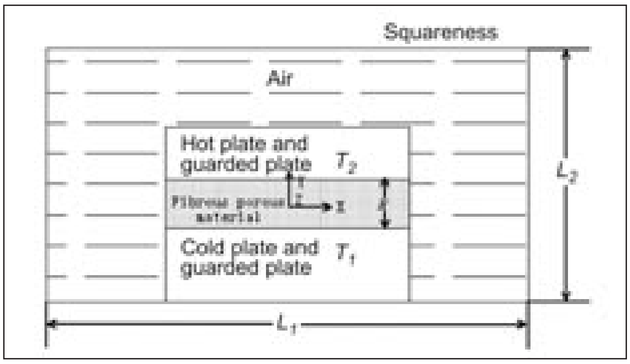

Fig. 1. Side view of the squareness

SIMULATION OF HEAT FLUX

The geometry model used for simulation, which has been established in the last paper (Part I), is shown in figure 1. According to the theory of permeation fluid mechanics, the fibrous porous materials can be regarded as a porous medium, with the assumption of which the heat transfer equations are constructed as follows:

- continuity equation:

$$div(\rho u) = 0 \tag{1}$$

where:
u is the volume average velocity;
ρ – the material parameter, listed in table 1.

- momentum equations:

$$div\left(\frac{\rho uu}{\phi}\right) = -\frac{\partial(\phi p)}{\partial x} + div(\mu grad(u)) + F \tag{2}$$

$$div\left(\frac{\rho vu}{\phi}\right) = -\frac{\partial(\phi p)}{\partial y} + div(\mu grad(v)) + F \tag{3}$$

$$div\left(\frac{\rho wu}{\phi}\right) = -\frac{\partial(\phi p)}{\partial z} + div(\mu grad(w)) + F \tag{4}$$

where:
ρ and μ are the static pressure and dynamic viscosity of the air,
F – the join force exerted on the air,

$$F = -\frac{\phi\mu}{\kappa}u + \phi G$$

κ and ϕ are the permeability coefficient and porosity;
G – the gravity acceleration;
k – unit vector in vertical direction,

$$G = (\rho_{ref} - \rho)gk; \quad \rho_{ref} = \rho(1 - \beta\Delta T); \quad \beta = \frac{1}{T_m}$$

T_m is the reference temperature,

$$T_m = \frac{T_1 + T_2}{2}$$

T_1 – the temperature of the cold plate and guarded plate;
T_2 – the temperature of the hot plate and guarded plate, according to the measure standard,
T_1 and T_2 are 20°C and 30°C.

- energy equation:

$$div(\rho uT) = div(a_e gradT) + q_R \tag{5}$$

where:
q_R is the radiative heat flux, which is minor enough to be ignored for the small temperature difference between the hot plate, cold plate and guarded plate [8];
a_e – the thermal diffusion coefficient, $a_e = \frac{\lambda}{\rho c}$;
λ and c – the material parameters, listed in table 1.

In the air, the heat transfer equations are similarly set as those of the fibrous porous materials, except the equations (2) ~ (4), which should be written as:

$$div(\rho uu) = -\frac{\partial(p)}{\partial x} + div(\mu grad(u)) + F \tag{6}$$

$$div(\rho vu) = -\frac{\partial(p)}{\partial y} + div(\mu grad(v)) + F \tag{7}$$

$$div(\rho wu) = -\frac{\partial(p)}{\partial z} + div(\mu grad(w)) + F \tag{8}$$

where $F = G = (\rho_{ref} - \rho)gk$.

The boundary conditions are as follows:

$$T\left(y = \frac{H}{2}\right) = 30°C, \; T\left(y = \frac{H}{2}\right) = 20°C \tag{9}$$

$$T\left(y = \frac{L2}{2}\right) = T\left(x = \frac{L1}{2}\right) = T\left(x = \frac{L1}{2}\right) = T\left(z = \frac{L1}{2}\right) = = T\left(z = -\frac{L1}{2}\right) = T_1 \tag{10}$$

$$p\left(y = \frac{L2}{2}\right) = p\left(x = \frac{L1}{2}\right) = p\left(x = -\frac{L1}{2}\right) = p\left(z = \frac{L1}{2}\right) = = p\left(z = -\frac{L1}{2}\right) = 101355pa \tag{11}$$

Apart from the above boundary conditions, the boundary conditions on the other faces are:

$$\frac{\partial T}{\partial n} = 0 \tag{12}$$

The equations (1) ~ (8), under the given boundary conditions (9) ~ (12), are discretized by FVM, which has already been discussed in detail in the last paper [1].

ANALYSIS OF EFFECT FACTORS OF THE TOTAL HEAT FLUX

According to the geological and thermal physical properties of the usual heat preservation materials, the scopes of geological and physical parameters used in numerical simulation are listed in table 1.

Based on the analysis of last paper, it is known the total heat flux q can be expressed as:

$$q = f(\lambda, \phi, \kappa, \mathrm{H}) \tag{13}$$

Changing the respective variable in formula (13), the corresponding total heat flux through the body of fibrous porous materials can be simulated and supposed to be measured by the guarded hot plate instruction. The trends are observed for the total heat flux changed

Table 1

PARAMETERS IN NUMERICAL SIMULATION, T_m = 25oC	
Parameters	Scope
Thickness, *H*, cm	0 ~ 5
Thermal conductivity, l, W/m · *K*	0.03 ~ 0.3
Permeability coefficient, κ, m^2	10^{-15} ~ 10^{-2}
Porosity, ϕ	0.1 ~ 0.99
Air density, ρ, kg/m^3	1.185
Air specific heat, *c*, kJ/kg · *K*	1.005
Air dynamic viscosity, m, kg/(m · s)	18.35 x 10^{-6}

with the related four variables, of which one variable changes with the other three variables fixed, to probing the way for improving the calculating formula of the thermal conductivity.

Figure 2 shows the variation of total heat flux as the thermal conductivity is increased. Seen from figure 2, it can be concluded that the porosity is not affecting the heat flux, the reason of which is supposed to be the porosity interplayed with the permeability coefficient; so, the role of porosity is substituted by the permeability coefficient, completely to be redundant. It can also be seen from figure 2 that the thermal conductivity is linear with the total heat flux, whatever the other parameters are. The relation between the total heat flux and thermal conductivity is expressed as:

$$q = a\lambda + b \tag{14}$$

of which the values of *a* and *b* are related with the thickness, *H*, and permeability coefficient, *k*. Figure 3 shows the variation of total heat flux as the permeability coefficient is increased. Because the permeability coefficient and total heat flux are varied in a wide span, respectively, we use the logarithmic coordinate for representing the permeability coefficient and total heat flux, respectively. Seen from figure 3, it can be concluded that the total heat flux is slightly varied with the permeability coefficient at the thickness of 1 cm. In fact, deduced from our numerical simulation, the total heat flux is not changed with a permeability coefficient below the thickness of 1 cm. It can also be asserted from figure 3 that the total heat flux is in piecewise function with the permeability coefficient at the thicknesses of 3 cm and 5 cm. At the thicknesses of 3 cm and 5 cm, respectively, when the permeability coefficient is higher than 10^{-4} m^2 or lower than 10^{-7} m^2, the total heat flux is not varied with the permeability coefficient; when the

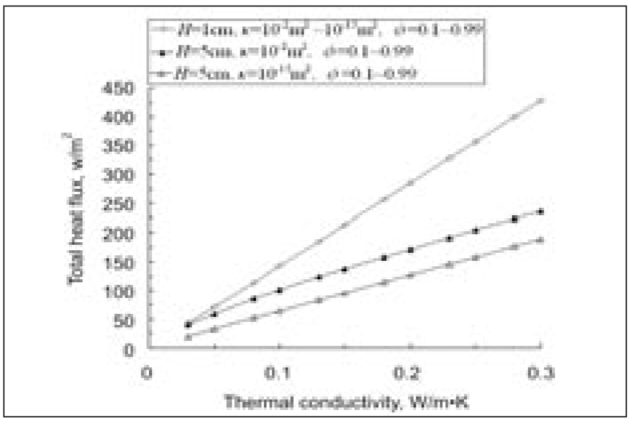

Fig. 2. Variation of total heat flux with increasing of thermal conductivity

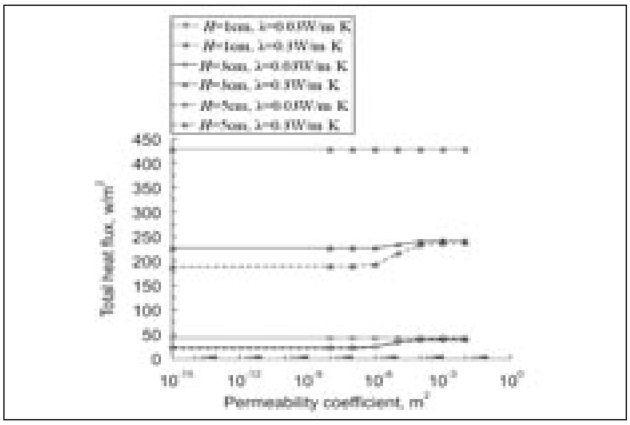

Fig. 3. Variation of total heat flux with increasing of permeability coefficient

permeability coefficient is within the span of 10^{-7} m^2 to 10^{-4} m^2, the total heat flux is increased with the increase in the permeability coefficient. This indicates that, when the permeability coefficient is higher than 10^{-4} m^2 or lower than 10^{-7} m^2, the values of *a* and *b* are only related with thickness; but, when the permeability coefficient is within the span of 10^{-7} m^2 to 10^{-4} m^2, the values of *a* and *b* are related with the permeability coefficient and thickness corporately.

IMPROVEMENT OF CALCULATING FORMULA FOR THERMAL CONDUCTIVITY

On the basis of the above analysis, it can be inferred that the total heat flux through the body of the fibrous porous materials is linear with thermal conductivity, according to the formula (14), of which the values of *a* and *b* are related with the thickness and permeability coefficient, respectively, but not related with porosity ϕ. The scope of the values *a* and *b* take is divided into three cases, as follows:

- at the situation of 10^{-4} m^2 ≤ κ ≤ 10^{-2} m^2, the values of *a* and *b* are only related with thickness;
- at the situation of 10^{-15} m^2 ≤ κ ≤ 10^{-7} m^2 , the values of *a* and *b* are only related with thickness;
- at the situation of 10^{-7} m^2 < κ < 10^{-4} m^2, the values of *a* and *b* are related with thickness and permeability coefficient corporately.

Improved formula for the cases of A and B

For the cases of *A* and *B*, which are and 10^{-4} m^2 ≤ κ ≤ 10^{-2} m^2 and 10^{-15} m^2 ≤ κ ≤ 10^{-7} m^2, respectively, the variation of the total heat flux with thermal conductivity can be obtained based on the linear relation at the different thicknesses, shown in figures 4 and 5.

Figure 4 and figure 5 only show the values of *a* and *b* on some given thicknesses. To deduct the values of *a* and *b* in the arbitrary thickness, the curve estimation is employed to fit the relations between *a*, *b* and the thickness. Through the curve fitting, it is found that the variation of a with an increasing thickness can be represented by the formula (15), the fitting degree of which is 1, viz. R^2 = 1; the variation of *b* with an increasing thickness can be fit with sextic, represented by formula (16), the fitting degree of which is 1, viz. R^2 = 1. So, with the formula (15) and formula (16), the values of *a* and *b* at the arbitral thickness can be calculated:

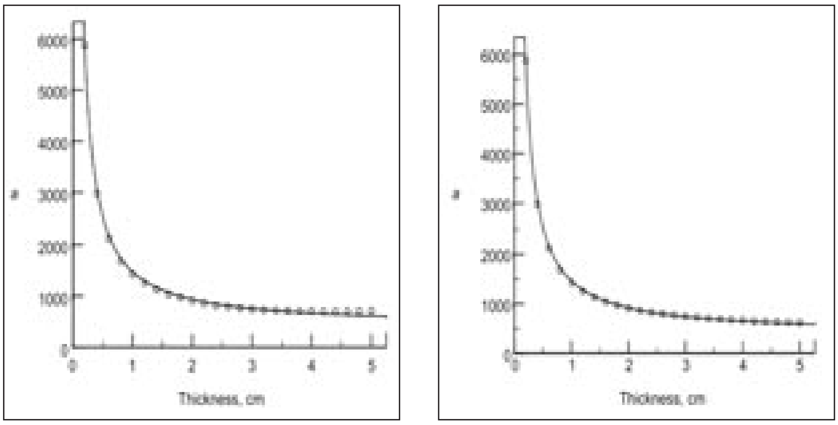

a *b*

Fig. 4. Variation of *a* with increasing of thickness:
a – 10^{-4} m^2 ≤ κ ≤ 10^{-2} m^2; ***b*** – 10^{-15} m^2 ≤ κ ≤ 10^{-7} m^2

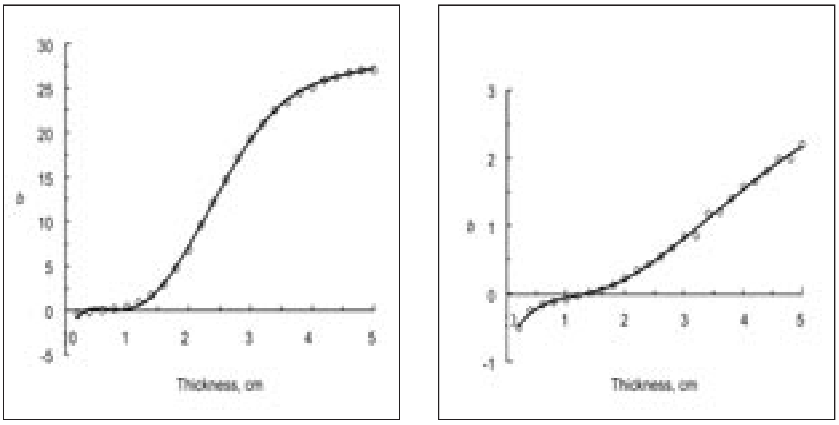

a *b*

Fig. 5. Variation of *b* with increasing of thickness:
a – 10^{-4} m^2 ≤ κ ≤ 10^{-2} m^2; ***b*** – 10^{-15} m^2 ≤ κ ≤ 10^{-7} m^2

Table 2

PARAMETERS IN THE IMPROVED CALCULATING FORMULA

	$d_0 \times 10^{-2}$	$d_1 \times 10^{-1}$	$c_6 \times 10^{-10}$	$c_5 \times 10^{-9}$	$c_4 \times 10^{-8}$	$c_3 \times 10^{-7}$	$c_2 \times 10^{-5}$	c_1	c_0
10^{-4} m^2 ≤ κ ≤ 10^{-2} m^2	3.99627	1.072957	–4.9000	9.5000	–6.8000	2.2000	–2.9000	1608.8	–2.9596
10^{-15} m^2 ≤ κ ≤ 10^{-7} m^2	3.81135	1.080564	–0.2000	0.3900	–0.3000	0.1100	–0.20527	190.62	–0.7809

$$a = d_0 + \frac{d_1}{H} \tag{15}$$

$$b = \sum_{i=0}^{6} c_i H^i \quad (i = 0,1...6) \tag{16}$$

where the values of d_0, d_1 and c_i are shown in table 2. The unit of the thickness is meter.

Improved formula for case C

For case *C*, which is 10^{-7} m^2 < κ < 10^{-4} m^2, the values of d_0, d_1 and c_i are varied with the permeability coefficient, shown in figures 6, 7 and 8. Through the curve fitting, it is found that the relations of d_0, d_1 and c_i with permeability coefficient can be expressed with the following formulas:

$$d_0 = 0.6058[-\log_{10}(\kappa)]^4 + 14.561[-\log_{10}(\kappa)]^3 + \\ +137.49[-\log_{10}(\kappa)]^2 - 576.42\log_{10}(\kappa) + 1287.7 \tag{17}$$

$$d_1 = -0.0011[-\log_{10}(\kappa)]^4 - 0.0308[-\log_{10}(\kappa)]^3 - \\ -0.3124[-\log_{10}(\kappa)]^2 + 1.4077\log_{10}(\kappa) + 8.42 \tag{18}$$

$$c_i = \alpha_2 + \frac{\alpha_1 - \alpha_2}{1 + e^{\frac{(\log_{10}(\kappa) - \alpha_3)}{\alpha_4}}}, \quad (i = 0,1...6) \tag{19}$$

where the calues of a_1 ~ a_4 are shown in table 2.

For cases *A* and *B*, the values of a and b can be calculated using the datum in table 2 and formulas (15) and (16). Then, combining the measured heat flux and formula (14), the thermal conductivity can be counted.

For case *C*, the values of a and b are evaluated with the datum in table 3, combining the formulas (17) ~ (19). Then, combining the measured heat flux and formula (14), the thermal conductivity can be counted. Formulas (14) ~ (19) combined with tables 2 and 3 construct the improved calculating formula for the

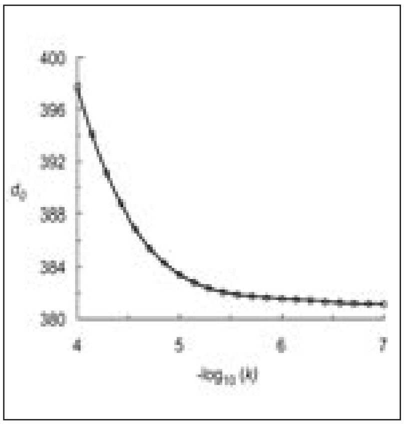

Fig. 6. Variation of d_0 with decreasing of permeability coefficient κ

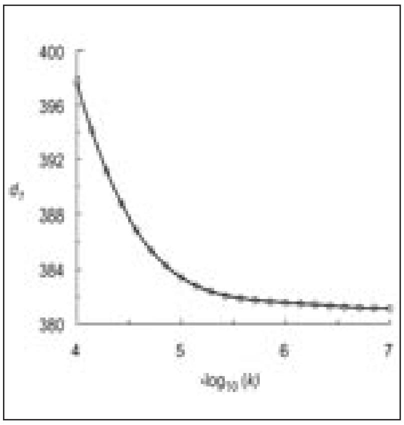

Fig. 7. Variation of d_1 with decreasing of permeability coefficient κ

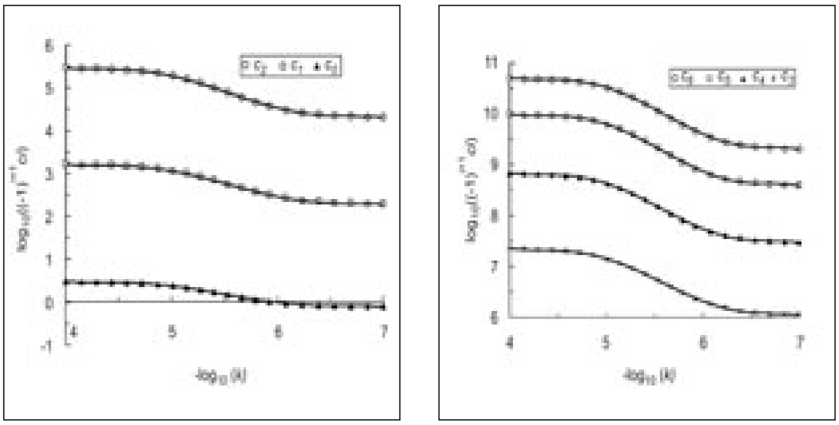

a *b*

Fig. 8. Variation of c_1 with decreasing of permeability coefficient κ increasing of thickness

Table 3

THE VALUE OF α IN FORMULA (19)				
c_i	α_1	α_2	α_3	α_4
c_0	–0.11177	0.47604	–5.48497	0.30954
c_1	2.26987	3.21479	–5.53561	0.32485
c_2	4.29988	5.47272	–5.53053	0.32401
c_3	6.0234	7.35446	–5.56769	0.33379
c_4	7.46253	8.84292	–5.55423	0.3185
c_5	8.5773	9.98697	–5.56233	0.31123
c_6	9.28507	10.6995	–5.58611	0.31609

thermal conductivity of fibrous porous materials, based on the above analysis. Actually, the permeability coefficients of normal fibrous porous materials are mostly less than 10^{-7} m^2, shown in table 3. Therefore, the most common sections are the formulas (14) ~ (16) and the second line in table 2. The computation of the improved formula is of such a complexity that it takes up a lot of time, but it can be simplified through programming.

EXPERIMENTAL PART

Three types of samples are shown in table 4, the third type sample are the materials sold on the market. The first two types of samples are made with different raw materials by the same method used for fabricating two series of wadding with different thicknesses. The total heat flux through a different thickness of wadding *1* and of wadding *2*, which are fabricated by the same method, is tested, while, for the case of non-woven *3*, the heat flux through one layer and respectively multiple layers are tested.

The KES-THERMO LABO II instruction, which is produced in Japan, is used for measuring the heat flux through the samples. The thermal conductivities calculated with our improved calculating formula and the original formula, viz. $\lambda = \dfrac{q \cdot H}{\Delta T}$ based on the assumptions of single component continuum materials and one-dimensional heat transfer, are executed as shown in figure 9.

Figure 9 shows the variation in thermal conductivity as thickness is increased. From figure 9, it can be seen that the thermal conductivities calculated on the same material are very close, when using the improved formula, but very fluctuant, as calculated with the original formula, which is based on the assumptions of single component continuum materials and one-dimensional heat transfer.

The thermal conductivity, which is the inherited property of the material, is supposed to be invariable whatever the thickness of the sample. Yet, as shown in figure 9, the thermal conductivities of some wadding materials have already surpassed the thermal conductivities of the fibers inside (4.2 ~ 8.4 x 10^{-2}W/m · K), the phenomenon of which obviously obey the basic laws of physics.

Table 4

INFORMATION OF SAMPLES				
Types of material	Material, mass friction	Thickness of sample, cm	Permebility coefficient, m^2	Porosity, %
Wadding 1	70% camel hair/ 30% polyester	1.51, 2.72 3.55, 4.84	9.83×10^{-9}	99.1
Wadding 2	30% sheep hair/ 70% polyester	1.42, 2.70, 3.94. 4.85	7.69×10^{-9}	99.4
Nonwoven 3	polyester	0.275 (one layer)	7.22×10^{-10}	99.5

Theoretically, the thermal conductivities of the same material should not vary in terms of the above analysis, which is in accordance with the computing results enabled by the improved formula established in this paper.

CONCLUSIONS

The mechanism of the heat transfer through the body of the fibrous porous materials, tested with the guarded hot plate, is different from that of the single component continuum materials. In this paper, the integral conductive and convective heat transfer model is established, to be solved with the FVM method, for simulating total heat flux through the body of fibrous porous materials.

The results show the total heat flux is not only related with the thermal conductivity, but also with the permeability coefficient and thickness simultaneously, but not in direct link with porosity. The total heat flux is linear with thermal conductivity. For the case the permeability coefficient is higher than 10^{-4} m^2 or lower than 10^{-7} m^2, the total heat flux is not varied with the permeability coefficient, but for the case the permeability coefficient is within the span of 10^{-7} m^2 to 10^{-4} m^2, the total heat flux increases with the permeability coefficient.

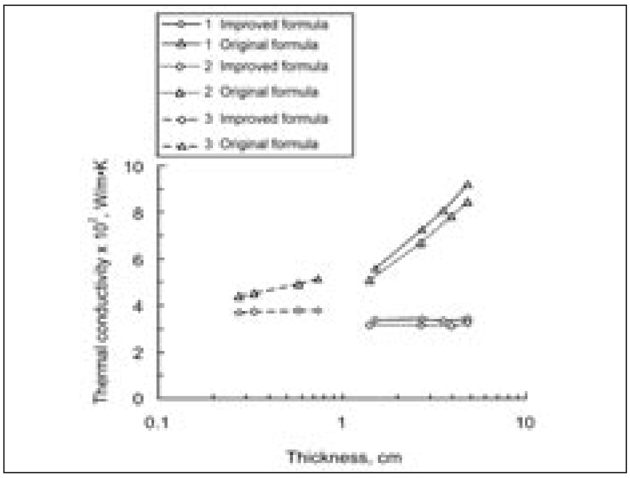

Fig. 9. Variation of thermal conductivity with increasing of thickness

On the account of the variation between total heat flux and thermal conductivity, permeability coefficient and thickness, the improved calculating formula is established through the curve fitting. Through the experimental part, it is proved that the thermal conductivity calculated by the improved calculating formula is stable and credible, but is very erratically calculated with the original formula, especially for the samples of big thickness. Although the fitting degree of the parameters in the improved calculating formula is 1, the calculating account is big; so, it should be simplified through programming within a practical application.

Acknowledgements

The authors of this article gratefully acknowledge the support of the Chinese National Science Foundation (NSFC 50973015).

BIBLIOGRAPHY

[1] Cui, P., Wang, F. M., Liang, Z. Y. *Study on the measured error of thermal conductivity of fibrous porous material. P.I. Error analysis.* In: Industria Textilă, 2010, vol. 61, issue 6, p. 276
[2] Boháč, V., Dieška, P., Kubičár, L. *The heat loss effect at the measurements by transient pulse method.* In: Measurement Science Review, 2007, vol. 7, issue 3, p. 24
[3] Hammerschmidt, U. *Guarded hot-plate (GHP) method: Uncertainty assessment.* In: International Journal of Thermophysics, 2002, vol. 23, issue 6, p. 1 551
[4] Xamán, J., Lira, L., Arce, J. *Analysis of the temperature distribution in a guarded hot plate apparatus for measuring thermal conductivity.* In: Applied Thermal Engineering, 2009,vol. 29, issue 4, p. 617
[5] Kubičár, L., Bohác, V., Vretenár, V. *Transient methods for the measurement of thermophysical properties: the pulse transient method.* In: High Temperatures-High Pressures, 2002, vol. 34, issue 5, p. 505
[6] Zuo, L., Zhu, S. K., Pan, N. *Determination of sample size for step-wise transient thermal tests.* In: Polymer Testing, 2009, vol. 28, issue 3, p. 307
[7] Cui, P., Wang, F. M. *The clothing layers' influence on its warming performance.* In: Industria Textila, 2009, vol. 60, issue 3, p. 115
[8] Yu, C. *Heat transfer and numerical analysis.* Tsinghua University Press, Beijing, 1981

Authors:

PENG CUI
FUMEI WANG
Donghua University
College of textiles
2999 North Renmin Road,
Songjiang District, Shanghai – China

ZHIYONG LIANG
Donghua University
College of science
2999North Renmin Road
Songjiang District, Shanghai – China
e-mail: zhyliang@dhu.edu.cn

Corresponding author:
PENG CUI
e-mail: cuipengdhu@gmail.com

Systemic approach to the design of knitted fabric with three-dimensional architecture. Part II*

LUMINIȚA CIOBANU

CĂTĂLIN DUMITRAȘ
FLORIN FILIPESCU

REZUMAT – ABSTRACT – INHALTSANGABE

Abordarea sistemică a proiectării tricoturilor cu arhitectură tridimensională. Partea a II-a

Tricoturile cu arhitectură tridimensională reprezintă o direcție de dezvoltare cu un potențial deosebit, mai ales în aplicațiile tehnice, și se împart în trei grupe: structuri multistrat/multiaxiale, structuri tip sandwich/spacer și structuri conturate spațial. Principala tehnică de realizare a tricoturilor conturate spațial este tricotarea de rânduri incomplete. Corelarea formei 3D a produsului cu desfășurata 2D a tricotului presupune definirea elementelor de bază și a liniilor de conturare. Elementele de bază sunt forme geometrice simple, care – prin repetiție – alcătuiesc desfășurata tricotului. Din punct de vedere al formei 3D, liniile de conturare reprezintă liniile de secționare necesare pentru a crea desfășurata, iar la nivelul acesteia reprezintă zonele de tricotare pe un număr incomplet de ace. Elementele de bază și liniile de conturare pot fi parametrizate, permițând proiectarea tricotului în corelație cu forma 3D dorită. Pentru modelarea dispunerii spațiale a tricoturilor, se propune un model inițial, care evidențiază distribuția forțelor ce generează geometria tridimensională a materialului tricotat.

Cuvinte-cheie: tricot 3D, conturare spațială, linie de conturare, element de bază, modelare

Systemic approach to the design of knitted fabric with three-dimensional architecture. Part II

Knitted fabrics with complex 3D architecture present an important development potential, especially in technical applications. They can be divided into three groups: multi-axial fabrics, sandwich/spacer fabrics and spatial fashioned fabrics. The main technique used to produce spatial fashioned structures is knitting on a variable number of needles. The correlation of the 3D product shape with the 2D geometry of the fabric requires the definition of the basic elements and fashioning lines. The basic elements are simple geometrical shapes that can be used to divide the 2D plan of the fabric. Considering the 3D shape, the fashioning lines represent section lines that are used to create the plan, where the knitting takes place on a variable number of needles. The basic elements and the fashioning lines can be described using parameters, thus allowing a fabric design that is correlated with the 3D shape intended to be obtained. Another interesting aspect is the modeling of the spatial shape of the fabrics, for which an initial variant is proposed, showing the stress distribution generating the 3D geometry of the knitted surface.

Key-words: 3D knitted fabric, spatial fashioning, fashioning line, basic element, modeling

Systemische Angehung des Entwurfs von Abstandsgewirken. II Teil

Die Abstandsgewirke vertreten eine Entwicklungsrichtung mit besonderem Potential, insbesondere in technischen Anwendungen und werden in drei Gruppen eingeteilt: Multischicht/Multiaxialestrukturen, Sandwich/Spacerstrukturen und Raumkonturstrukturen. Die Hauptfertigungstechnik der Raumkonturstrukturen ist das Wirken von unvollständigen Reihen. Die Übereinstimmung der 3D-Form des Produktes mit der 2D-Entwicklung des Gewirkes setzt voraus die Definierung der Basiselemente und der Konturlinien. Vom Sichtpunkt der 3D-Form, repräsentieren die Konturlinien die nötigen Schnittlinien um die Entwicklung zu generieren und von deren Sichtpunkt repräsentieren sie Gewirkzonen mit unvollständiger Nadelanzahl. Die Basiselemente und die Konturlinien können parametrisiert werden und erlauben somit den Entwurf der Gewirke in Übereinstimmung mit der gewünschten 3D Form. Für die Modellierung der Abstandslage der Gewirke wird ein ursprüngliches Modell vorgeschlagen, welches die Distribution der Kräfte, welche die tridimensionelle Geometrie des Materials generiert, hervorhebt.

Stichwörter: Abstandsgewirke, Raumkonturierung, Konturlinie, Basiselement, Modellierung

The shape of textile fabrics/products is an important factor in the design stage, because it influences the selection of the raw material, structure and technology. The 3D fabrics are found in different applications, many times a certain destination imposing the shape of the fabric/product. The field of technical textiles is the one where the complex shape fabrics had the most significant development, due to the high level of the applications, the restrictions imposed by the specific requirements, the process of the high performance raw materials and the need to simplify the subsequent processing.

Spatial fashioned fabrics are fabrics where the 3D geometry is obtained through fashioning, when the knitting is carried out on a variable number of needles [1–6].
The 3D geometry is generated by the different amount of rows knitted along the panel width, the surplus stitches being placed spatially. These fabrics are produced on electronic flat knitting machines for which the carrier course is variable.

DESIGN OF KNITTED FABRICS WITH SPATIAL GEOMETRY

The design of such fabrics considers two aspects: the fabric shape and the fabric structure and structural parameters.
When considering the fabric shape, the 3D geometry is obtained using fashioning lines that were classified and discussed in the first part of this paper [7]. The most important parameters for the design of a fashioning line are:

- The line increment Δa and Δr, representing the number of needles (wales) that stop/start working and the number of rows at each variable stroke;
- The line geometrical parameters – its dimensions (height h and width l) and slope;
- The missing index (the number of rows when a stitch misses due to working on a variable number of needles);
- The shape amplitude H, representing the height of the spatial fabric in reference to its original planar geometry.

* Part II. Part I has been published in Industria Textilă magazine, 2010, vol. 61, issue no. 3, p. 129

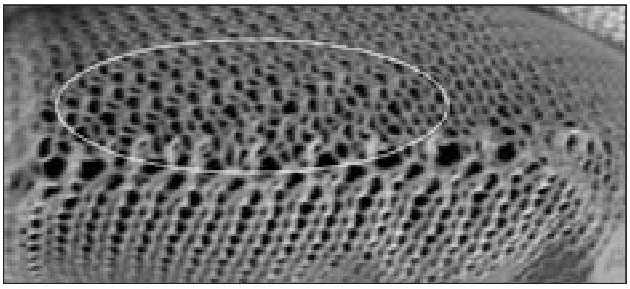

Fig. 1. Non-uniform stitch aspect along the fashioning line, for PES HT fabrics

THE CONTROL OF THE 3D GEOMETRY THROUGH FASHIONING LINES

The shape and the dimensions of the 3D fashioning (including the amplitude) depend on:

- The yarns used – mainly their elasticity modulus and bending rigidity;
- The fashioning lines – increment, slope, missing index, the type of the fashioning line (symmetrical or asymmetrical);

The technological parameters/structural parameters – position of the quality stitch cam/stitch density.

The mechanic characteristics of the yarn are an important factor of the knitting process, influencing the stitch aspect and the amplitude of the spatial geometry. The knitting process implies two types of strains – tensile and bending (at very low curvature radius).

The use of classic yarns, characterised by a higher elasticity modulus and lower bending rigidity favours the 3D geometry, the stitches having a uniform aspect. In the case of high performance yarns (glass, aramid or PES HT) with high bending rigidity and lower proportional limit, specific to high performance fibres (glass, aramids or PES HM, HT), the spatial fashioning rises problems regarding the yarn knittability and the strain distribution in the knitted structure. The spatial amplitude is reduced, and the stitch aspect in the fashioning area is not uniform, as it is illustrated in figure 1.

The fashioning line influences the 3D geometry of the fabric through its increment, slope and type. The following aspects can be mentioned:

- A low increment (as number of needles Δa as well as rows Δr) gives a higher amplitude for the spatial geometry. Actually, it is better to use an increment of Δa = 1, 2 or 3 needles, higher values reducing significantly the spatial geometry of the fabric. The value of Δr can be chosen according to the line slope, generally Δr = 1 or 2 rows. Higher slope and amplitude can be obtained with higher values for Δr, but limits must be imposed, higher values for Δr determining a puckering effect around the fashioning line and therefore an unpleasant fabric aspect.
- Higher slope means higher amplitude of the 3D geometry. Still, the fashioned area is smaller. The line slope is directly related to the line increment and the stitch dimensions.
- The type of fashioning line affects the 3D geometry of the fabric. A symmetrical line will generate a symmetrical geometry, characterised by the highest amplitude. An asymmetrical line will limit the three dimensional effect, depending on the maximum missing index. For example, if all needles are reintroduced into working in the same row, then the fashioning effect appears only in the inferior zone, as illustrated in figure 2.

Fig. 2. Spatial geometry for a fashioning line where all needles restart working at once

The technological parameters and implicitly the structural parameters are extremely important for the spatial fashioning because:

- A lower position for the quality stitch cam (corresponding to higher density and lower stitch length) determines a smaller fashioning effect. Lower values for the stitch length (within technological limits) will increase the 3D geometry.
- The yarn tension also influences the three dimensional effect, higher tension increasing the effect. There are limitations regarding the possible maximum level, depending on yarn type and maximum missing index, in order to avoid yarn break in the missed stitches, especially on the edges and a non-uniform fabric aspect.
- The take-down force must be controlled in the fashioning area, where the take-down values must be lowered. Too much take-down can lead to stitch over tensioning on the fashioning line. In fact, take-down is one of the main technological problems regarding the spatial fashioning due to the different strain state in the fabric.

DESIGN OF THE SPATIAL FASHIONED FABRICS

When designing a spatial fashioned knitted fabric, the basis is the 3D shape, its lateral area being transformed into the 2D plan of the fabric that defines the surface to be knitted and the fabric fashioning. There are more ways of transforming the 3D shape into a plan, according to the basic element used to decompose the lateral area of the solid body, but not all of them are suited for the knitting process.

Regardless of the desired 3D shape, its lateral area must be equal to the area of the fabric. It must be underlined that this equality is not accurate, due to the fact that the knitted fabric is not a continuum. It is made of stitches with certain dimensions. The 3D shape – fabric 2D plan correlation will determine the fabric dimensions, the basic elements and the fashioning lines.

A frustum of a cone is given as an example (fig. 3). The basic element used for the fabric plan is a trapezoid made of two triangles ABC and EDF and a rectangle BCDE.

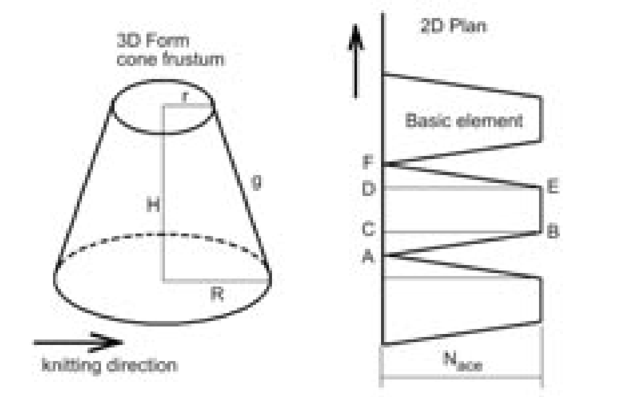

Fig. 3. Frustum of a cone and the fabric plan

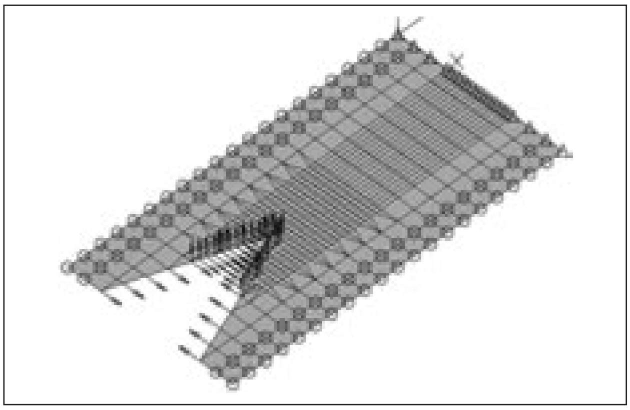

Fig. 4. FEA model

The lateral area of a cone frustum is:

$$A_{tr\ con} = \pi g(R+r) = \pi\sqrt{H^2+(R-r)^2}(R+r) \qquad (1)$$

The area of the basic element is:

$$A_{element} = N_0 \cdot s_0 \cdot n \qquad (2)$$

where:

N_0 = the number of stitches in the basic element;

s_0 = stitch area = $A \cdot B$, mm^2;

A = stitch pitch and B = stitch height;

n = repeats of the basic element within the fabric plan.

The number of stitches in the basic element is determined with the relation:

$$N_0 = 2\sum_{i=1}^{m}(N_{ace} - i\Delta a)\cdot \Delta r + N_{ace}\cdot N_r \qquad (3)$$

where:

N_{ace} = number of working needles in one bed;

N_r = number of rows where all needles are working (corresponding to rectangle BCDE from the basic element);

m = increment repeats on the fashioning line;

Δa, Δr = increment of the fashioning line.

The lateral area of the 3D shape is equal to the fabric area:

$$A_{tr\ con} = A_{tricot}$$

and therefore

$$A_{\text{tr con}} = \pi g(R+r) = \pi\sqrt{H^2+(R-r)^2}(R+r) = = A_{\text{fabric}} = 2\sum_{i=1}^{m}(N_{\text{ace}} - i\Delta a)\cdot \Delta r + N_{\text{needles}}\cdot N_r \qquad (4)$$

The following relations define the equality between the dimensions of the cone frustum and the fabric plan:

$$\pi r = n \cdot N_r \cdot B \qquad (5)$$

$$\pi R = n\cdot(N_r + 2m\cdot\Delta r)\cdot B \qquad (6)$$

$$g = N_{\text{ace}}\cdot A \qquad (7)$$

$$\pi(R-r) = n\cdot 2(m\cdot\Delta r) \qquad (8)$$

The stitch height and pitch are established in an initial design stage, according to the machine characteristics (gauge), yarn count, T_{tex}, and technological parameters, especially the position of the quality cam. The equations presented above give the repeats of the basic element and the repeats of the fashioning line increment, m, as well as the number of rows where all needles work, N_r.

MODELLING SPATIAL KNITTED FABRICS

In order to create a model simulating the fabric geometry in the fabric zones with spatial geometry, an initial model generated with flat elements is used. The model offers 5 degrees of freedom per node (three translation and two rotations). This initial model is based on the simplifying hypothesis of considering the fabric a homogenous material, with the physical mechanical properties of the yarn throughout its mass. The mechanical properties are illustrated in table 1 for two types of technical yarns. The fabric thickness was considered to be 0.3 cm.

In order to simulate the fabric behaviour, the model was considered fixed at its superior part (all degrees of freedom are constrained). On the fabric edges, only the *z*-axis translation and the *x*-axis rotation were constrained. This way, only the edges displacement in the xy plan is modelled, situation that corresponds to reality. The considered load is given by forces concentrated in the nodes that are acting along the x and zaxes, their values being 20 N for the *x*-axis and 10 N for the *z*-axis. These values represent the forces that are considered to be required, to pull the spatial fabric back into the plan. The forces are placed in the nodes defining the spatial zone and have a triangular variation. The maximum value is placed at the edge zone for *x*-axis (corresponding to the maximum stitch missing index), and in the area of maximum spatial amplitude for y-axis.

The data was processed using FEA Algor v 20.2 software. The resulting model is illustrated in figure 4.

The preliminary results show the presence of a strain state in the fashioned areas that forces the fabric to a

Table 1

YARN TENSILE CHARACTERISTICS

Yarn	Breaking force, N	Tenacity, cN/tex	Young, N/tex	Elongation, %	Resilience, J/g
Glass 408 tex	229.87	56.34	84.65	2.46	6.86
PES HT 2 · 114 tex	149.24	65.51	6.22	17.37	64.03

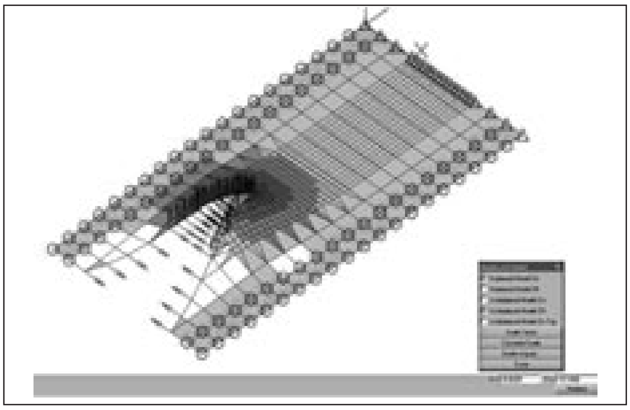

Fig. 5. Model with deformations

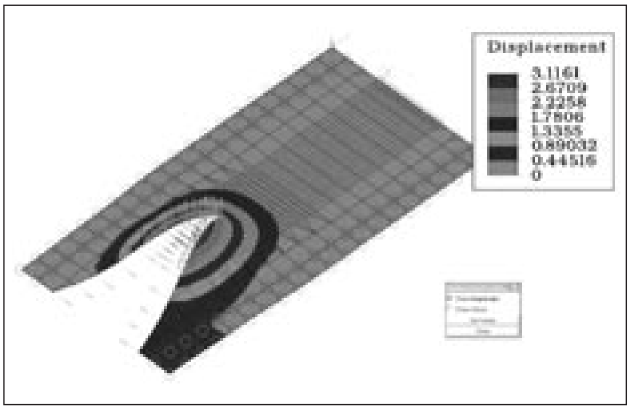

Fig. 6. Displacement distribution according to model

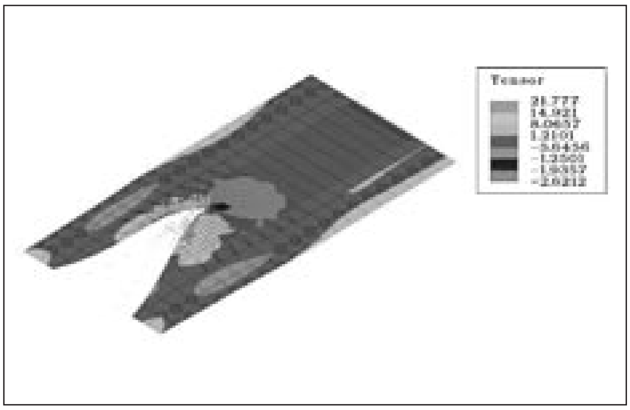

Fig. 7. Distribution of normal stress σ_y

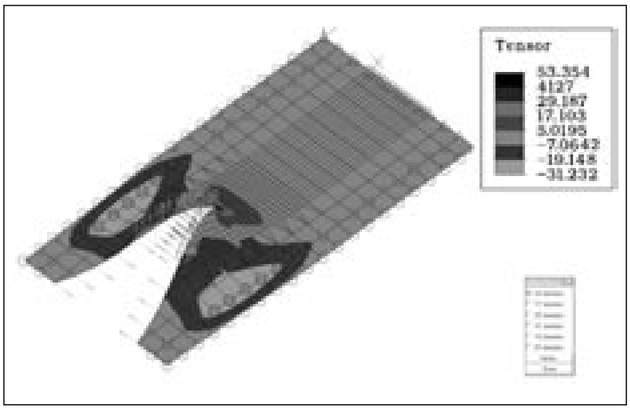

Fig. 8. Distribution of normal stress σ_x

spatial geometry. The simulation gives information regarding the zones where the generated tension is transferred, characterised by tensile and compression strains.

Following the model processing, the results obtained are illustrated in figures 5 to 8.

Different variants of loading were considered, in order to obtain the model, characterised by different deformation possibilities. The comparison with the real geometry led to the presented loading variant. The model gives a general idea over the forces within the systems.

CONCLUSIONS

The knitted fabrics with three-dimensional architecture represent a dynamic domain of the knitted structures, especially for technical applications. The spatial fashioned fabrics have a significant development in the recent period, the literature offering a significant amount of references concerning these applications.

The design of spatial knitted fabrics, regardless of the desired 3D shape, concerns the basic elements of the resulting 2D fabric plan and the parameters of the fashioning lines. The knowledge of the spatial effect generated by the fashioning lines is required for an accurate design, as well as the influence of different factors (type of yarns, type of fashioning line, technological parameters).

The fabric and the basic elements dimensions, the fashioning line dimensions, are determined based on the equality between the lateral area of the 3D shape and the area of the 2D fabric plan, taking into consideration the structural parameters (stitch densities, stitch dimensions).

The next step in designing spatial fabrics is the modeling of the 3D geometry considering the forces that generate this geometry. The model presented in the paper is an initial step in modeling for this type of knitted fabrics. The model is based on the simplifying hypothesis that the fabric is a homogenous material, which is characterized by the properties of the raw material throughout its mass. The next stage will be to generate a model considering the real stitch geometry.

Acknowledgements

The current paper is published in the frame of the research project PN II ID 376/2007, financed by the Romanian Government, through CNCSIS.

BIBLIOGRAPHY

[1] Ciobanu, L. *Contribuţii la producerea şi dezvoltarea tricoturilor cu destinaţii tehnice.* Teză de doctorat. Universitatea Tehnică Ghe. Asachi, Iaşi, 2003

[2] Cebulla, H., Diestel, O., Offerman, P. *Modelling and production of fully fashioned biaxial weft knitted fabrics.* TECNITEX 2001, AUTEX *"Technical Textiles: Designing Textiles for Technical Applications"*, vol. I, editor Araujo, M.D., Portugal, 2001, ISBN 972-98468-3-9, p. 263

[3] Dias, T., Fernando, A., Choy, P. K., Xie, P. *Knitting seamless three-dimensional shell structures on modern electronic flat bed knitting machines.* Bolton College, 1999, p. 36

[4] Song, G., Wu, J., Wei, Y. *Computer aided-design of three-dimensional knitwear.* In: JOTI, vol. 97, nr. 6, p. 549
[5] Power, J. *Knitting shells in the third dimension.* In: JTATM, vol. 4, nr. 4, 2004, p. 1
[6] Hong, H., Araújo, M. D., Fangueiro, R. *The use of flat knitting machines for the production of 3D technical fabrics.* TECNITEX 96, Torino, 21–23 November, 1996. Congress Papers, vol. 2. Centro Tessile Cotoniere e Abbigliamento, Firenze, p. G 47-G 53
[7] Ciobanu, L., Dumitra, C., Filipescu, F. Systemic approach to the design of knitted fabric with three-dimensional architecture. Part I. In: Industria Textilă, 2010, vol. 60, issue 3, p.129

Authors:

Dr. ing. LUMINIȚA CIOBANU
Asistent FLORIN FILIPESCU
Universitatea Tehnică Ghe. Asachi
Facultatea de Textile-Pielărie și Managementul Industrial
Bd. D. Mangeron nr. 53, 700050 Iași
e-mail: lciobanu@tex.tuiasi.ro

Conf dr. ing. CĂTĂLIN DUMITRAȘ
Institutul Național de Inventică
Bd. Carol I nr. 3–5, 700506 Iași
e-mail: dumitrascata@yahoo.com

DOCUMENTARE

Nanotehnologie

PROIECTUL NANOSILVER PRIVIND IMPACTUL NANOPARTICULELOR DE ARGINT ASUPRA MEDIULUI

Cu toate că peste 1 000 de kg de particule de nano-argint sunt deja folosite, în fiecare an, în zonele sensibile din punct de vedere ecologic, se cunosc extrem de puține informații despre efectele lor asupra mediului.

Cercetătorii de la ***Institutul Hohenstein***, din Bonnigheim/Germania, împreună cu 16 parteneri – din instituții de cercetare, industrie și autorități de reglementare – lucrează la un proiect major, pentru a investiga comportamentul, localizarea și efectul particulelor de argint asupra mediului înconjurător.

Rezultatele acestei acțiuni, efectuată ca răspuns la apelul Ministerului Federal al Educației și Cercetării din Germania, pot fi de folos pentru industria textilă, în creșterea competitivității acesteia, dar și pentru publicul larg.

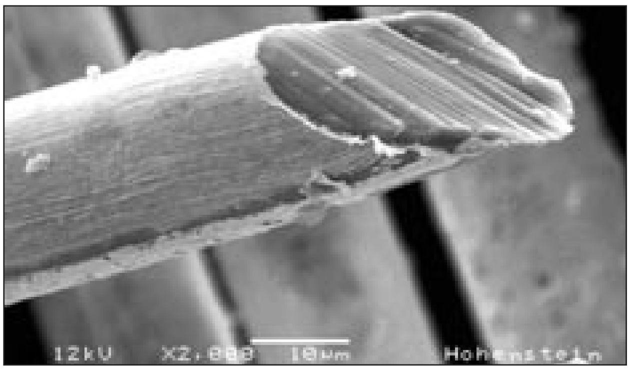

Fig. 1

Textilele tratate cu nanoparticule de argint (fig. 1) nu produc niciun efect dăunător asupra mediului înconjurător.

Institutul Hohenstein pentru Inovarea Textilelor dorește, pentru prima dată, să facă lumină în ceea ce privește efectul, din punct de vedere ecologic, al tratamentelor cu nanoparticule de argint aplicate produselor textile, utilizate zi de zi.

Efectul antimicrobian al nanoparticulelor de argint, folosite de secole pentru purificarea apei potabile, și nu numai, previne colonizarea textilelor cu bacterii patogene sau cu bacterii care cauzează mirosul neplăcut. Textilele tratate în acest fel sunt utilizate pentru diverse aplicații, incluzând:

- textilele medicale – lenjeria de corp specială pentru cei care suferă de neurodermatită, halatele pentru operații, bandajele;
- îmbăcămintea pentru sport și agrement;
- echipamentele individuale de protecție;
- textilele de interior – pături și perdele;
- textilele tehnice, inclusiv cârpe de curățat și filtre.

Liderul de proiect, Dr. Edith Classen, dorește să demonstreze că acest tratament nu are niciun efect dăunător asupra microflorei din apă, sol sau apele subterane: *„Cu acest proiect major, umplem un gol în cercetarea textilă... Datele obținute privind mărimea, forma și proprietățile de suprafață ale nanoparticulelor de argint vor forma o bază de date importantă pentru evaluarea riscului pe care îl pot prezenta textilele tratate cu aceste nanoparticule pentru mediul înconjurător".*

Pe parcursul proceselor de producție a materialor textile, de utilizare, spălare sau deversare a apelor reziduale, argintul nu afectează diversele medii cu care vine în contact, ci are un efect antibacterian.

Smart textile and nanotehnology, februarie 2011, p. 10

Quality evaluation model for clothing materials

CRISTIAN-CONSTANTIN MATENCIUC IONUȚ DULGHERIU

REZUMAT – ABSTRACT – INHALTSANGABE

Model de evaluare a calității materialelor destinate realizării vestimentației

Lucrarea prezintă un model de evaluare a calității unei grupe de materiale alcătuite din înlocuitori de piele, destinate realizării articolelor de vestimentație pentru femei. Deși există diverse modalități de abordare, în prezentul articol s-a folosit noțiunea de indice global de confort, stabilit în baza determinării și cuantificării indicatorilor de influență a confortului termofiziologic și senzorial, care – împreună cu indicatorii specifici valorii de prezentare și durabilitate – pot exprima per ansamblu valoarea de întrebuințare a materialelor, produselor și structurilor vestimentare.

Cuvinte-cheie: confort termofiziologic, confort senzorial, indice global de confort, comportare în mediu umed, izolare termică, permeabilitate la aer, etalon

Quality evaluation model for clothing materials

The paper presents a quality evaluation model for a group of materials made of leather substitutes, intended for the manufacture of women clothing products. Even if there are various other approaches, the notion "global comfort index" is introduced here, being set on the basis of determination and quantification of indicators influencing the sensorial and thermo-physiological comfort, which – together with the specific indicators of the sustainability and presentation value – can express on the whole the usage value of the clothing materials, products and structures.

Key-words: thermo-physiological comfort, sensorial comfort, global comfort index, behaviour in wet environment, thermal insulation, air permeability, benchmark

Qualitätsbewertungsmodell für Bekleidungsmaterialien

Die Arbeit präsentiert ein Qualitätsbewertungsmodell einer Materialgruppe von Ledersubstituten bestimmt für Damenbekleidungsartikel. Obwohl unterschiedliche Angehmethoden existieren, wurde im Artikel der Begriff „Globales Komfortindikator" verwendet, bestimmt und kuantifiziert aufgrund der thermophysiologischen und sensoriellen Einflussindikatoren, welche – gemeinsam mit den spezifischen Indikatoren der Werte für Vorstellung und Nachhaltigkeit – den Gesamtutzwert der Materialien, Produkte und Bekleidungsstrukturen ausdrücken kann.

Stichwörter: thermophysiologischer Komfort, sensorieller Komfort, Globales Komfortindikator, Nassverhalten, thermische Isolierung, Luftpermeabilität, Muster

Although the research in the field of clothes and shoes highlight as a main objective the accomplishment of a much higher dimensional correspondence between body and product, it was considered that the general comfort state is not influenced by this correspondence.

The knowledge of the objective and precise determination of the main features of the ensemble of sanogenetic indicators become thus relevant: the air permeability, vapour permeability, hygroscopicity, hydrophilicity, porosity and thermal conductivity etc.

Since the notion of quality is defined by an ensemble of features and – even if connections between the sanogenetic indicators may be made – the indicators that characterize the presentation value, the durability indicators and the indicators specific for the behaviour at wearing, are conditioned, each of them, by a multitude of influential factors. The research proves that the relations are stronger in the case of physiological or sanogenetic indicators.

Under these conditions, the research of the present paper was focused especially on the influencing indicators of the thermal and physiological comfort, without neglecting some factors defining the sensorial comfort.

Clothing, by its structure, has the capacity to influence the physiological functions of the human being and has in its turn similar functions with the skin, namely those of protection and thermal regulation; it can be thus granted the quasi-physiological character. It can also be considered as "the second skin", ensuring a full mobility of the person who is dressed. All these features are included in the quality ensemble that cannot be isolated from the usage value and generally from the products value.

From a physiological point of view, the main role of the clothing used by people is to ensure the load of the blood flow and the full use of physical and intellectual abilities of the human being, by creating a comfort sensation, of well-being, even in an unfavourable environment, even harsh to stand.

The normal thermal process of the human body is ensured only by the conditions in which the clothing owns the three essential properties that define quality from this point of view, namely: the capacity for thermal insulation (of retaining the heat of the body), the capacity for continuous absorption of humidity and its evaporation, and the capacity of permanently airing the body.

The present research focused on a number of ten articles, most of them leather replacements/substitutes on a textile support, subjected to a superior chemical finishing process, the main features being the coating with vinyl poly-chloride, materials that can be especially used to make light products intended for women. Among such products there are jackets, waistcoats, evening gowns etc.

They are recommended to be used in seasons with moderate temperatures and as a last layer in the clothing ensemble.

As it was already specified, experimental research was done not only for the features specific to the sensorial

Table 1

Name	Hydrophily, *H*, mm				Hygroscopicity, I_h, g/m^2 · h		Vapour permeability, μ, g/m^{2}h		Air permeability, *Pa*, l/sm^2		Thermal insulation, λ, kcal/m·h·c		Porosity, P_z, %		Global index	
	U	*p*	*B*	*p*	Value	*p*	Value	*p*	Value	*p*	Value	*p*	Value	*p*	*U*	*B*
Novomat extra	118	100	118	100	0.127	62.79	4.33	62.39	0.693	16.64	0.035	87.5	33.75	55.17	384.49	384.49
Arel	28	23.72	3	2.54	0.0404	11.59	4.75	68.44	2.08	50	0.0272	68	50.46	82.49	304.24	283.06
Lancansin 2	5	4.23	12	10.16	0.08	22.96	3.98	57.34	2.49	60	0.028	70	40.6	66.37	280.9	286.83
Novomat extra 1	13	11.01	2	1.69	0.3483	100	4.68	67.43	1.387	33.2	0.026	65	27.23	44.51	321.15	311.83
Lancansin 4	92	77.96	60	50.84	0.0062	1.78	6.94	100	2.765	66.4	0.036	90	61.17	100	436.14	409.02
Lancansin 3	10	8.47	10	8.47	0.1329	38.15	3.37	48.55	3.740	90	0.0319	79.75	50.60	82.72	347.64	347.64
Alsin 2	115	97.45	105	88.98	0.2808	80.62	5.41	77.95	0.693	16.64	0.037	92.5	35.83	58.57	423.73	415.26
Lancansin 1	72	61.10	92	77.96	0.1254	36	3.15	45.38	1.387	33.2	0.035	87.5	51.63	84.40	347.58	364.44
Altin	2	1.69	0	0	0.0479	13.75	5.54	79.82	2.08	50	0.023	57.5	51.05	83.45	286.21	284.52
Lancansin 7	78	66.10	40	33.89	0.0841	24.14	4.12	59.36	4.165	100	0.040	100	59.59	97.41	447.01	414.8

comfort that generally define the touch of materials in contact with the human body, but also, after establishing the thermo-physiological comfort index, as well as the sensorial comfort index, these were incorporated in a total index that may express the ensemble quality of materials and products.
This index may lie at the basis of the scientific research of clothing materials, products and structures and, in this context, it was necessary to establish an ensemble of variants, for which limits were determined for the comfort influence parameters, which also explains the numerical expression of their usage value. This manner of defining the quality is imposed when, within the same group of materials, a great number of variants is included and the technologies for products manufacture are alike.
From the centralized tables that made up databases, apart from some structural properties of materials, treatments and special names of these result. These data were at the basis of the mathematical modelling, by means of 2D and 3D system processing, in the first case using the Excel software program and, in the latter, the application TableCurve 3D v2, designed by the company Jandel Scientific Software.

THE THERMO-PHYSIOLOGICAL COMFORT INDEX

The thermo-physiological comfort is determined by the interaction between body and environment and it is reached when the heat and humidity transport from the body through the clothing is regulated in such a way that the energy of the human body is balanced and, in the clothing microclimate, there are values of temperature and humidity felt as comfortable.
In order to ensure the thermo-physiological comfort, the lingerie or sports products must absorb the intense perspiration and transmit it to the surrounding environment.
In the case of coated materials under study, the possibility of their use should be analysed in such clothing products and structures so that, under appropriate micro- or macroclimate conditions, they should ensure a corresponding comfort state.
Even if they have reduced air permeability, this is compensated by their vapour permeability, as well as by a thermal conductivity within admitted limits, specific to the materials intended for clothing products. As it is also shown by the tables containing centralized experimental data, these materials have as well accepted values for hygroscopicity, hydrophilicity and even for porosity, parameter involved in the modification of the general comfort state.
The values calculated for different comfort characteristics may be included, through corresponding shares, in an index conventionally called global comfort index. This index may be at the basis of designing on scientific criteria both the products, and the clothing structures, but it can also allow the appreciation from a qualitative point of view of the textile surfaces, leathers and substitutes.
During the present stage of the test technique in the field of clothing products, when replacing the long-term and expensive tests at wearing with the laboratory tests, a main requirement is represented by the figure expression of some specific indicators, with the aim of appreciating the quality of any material intended for clothing products. As a consequence, the comfort indices are determined starting from the values of some characteristics considered as "benchmarks", no matter what their function and index, for which a 100 score is assigned.
If low values are imposed for a certain characteristic, the calculi are made by means of the inverse proportion rule, that is the 100 score is multiplied by the corresponding value and it is divided by the higher value. The *P* score is thus obtained, assigned to the other variant.
The thermo-physiological comfort index highlights the limits of the comfort parameters that can lie at the basis of the design norms setting on scientific criteria, for various clothing ranges and items. As long as new variants having the same use may appear, the framing within the limits of the global comfort index may be tested, as well as that of other newly designed clothing items and structures.
The included characteristics with their corresponding shares in the value of the thermo-physiological comfort index are hydrophilicity, hygroscopicity, vapour permeability, air permeability, porosity and thermal insulation. The determination methods and the calculus procedures comply with those used by the specialty literature [1, 4, 5, 6].
The values obtained for the thermo-physiological comfort index are included in table 1, with the specification

Table 2

Item	Drapeability		Flexibility								Creasing				Global index	
			U				B				U		B			
	Cd, %	p	S, f(h)	p	S, f(h)	p	S, f(h)	p	S, f(h)	p	λ, %	p	λ, %	p	U	B
Novomat extra	62.5	100	77	92.77	78	66.66	88	100	80	89.88	83	83	73	73	342.43	362.88
Arel	52.8	84.48	77	92.77	71	60.68	86	97.72	89	100	95	95	97	97	332.93	379.2
Lancansin 2	37.6	60.16	69	83.13	117	100	80	90.90	86	96.62	98	98	100	100	341.29	407.84
Novomat extra	49.7	79.52	76	91.56	73	62.39	80	90.90	87	97.75	88	88	88	88	321.47	356.17
Lancansin 4	53.4	85.44	78	93.97	92	78.63	82	93.18	88	98.87	93	93	80	80	351.04	357.49
Lancansin 3	60.0	96.04	82	98.79	108	92.3	81	92.04	84	94.38	97	97	80	80	348.13	362.46
Alsin 2	42.2	67.6	70	84.33	62	52.99	78	88.63	89	100	80	80	73	73	284.92	329.23
Lancansin 1	60.03	96.04	80	96.38	87	74.35	78	88.63	86	96.62	98	98	91	91	364.77	372.29
Altin	47.3	75.68	80	96.38	88	75.21	79	89.77	87	97.75	79	79	90	90	326.27	353.2
Lancansin 7	61.8	98.88	83	100	91	77.77	88	100	87	97.75	100	100	86	86	376.9	382.63

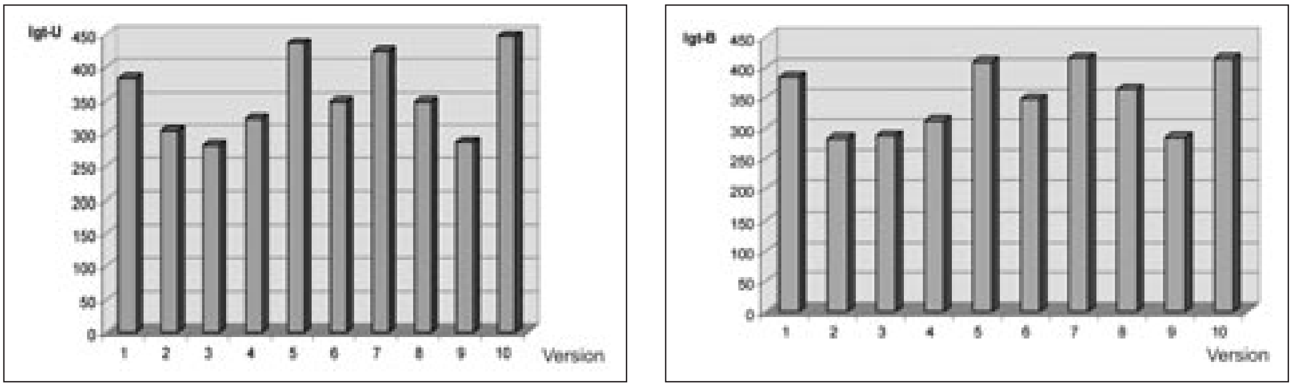

Fig. 1. Thermo-physiological comfort index

that the corresponding scores set for the two directions, respectively warp and weft, were summed up accordingly. As the contents of the tables and the graphical representations from figure 1 show, it was used the analysis of the limits for a group of 10 materials, without too many differences for the two directions. As the charts show, the thermo-physiological comfort index was noted with Igt-U on the warp direction and with Igt-B on the weft direction. Taking into account that, at the increase of material volume, that is of porosity, the contents in vapour assimilated by the environment also increases, a 3 D system processing was used, as also previously shown, by means of applying the TableCurve 3D v2, designed by the company Jandel Scientific Softwaer. It was also considered the way the air permeability may be associated with these parameters. The chart from figure 2 allows interpretations in this respect, taking into consideration the function displayed with the adequate correlation coefficient. General interpretations may also be made in the case when the hygroscopicity is replaced with the thermal insulation or the vapour permeability. Thus, the displayed mathematical model having the form:

$$z = a + b/x + c \cdot y$$

was verified with the average values for hygroscopicity z, porosity x and air permeability y, under the conditions:

$$a = 0.22;\ b = 15.4;\ c = 0.02$$

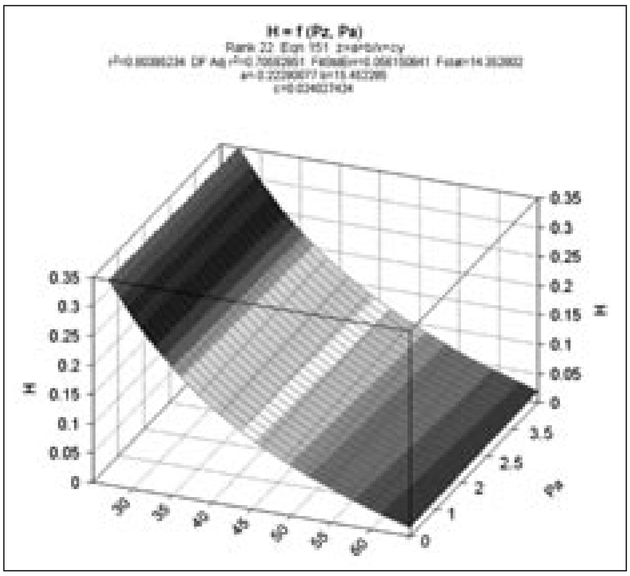

Fig. 2. The relation between hygroscopicity, air permeability and porosity

THE SENSORIAL COMFORT INDEX

The sensorial comfort is determined by the sensations felt at contact, the mechanical touch between the material and skin. The lingerie being the first textile layer on the body, must ensure an optimal sensorial comfort. In this respect, on one hand, agreeable sensations, such as smooth, flexible, etc and, on the other hand, non-agreeable, irritating sensations, such as coarse, scratching, stinging, sticking may be addressed. For example, as for knits, the contact surfaces with the body may be described by the size and position of stitches in the knit, as well as by the thread thickness and surface. As the sensations felt during the contact

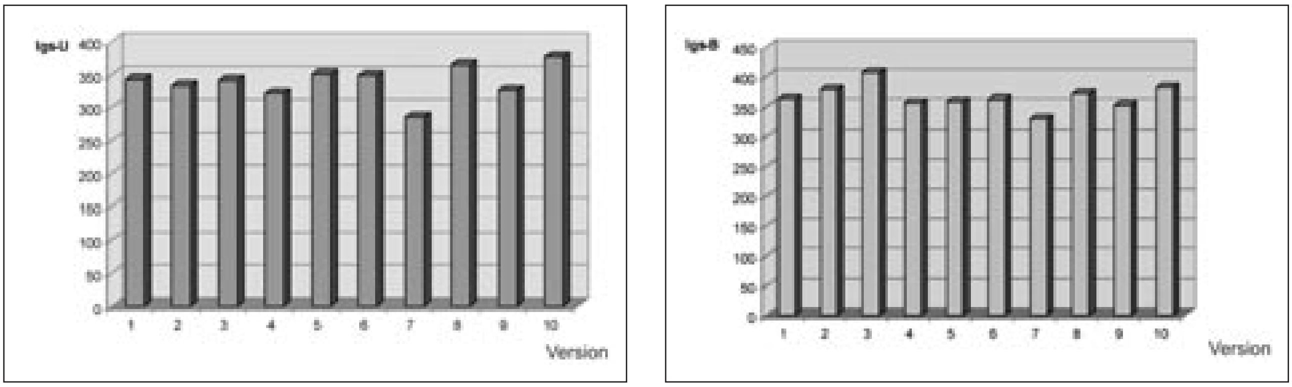

Fig. 3. The chart of the sensorial comfort index

Table 3

Item name	Global index 1		Global index 2		Total index	
	U	*B*	*U*	*B*	*U*	*B*
Novomat extra	384.49	384.49	342.43	362.88	726.92	747.37
Arel	304.24	283.06	332.93	379.2	637.17	662.26
Lancansin 2	280.9	286.83	341.29	407.84	622.19	694.67
Novomat extra 1	321.15	311.83	321.47	356.17	642.62	668
Lancansin 4	436.14	409.02	351.04	357.49	787.18	766.51
Lancansin 3	347.64	347.64	384.13	362.46	731.77	710.1
Alsin 2	423.73	415.26	284.92	329.23	708.66	744.49
Lancansin 1	347.58	364.44	364.77	372.29	712.37	736.73
Altin	286.21	284.52	326.27	353.2	612.48	637.72
Lancansin 7	447.01	414.8	376.9	382.63	823.91	797.43.

between material and skin are difficult to evaluate, in order to define the touch [6], the following characteristics were set: draping, flexibility and creasing. The calculi for the scores and for the sensorial comfort index in the two directions were grouped in table 2, while the graphical representations are presented in figure 3. As in the case of the thermo-physiological comfort, minor differences were perceived in the two directions. The sensorial comfort index was noted with Igs-U on the warp direction and with Igs-B on the weft direction. The notations are viable also when it is about the direction of wales or rows: if the textile support is made of knitwear. It is to be noticed that these materials are characterized by a special flexibility, which has an important weight in the value of the sensorial comfort index. It should also be specified that the thickness of these materials is also recorded in limits very close to 0.34–0.4 mm.

The 3D system processing allowed the obtaining of a complex interdependence function between creasing, flexibility and draping, as it results from figure 4. The selected complex mathematical model is inserted in the figure, together with the correlation coefficient. This is also verifiable, as in the case of the thermo-physiological comfort index. The same significances being involved for *y*, *x* and *y*, the mathematical model is of the form:

$$z = a + bx + c/y$$

THE GLOBAL COMFORT INDEX

The global comfort index was obtained by summing the thermo-physiological comfort index and the sensorial comfort index. The obtained values, on which the graphics from figures 5 and 6 were drawn, are centralized in table 3. For each variant, similar values for the two directions are highlighted and, for the entire group, there are close limits for all materials, which have in fact the same use.

The results of the research about the setting of the global comfort index are associated with the goal of scientific processing of products, especially when they correspond to a range of variants and to a great number of determinations.

These also contribute to the numerical expression of the usage value of products, in relation to the properties under analysis. In this case, too, after the processing in

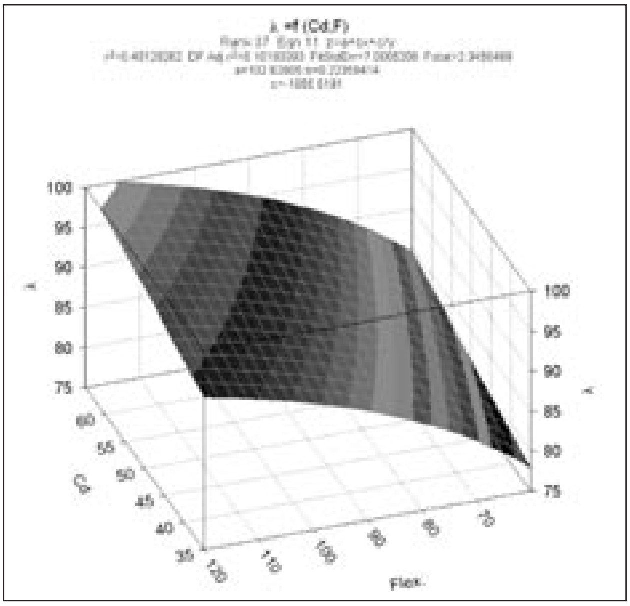

Fig. 4. The relation among creasing, draping and flexibility

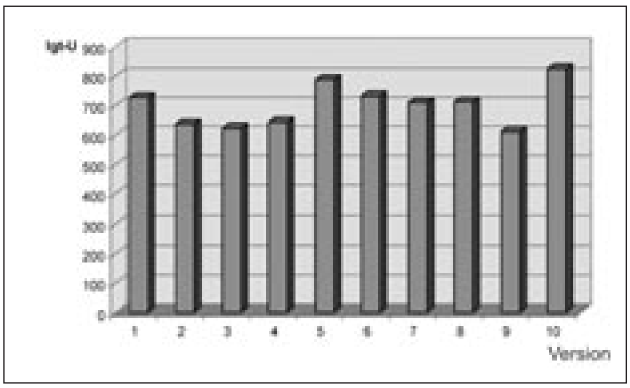

Fig. 5. The chart of the global index (warp)

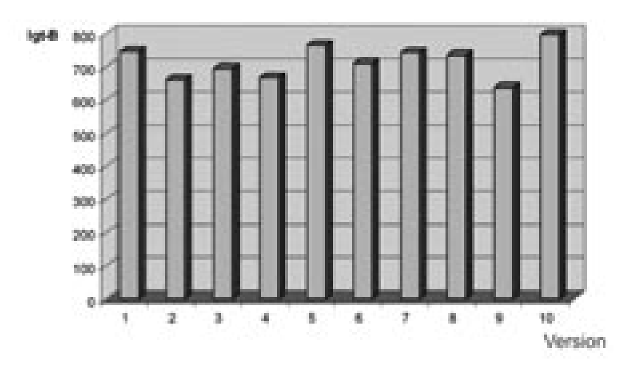

Fig. 6. The chart of the global index (weft)

the 3D system, interdependences were set between the total or global comfort index and the sensorial comfort index, on one hand, and with the thermo-physiological index on the other hand. The graphics from figures 7 and 8 allow related evaluations, also proving that the direction of test orientation does not allow the value of the global comfort index.

The global comfort index [7] resulted after the addition of the scores for the studied variants, with values written in the tables and graphically represented in ensemble drawings, also highlighted the limits of the comfort indicators that can be at the basis of the completion of design norms. These have, in the present stage, specific properties for all clothing items. In this case, too, as new types of materials having the same use appear, the framing within the limits of the global comfort index may be tested for other newly designed clothing materials, items or structures.

According to the indications from figures 6, and 7, mathematical models were selected in both cases taking the form:

$$z = a + bx + c/y$$

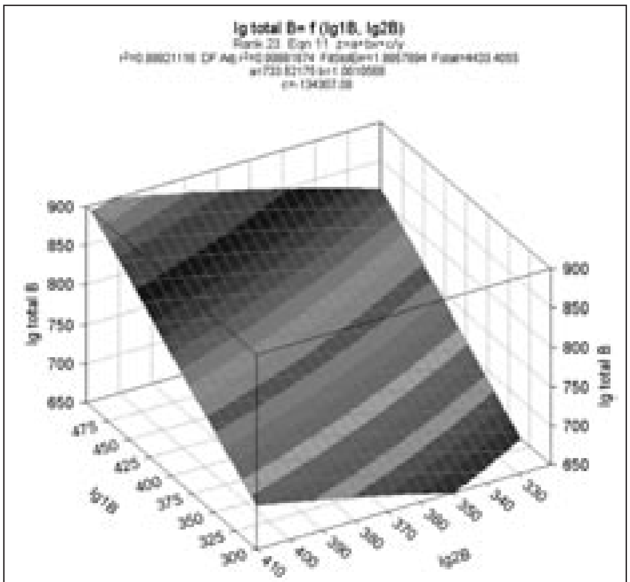

Fig. 7. The relation among the global comfort index and the thermo-physiological and sensorial comfort index (weft)

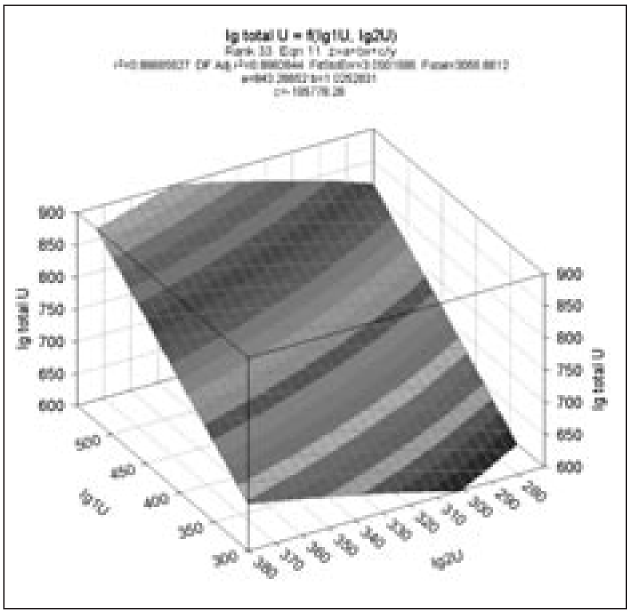

Fig. 8. The relation among the global comfort index and the thermo-physiological and sensorial comfort index (warp)

CONCLUSIONS

- From the analysis of the data recorded in the tables, as well as from the analysis of the variation interval of the values from the graphics, very few deviations from the benchmark are registered, implying that, by using this expression and representation manner, the presence within the variation interval of some other characteristics may be analysed.
- The method of expressing quality based on the calculus of the global comfort index, which in its turn may be included in a global quality index, may be helpful when shaping the notion of quality for adequate clothing materials, products and structures.
- The research may be continued for other variants too, which would contribute to the elaboration of a database very useful in the analysis technique of value.
- The results of the present research may be interpreted accordingly, by means of a minute analysis of charts and limits recorded in the tables, their understanding being also conditioned by the knowledge of the fundamental theoretical essentials of definition, expression and calculus of the clothing comfort parameters.
- The fact that both the thermo-physiological comfort index and the sensorial comfort index have values ranging in the interval 280–450, and the total index, irrespective of its direction, ranges in the same interval, that is 610–820, confirms the truthfulness of the research results, and the proposed model may be extended to other groups of materials.
- From the analysis of tables and charts, we can appreciate that the no. 100 variant may be considered the reference and, on the whole, the benchmark.

BIBLIOGRAPHY

[1] Mitu, S. *Confortul și funcțiile produselor vestimentare.* Editura Ghe. Asachi, Iași, 2000

[2] Mitu,S., Mitu, M. *Modificarea parametrilor fiziologici la diferite condiții de stare și structuri vestimentare cu sacou.* În: Industria Textilă, 2003, issue 2

[3] Mitu, S., Hâncu, S., Căprariu, C., Capmare, L., Ţuca, M. *Transfer de căldură şi masă prin îmbrăcăminte.* În: Industria Textilă, 2007, vol. 58, issue 5
[4] Mitu, S., Hâncu, S., Matenciuc, C., Bârlădeanu, E. *Limitele indicatorilor sanogenetici pentru ansambluri vestimentare cu noi particularităţi structurale.* În: Industria Textilă, 2008, vol. 59, issue 1, p. 14
[5] Mitu, S., Matenciuc, C. C. *Modificarea parametrilor de confort prin utilizarea pieilor naturale în produse vestimentare.* În: Industria Textilă, 2009, vol. 60, issue 1, p. 26
[6] Mitu, S. *Metode şi rezultate experimentale privind stabilirea indicelui global de tuşeu.* În: Industria Uşoară, 1992, issue 1
[7] Mitu, S., Mitu, M. *Relaţia dintre masa structurii vestimentare cu jachetă şi cheltuielile energetice ale organismului.* În: Industria Textilă, 2010, vol. 61, issue 3, p. 17
[8] Loghin, C., Nicolaiov, P, Ionescu, I., Hoblea, Z. *Functional design of equipments for individual protection.* In: Management of technological changes, 2009, vol. 2, p. 693
[9] Loghin, C., Ursache, M., Ionescu, I. *Experimental research on the sewability of ferromagnetic micro-wires.* In: Tekstil ve Konfeksiyon, 2010, vol. 20, issue 4

Authors:

Drd. ing. CRISTIAN-CONSTANTIN MATENCIUC
Drd. ing. IONUŢ DULGHERIU
Universitatea Tehnică Gheorghe Asachi
Facultatea de Textile-Pielărie şi Management Industrial
Bd. D. Mangeron nr. 53–55, 700050 Iaşi
e-mail: cmatenciuc@tex.tuiasi.ro

DOCUMENTARE

Tehnologie chimică

DUBLĂ APĂRARE ÎMPOTRIVA RADIAŢIILOR

Oamenii de ştiinţă de la ***Institutul Hohenstein*** şi ***Denkendorf ITCF*** au dezvoltat primele textile din lume, care împiedică trecerea radiaţiilor electromagnetice (EM) şi infraroşii (IR).

Până în prezent, materialele textile de protecţie puteau să constituie o barieră doar pentru o singură sursă de iradiere – fie contra radiaţiei electromagnetice, fie contra radiaţiei termice, fie contra radiaţiilor solare intense. Fibrelor artificiale le este conferit efectul de screening, fie prin încorporare sau prin acoperirea lor cu oxid de indiu şi staniu (ITO), un compus transparent, utilizat, de asemenea, la ecranele tactile sau telefoanele inteligente.

Fig. 1

Testele efectuate pe materialele textile supuse tratamentului au arătat că acestea posedă o bună rezistenţă la spălare, abraziune şi intemperii. De asemenea, s-a dovedit că tratamentul nu este dăunător din punct de vedere biologic, iar articolele de îmbrăcăminte confecţionate din aceste materiale sunt confortabile în purtare (fig. 1).

„Aceste materiale inovatoare nu numai că sunt extrem de eficiente împotriva radiaţiilor, dar sunt şi bune conducătoare de electricitate, deci au proprietăţi antistatice... Acest lucru le face ideale pentru a fi utilizate atât în fabricarea echipamentelor individuale de protecţie pentru pompieri, lucrătorii din turnătorii şi atelierele de sudură, cât şi în industria semiconductorilor sau pentru personalul de întreţinere care lucrează la sistemele de telecomunicaţii" – a explicat Dr. Edith Classen – şeful de proiect.

De asemenea, noile materiale pot fi utilizate în industria articolelor textile de interior şi a articolelor tehnice. *„Vă puteţi imagina confecţionarea jaluzelelor, de exemplu, care nu numai că împiedică trecerea radiaţiei solare din timpul verii, pentru a menţine camera rece, dar în acelaşi timp, oferă şi o bună protecţie împotriva radiaţiilor electromagnetice, provenite de la stâlpii de telefonie mobilă din apropierea unor imobile"* – a adăugat Dr. Edith Classen.

Aceste materiale multifuncţionale prezintă interes şi pentru domeniul militar, putând fi folosite la confecţionarea uniformelor militare, pentru a face ca purtătorul să fie invizibil pentru camerele video cu infraroşu şi, în acelaşi timp, pentru a oferi protecţie împotriva radiaţiilor electromagnetice.

Smarttextiles and nanotehnology, februarie 2011, p. 7

Performance evaluation module for textile materials

JEAN MARIE BACHMAN
MARCO BARBIERI
IULIANA DUMITRESCU

REZUMAT – ABSTRACT – INHALTSANGABE

Modul de evaluare a performanţelor materialor textile

Obiectivul proiectului EnviroTex-Design constă în dezvoltarea unei platforme de servicii web, pentru întreprinderile mici şi mijlocii din domeniul textile-pielărie. Platforma de design colaborativ are ca scop stimularea colaborării dintre întreprinderi, asistarea utilizatorilor în formularea de întrebări ce răspund nevoii lor de informaţii, găsirea celor mai adecvaţi parteneri pentru a reacţiona rapid la oportunităţile pieţei, îmbunătăţirea modului de diseminare a cunoştintelor între întreprinderile de profil.

Cuvinte-cheie: servicii web interactive, platformă virtuală de design, performanţă, textile

Performance evaluation module for textile materials

The objective of the EnviroTex-Design project is to develop an interactive web-services platform for Clothing & Leather/Footwear SMEs. The Collaborative Virtual Design Platform aims to stimulate collaboration between enterprises, to assist users in formulating queries to meet their information needs, to find the most suitable partners to react quickly to the new market opportunities, to enhance effective knowledge sharing between SMEs.

Key-words: interactive web-services, Virtual Design Platform, performance, textile

Leistungsbewertung der Textilmaterialien

Das Objektiv des Projektes Enviro-Tex Design besteht in der Entwicklung einer Webdienst-Platform für KMU aus dem Bereich Textilien/Leder. Die kollaborative Designplatform hat als Zweck die Stimulierung der Partnerschaft zwischen Unternehmen, die Asistenz der Benutzer in der Formulierung von Fragen entsprechend ihrer Informationsbedürfnissen, die Entdeckung der besten Partner für eine gute Marktänderungreaktionsbereitschaft, die Verbeserung der Dissemination der Kenntnisse zwischen Profilunternehmen.

Stichwörter: Interaktive Webdienste, Virtuelle Designplatform, Leistung, Textilien

To be competitive, the small and medium-sized enterprises needs be innovative, flexible, and reactive to the market demands. Due to globalization and fierce competition, the future market position of SMEs is strongly related to their capacity to cooperate with worldwide partners, and of fast access to the existing knowledge. Currently, information resources are scattered about various web sites, making it difficult for SMEs to efficiently access them. At the same time, the consumers need comfortable, modern, healthy, qualitative and low cost garments.

In this line, the FP7 project *"Virtual Collaborative Design Environment"*, Acronim: *Enviro-Tex-Design*, developed a web-based platform for collaborative Design, Development and Delivery of garments and leather products.

The collaborative platform provides to designers, retailers and manufacturers a quickly and collaboratively guidance of the whole design process from the very beginning till the development of the end product with the desired performance characteristics and special concern to environmental, health and toxicological regulations and standards.

The virtual platform will be an efficient knowledge system and a key success factor for geographically distributed networked enterprises, sharing resources and reacting rapidly to the market demand.

It is the most cost efficient way to create innovative textile and leather products taking into account the international market dynamic changes.

THE STRUCTURE AND COMPONENTS OF THE "COLLABORATIVE 3D VIRTUAL DESIGN PLATFORM"

The platform architecture

To respond to textile and shoes market needs, to automate the product design and to enable marketplace collaboration, the collaborative platform integrates the following modules:

- an intuitive 3D user interface enabling real time interaction between customers and producers;
- performance evaluation module enabling producers and/or designers to assess the performance of their final products during the design phase without the need to manufacture and test physical prototypes;
- an extensive interactive, collaborative digital material library (with access security) which will allow designer owners to help users to choose the textile products (fabric, yarns, fibres, accessories) with required end-use properties and access to their designs anytime anywhere;
- health-environment-safety (EHS) decision making toolbox – to determine the toxicological & environmental impacts in the design stage;
- a dynamic real time simulation and visualisation sub system enabling the transformation of the virtual prototype into a physical one and speeding up the product design and manufacture;
- technical datasheet generator enabling designers to define production process and automate generation of the technical data sheets;
- a regional network of enterprises (Extended Micro-Factory) to fast identification and dynamic setting-up of a supply chain tailored on the new product characteristics, based on objective parameters allowing to assess the rating of both suppliers and customers.

The *"Collaborative 3D Virtual Design Platform"* provides users with information and tools as well as an integration framework to:

– collect information about material's properties and performances;
– select the functionalities and properties of the materials;

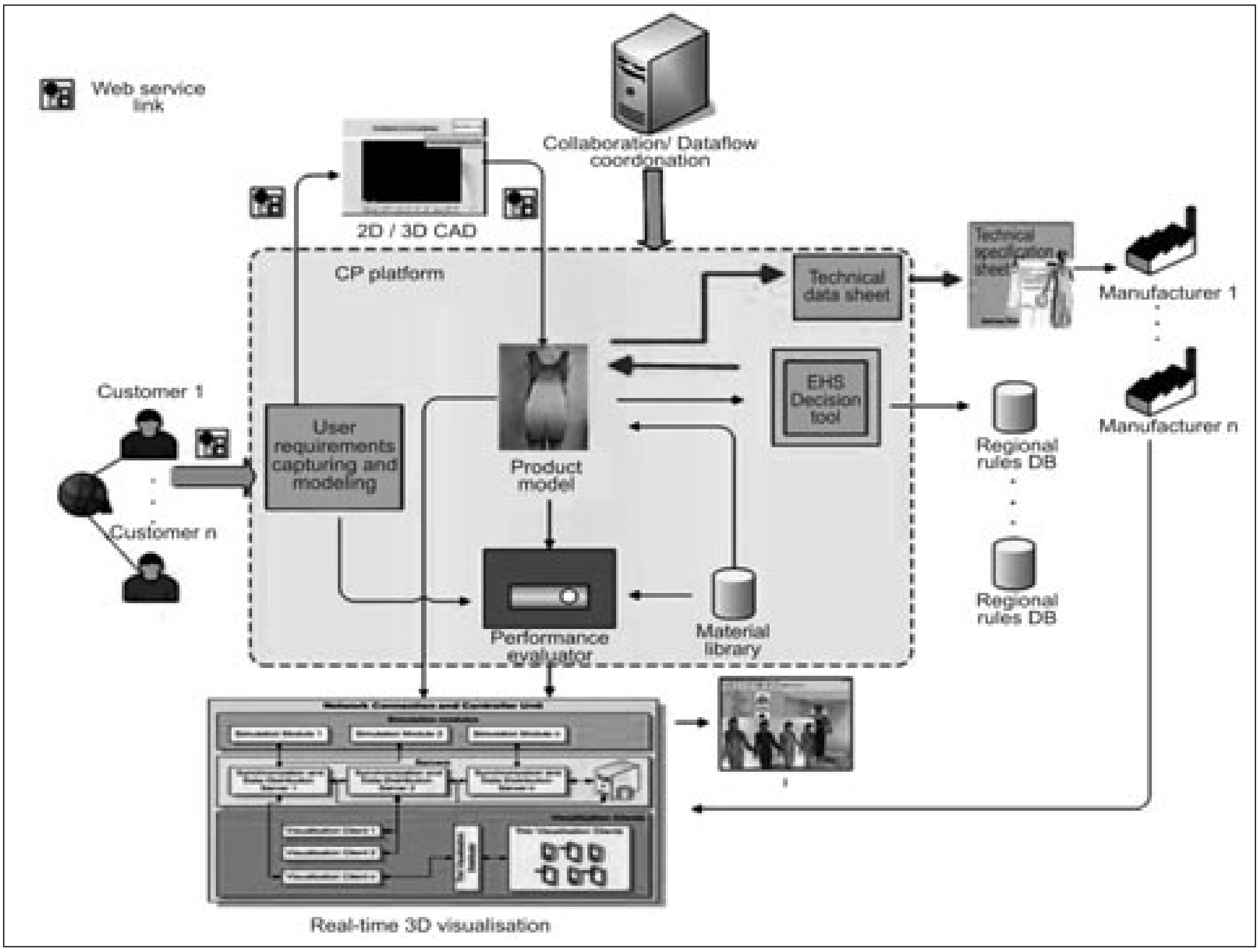

Fig. 1. Collaborative virtual platform

– select the cost-efficient technologies;
– avoid the environmental impact;
– communicate on products' compliance with performance and EHS requests/certifications (anti-allergic, anti-bacterial, eco label), REACH demands;
– generate a data-set of technical sheets and production sheets;
– to select one or several potential partners to involve them in their product chain;
– develop of "Rapid Prototyping" enabling the transformation of the virtual prototype into a physical one;
– develop new products.

The Collaborative Platform (fig. 1) will be a highly optimised and fast network communication for real-time data exchange, enabling designers and producers to define production process and avoid long and expensive testing and sample manufacturing.

PERFORMANCE EVALUATION MODULE (PEM)

PEM is a decision tool to evaluate the global performance of a product before manufacturing. It enables product designers to compare different materials properties, to evaluate the global performance, to select the best functionality of the garment, to benchmark products and components allowing them to create new products, based on selected physical and mechanical textile parameters.

PEM can be used, as separate software or integrated in the collaborative platform, as decision support in textile industry and for studies in research institutes.

The software enables companies to quantify their material performances and identify economically advantageous improvement opportunities, making transparent decision on product development and investments.

The objective evaluation of the performance for the final product (garment) and for the components of the garment (fibers, yarns, fabric) is based on a modeling method combining a variety of non-homogeneous standardized characteristics associated to a product type. The method allows selecting a set of relevant characteristics, defining quantitative scoring combination formula, and calculating the score according to this formula.

It is configurable via user-defined fields, it is interactive (the user can select automatically the data from material library or add manually its own data or introduce the unknown data calculated in Matrix Interaction); it is flexible allowing the selection the desired data from more than 100 properties existing in the material library and in the companies historic database.

The global performance of a product is the result of a mathematical calculation which integrates all parameters considered relevant to quantify the response of the product.

The innovative elements of PEM consist in:
– PEM can calculate the performance of any object and its components no matter the unit measurement and value range of the parameters, the level of involving, the domain of interes etc. (e.g. physical properties, costs, sensitive perceptions, subjective

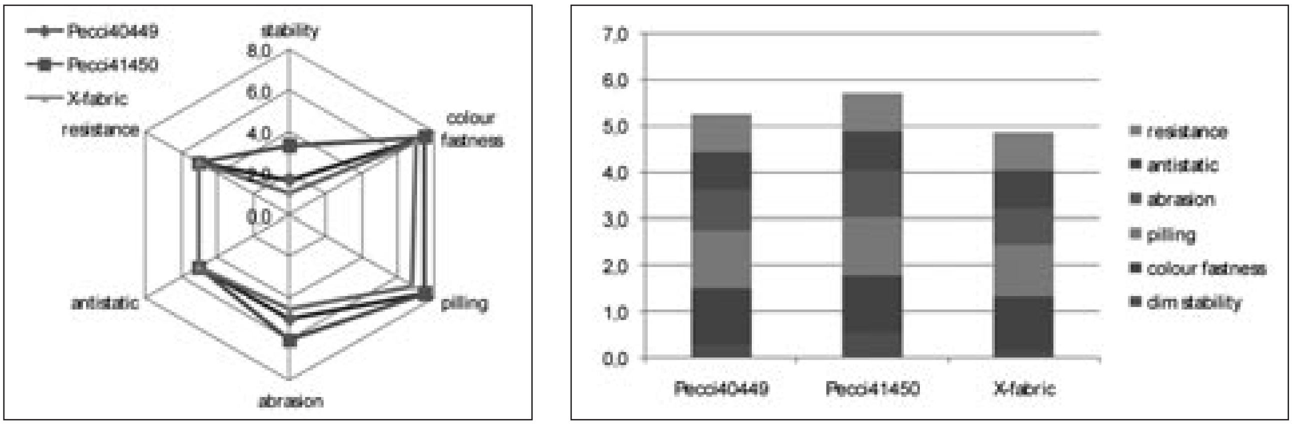

a *b*

Fig. 2

aspects, environmental impacts, safety considerations). The only requirement is that each parameter has an objective numerical value measured (determined) on a standardised scale. All the values are normalized;

- PEM integrates in its calculation weightings which take into account the hierarchical importance of elements entering in the calculation. The weightings are introduced to take into account the use context of the product in the performance evaluation. PEM offers the possibility to give different performance values for the same product in different use contexts. The differentiation of the use contexts is determined by the weightings. These weightings are peculiar to each type of use, so they are defined by the designer/contractor himself;
- PEM calculates the performance based on objective measurements (property values) according to international standards, of the product parameters and on subjective weighing factors.
- PEM calculates the performance and a performance completeness rate. The completeness rate indicates to the user if the performance evaluation takes into account all parameters he has configured for the calculation. Effectively certain parameter values can be missing;
- PEM can extrapolate missing property values using Behavioral Modeling Tool (sub-module of PEM);
- PEM, in case of modeling a property value, returns a performance confidence rate. The confidence rate characterizes the confidence on the performance calculation. The confidence rate takes into account the modeled parameters and their modeling confidence returned by Behavioral Modeling sub Tool.

The performance value is used either to check the appropriateness of the response of the object with the user specifications or to rank different products to make a choice. The performance value is displayed on a scale, normally [0, 10]). PEM positions the performance on this scale taking into account the acceptability interval defined by user. The acceptability interval is defined by a lower value and an upper value meaning the product is acceptable according to the user specification.

In order to facilitate the user interpretation PEM proposes two types of graphs of figure 2.

PEM proposes also a detailed display of the global performance by spider diagram or bar diagram. The global performance is decomposed on functionality performance or sub-functionality performance or even in property performance at the user demand, as better explained below.

CONCLUSIONS

The Collaborative Platform developed in *EnviroTex Design* project will offer to SMEs:

- reduction of design, prototyping and production time and costs;
- better interaction among customers and producers;
- anticipation of issues that are normally considered after the design phase;
- a collaborative 3D virtual environment enabling multidisciplinary teams cooperating in the product design to collect at early stage emerging demands and constraints;
- decision making tools and guidelines supporting toxicological and environmental constraints all along the design process;
- a performance evaluation application enabling the selection of the best functionality according to the expected performance;
- a production enabling an automatic generation of technical data sheets integrating performance parameters.

Authors:

Senior researcher dr.
JEAN MARIE BACHMANN
Institut Français Textile Habillement (IFTH)
270 Rue Faubourg Croncels
10000 Troyes, France
e-mail: jmbachmann@ifth.org

Senior researcher dr.
MARCO BARBIERI
Tecnotessile, Via del Gelso
1359100 Prato, Italy
e-mail: marco.barbieri@tecnotex.it

Senior researcher dr. eng.
IULIANA DUMITRESCU
The National Research & Development
Institute for Textiles and Leather
16 Lucrețiu Pătrășcanu Street
030508 Bucharest
e-mail: certex@ns.certex.ro

INOVAŢIE ŞI DESIGN ÎN CONDIŢII DE CRIZĂ

Datorită conjuncturii economice actuale, producătorii sunt forţaţi să găsească noi soluţii de ieşire din criză, astfel încât această perioadă să fie una de tranziţie, să reprezinte doar o etapă parcursă şi nu un moment de încheiere a activităţii. Nici producătorii din industria textilă nu sunt ocoliţi de dificultăţi, în această perioadă, astfel încât se impune o abordare strategică a întregii activităţi bazată pe inovaţie şi design, care să permită menţinerea în activitate a acestora şi chiar penetrarea unor noi pieţe de desfacere.

Articolele textilele sunt pentru om cea de-a doua piele şi vorbesc despre: cine suntem, vârsta, sexul, clasa socială, cultura căreia îi aparţinem, ori aparteneţa la un grup. Articolele textile ne însoţesc, practic, peste tot, acasă, la locul de muncă şi în vacanţă, având o multitudine de aplicaţii şi, din acest punct de vedere, se poate afirma că, pentru textile, nu există înlocuitori în zona articolelor de îmbrăcăminte sau în cea a decoraţiunilor de interior. Datorită noilor descoperi în domeniul materialelor textile, este uşor de anticipat extinderea utilizării acestora în mult mai multe domenii decât în prezent.

Având în vedere proprietăţile multifuncţionale ale textilelor inteligente, se preconizează că acestea vor avea o aplicabilitate crescută în viitor, semnificativ mai mare decât aplicaţiile tradiţionale existente în prezent.

Deşi concurenţa globală aduce pe piaţă produse obţinute în ţări cu mână de lucru ieftină, domeniul textil din Uniunea Europeană deţine o pondere însemnată în cadrul acestei industrii, însumând o forţă de muncă de 2,3 milioane de persoane, cu vânzări de peste 210 milioane de euro. La nivel mondial, industria europeană de textile deţine prima poziţie în exporturi şi a treia în exportul de îmbrăcăminte, datorită rolului de lider în inovare, design şi creativitate.

Posibilităţii de creşterea a performanţelor firmelor prin inovare, creativitate şi design

Cei trei termeni – *inovare, creativitate şi design* – sunt o posibilă reţetă de ieşire din criză, deoarece, gestionaţi corespunzător, ei pot reprezenta activele cele mai valoroase ale firmelor. Inovarea constituie baza proprietăţii intelectuale şi necesită o protecţie corespunzătoare împotriva contrafacerilor, astfel încât articolele proprii să aducă rezultatele economice estimate de producător.

În condiţiile actualei crize economice, misiunea strategică a unei organizaţii este găsirea unei căi care să-i permită câştigarea unui avantaj net asupra concurenţilor, cu cheltuieli cât mai reduse. În astfel de condiţii, mai importantă decât performanţa în sine este performanţa în raport cu concurenţii.

Conform literaturii de specialitate, firmele textile pot opta pentru una din următoarele căi de întărire a poziţiei concurenţiale[1]:

- ***Concentrarea asupra unor factori-cheie*** de reuşită, prin creşterea propriilor atuuri concurenţiale, şi anume prin modificarea repartiţiei resurselor proprii, în scopul creşterii cotei de piaţă, ceea ce poate să constituie un factor-cheie, care să-i ofere organizaţiei respective un avantaj competitiv. Dacă resursele sunt repartizate în aceleaşi proporţii cu cele ale concurenţilor, poziţia organizaţiei faţă de aceştia va fi modificată.
- ***Focalizarea pe anumite segmente,*** în care organizaţia şi-a dovedit superioritatea sa relativă faţă de concurenţi şi cunoaşterea slăbiciunilor acestora. Organizaţia poate obţine astfel profit, pe următoarele căi:
  - prin valorificarea superiorităţii dobândite în domenii în care nu se confruntă direct cu principalii săi concurenţi, de exemplu pe baza avansului tehnologic al anumitor produse sau a eficacităţii unei anumite reţele de vânzare;
  - pe baza unei diferenţe evidente între organizaţie şi principalii săi concurenţi, în ceea ce priveşte aspectele financiare sau structura activelor.
- ***Modificarea ordinii stabilite***, în sectoare aflate în stagnare sau cu creştere lentă, prin adoptarea unei strategii bazate pe iniţiative ofensive, care să răstoarne factorii-cheie pe care se bazează avantajul relativ al concurentului. O astfel de strategie necesită un studiu atent şi precis al pieţei.
- ***Dezvoltarea de produse noi, prin inovaţie şi design,*** ce aduc mai multe avantaje clienţilor, în special în sectoarele puternic concurenţiale.

Inovarea, conform Comunicării Comisiei Europene[2], constă în:

- înnoirea şi lărgirea gamei de produse, servicii şi pieţe asociate;
- stabilirea de noi metode de producţie, aprovizionare şi distribuţie;
- introducerea unor schimbări în management, marketing, organizarea muncii, condiţiile de muncă şi instruirea personalului.

Prin urmare, se impun a fi analizate următoarele tipuri de inovări:

- ***Inovarea de produs*** se referă la produse sau servicii noi sau semnificativ îmbunătăţite, care diferă de produsele precedente, realizate de organizaţie. Acestea includ schimbări semnificative în specificaţiile tehnice în componente şi materiale soft încorporate, utilizare *„prietenoasă"* (facilităţi în procesul de utilizare) şi alte caracteristici funcţionale. Spre deosebire de inovarea de proces, ele se vând direct clienţilor.
- ***Inovarea de proces*** aparţine atât sectoarelor industriale, cât şi sectorului serviciilor şi presupune metode noi sau îmbunătăţite, sisteme noi de transport şi distribuţie. Acestea includ schimbări semnificative în tehnologiile specifice, echipament şi/sau soft, efectuate în scopul îmbunătăţirii calităţii, eficienţei şi

[1] Kenichi Ohmae, Mc Kindez. *Le genie du stratege*, Ed. Dunod, Paris 1991

[2] Planul naţional pentru Cercetare-Dezvoltare şi Inovare. Programul 5/2007/2013

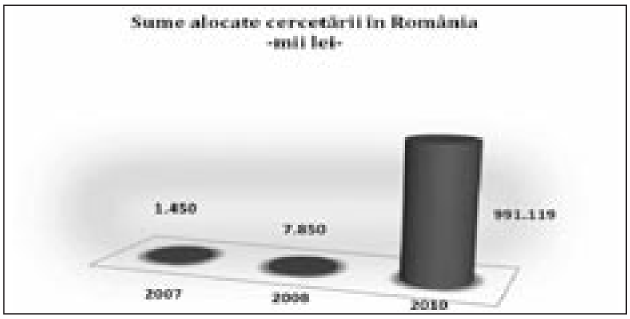

Fig. 1. Cuantumul sumelor alocate cercetării în România, în ultimii 3 ani

flexibilității unei activități productive sau a unei activități de aprovizionare și al reducerii riscurilor privind siguranța și protecția mediului ambiant.

- ***Inovarea în plan organizatoric*** implică, de obicei, schimbări importante în lanțul de furnizori ai firmei, fiind puțin dependentă de tehnologie; se exclud inovările de ordin pur organizațional.
- ***Inovarea de marketing*** se referă la schimbări semnificative pentru cunoașterea modului în care piețele de desfacere ale organizației acceptă schimbări în designul și ambalarea produselor.

Locul inovării în economie

Inovarea, indiferent de tipul acesteia, trebuie să fie nouă pentru organizație, dar nu este necesar să fie nouă pentru sectorul de activitate din care face parte organizația sau pentru piață.

Ținând seama de faptul că inovarea, mai ales cea de produs și cea de proces, depinde de capacitatea financiară a organizației și are un înalt nivel de risc, numărul organizațiilor inovatoare de produs este foarte redus. Chiar și în perioada premergătoare crizei actuale (2004–2006), față de numărul total de întreprinderi, exista un mare decalaj între procentul organizațiilor inovatoare de produs (1,9%) și cel al celor noninovatoare, cu inovări nefinalizate și abandonate (78,9), conform datelor Institutului Național de Statistică[3].

Pentru a evalua performanțele de inovare realizate de statele europene, la inițiativa Comisiei Europene a fost dezvoltat instrumentul numit *Tablou de bord european al inovării* („European Innovation Scoreboard" – EIS), care permite analiza comparativă a performanțelor activităților de inovare ale Statelor Membre ale U.E., precum și ale altor națiuni inovative[4].

Damanpour definește inovația ca „adoptarea unui dispozitiv, sistem, program, proces, produs, serviciu sau a unei politici, ca element de noutate pentru organizația care le însușește". Compania de consiliere generală în management din S.U.A., *Boston Consulting Group (BCG),* apreciază că „inovația este procesul de realizare a unor îmbunătățiri, prin introducerea a ceva nou. Acesta poate fi un nou produs inventat, o nouă lege emisă de guvern sau, pur și simplu, o nouă idee care încurajează gândirea nouă".

Pentru a evalua nivelul cercetării din România, iată câteva cifre relevante (Camera Deputaților)[5]:

- în 2008, pentru proiectele în derulare din 2007 s-au alocat 1 450,446 mii de lei, fiind finanțate un număr de 13 proiecte din perioada 2007–2009;
- în 2009, pentru proiectele în derulare din 2008, s-au alocat 7 849,554 mii de lei, fiind finanțate 42 de proiecte;
- suma alocată pentru 2010, de 991 119 mii de lei, dintre care 200 000 de lei pentru creșterea competitivității în industrie (fig. 1).

Inovația este considerată, în general, ca fiind motorul principal al creșterii economice în economia globală de astăzi. Prin introducerea în practică a inovațiilor se pot obține produse cu caracteristici îmbunătățite de calitate, servicii de calitate superioară, procese de producție noi, mai eficiente și mai curate (ecologice), modele îmbunătățite ale sistemului de management al afacerilor, metode moderne de management al forței de muncă etc. Există multiple motivații ale întreprinderilor și organizațiilor pentru a inova, printre care: creșterea cotei de piață, cucerirea de noi piețe, ameliorarea calității produselor, lărgirea gamei de produse, înlocuirea produselor învechite, reducerea impactului asupra mediului etc. Inovația este indisolubil legată de creativitate (categorie din care face parte acest articol). Inovarea și creativitatea sunt procese care se intercondiționează, deoarece găsirea soluției la problemele ce apar într-un proces de inovare necesită creativitate. Inovația vizează o aplicare comercializabilă în practică a unei invenții. Totuși, inovația este posibilă și fără o prealabilă invenție[6].

În contextul economic actual, problema priorității între dezvoltarea de produse noi sau de noi tehnologii se pune în mod diferențiat, în raport cu ramura de activitate în care se încadrează întreprinderea, cu perspectivele ei și cu potențialul creativ de care dispune.

Ediția online a prestigioasei reviste *Nature* face o analiză a procentului din PIB pe care diferite țări și U.E. le dedică cercetării și inovării. Media acestuia în U.E. este, în continuare, în urma Statelor Unite și a Japoniei, iar România este la jumătate din media U.E. Cifrele sunt prezentate în studiile *„2008 Innovation Scoreboard"* și *„2008 Science, Technology and Competitiveness"* și sunt citate de Comisia Europeană. Aceste studii arată că media U.E. la investițiile în cercetare și inovație[7] (Research and Development, R & D) este de aproape 1,8%. Mai mult, aceasta nu a mai crescut din anul 2000. U.E. este în continuare cu mult în urma S.U.A. și a Japoniei în ceea ce privește procentul din PIB dedicat cercetării științifice: 1,8% din PIB pentru cercetare, deși la un summit din anul 2002, de la Barcelona, U.E. își propunea să ajungă la 3% până în 2010. Iată câteva cifre elovente în acest sens: România – de la 0,2%, în 2000, la 0,8%, în 2008; pentru alte țări însă, tot raportul U.E. anunță o creștere, după cum urmează: pentru China – de la 0,90%, în 2000, la 1,42%, în 2008; S.U.A. – de la 2,74%, în 2000, la 2,61%, în 2008; Japonia – de la 3,04%, în 2000, la 3,39%, în 2008[8] (fig. 2).

---

[3] *http://www.insse.ro/cms/files/pdf/ro/cap13.pdf*

[4] Damanpour, F. & Wischnevsky, J. D. *Research on organizational innovation: Distinguishing innovation-generating from innovation-adopting organizations*. Journal of Engineering and Technology Management, vol. 23, 2006

[5] *http://m.cdep.ro/interpel/2010/r2579A.pdf*

[6] OSLO *Manual Guidelines for collecting and interpreting innovation data*, 3rd, ed. OECD/European Communities, 2005

[7] European Commission: *European Innovation Scoreboard. Comparative analysis of innovation performance*, ianuarie 2009

[8] Revista Nature, *http://www.nature.com/news/2009/090128/full/457523d.html*

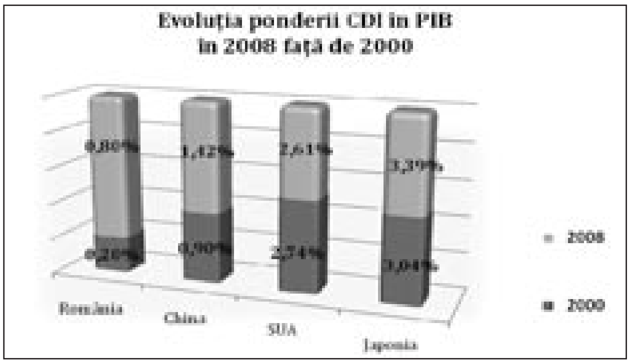

Fig. 2. Evoluția ponderii sumelor alocate CDI în PIB, în 2000 și 2008

Inovarea de produs și de proces au la bază rezultatele activității de cercetare-dezvoltare-inovare (CDI), obținute în entitățile de cercetare cu acest profil: institute de cercetare-dezvoltare sau departamente din universități[9].

Pentru reducerea decalajelor tehnologice și de competitivitate foarte mari, față de țările membre ale U.E., manifestate în țara noastră, în principal, prin nivelul scăzut al inovării în întreprinderi, prin capacitatea redusă de absorbție a rezultatelor din cercetare de către agenții economici, prin slaba dezvoltare a activității de cercetare-dezvoltare de către agenții economici, precum și prin nivelul redus al cercetării-dezvoltării proprii, de la nivelul firmelor, au fost inițiate programe pentru accesul întreprinderilor la activitatea de cercetare-dezvoltare-inovare, finanțate din fonduri structurale europene, în special pentru IMM-uri.

Astfel de programe au ca obiective specifice: sprijinirea intrării pe piață a noilor afaceri cu caracter inovativ (bazate pe rezultatele activității de cercetare-dezvoltare, obținute în institute de cercetare-dezvoltare și în universități), cu scopul de a asigura transferul de cunoștințe și de tehnologie și de a acorda asistență respectivelor întreprinderi, în domeniul începerii de noi afaceri, dar și generarea de rezultate de interes economic, prin transpunerea cercetărilor în produse, tehnologii și servicii îmbunătățite, cu cerere mare pe piață, și dezvoltarea capacității de inovare a întreprinderii, prin îmbunătățirea infrastructurii de cercetare-dezvoltare, pentru creșterea calității activității proprii de cercetare-dezvoltare.

Dezvoltarea tehnologică a firmelor este considerată ca fiind principalul factor pentru creșterea competitivității acestora, de aceea inițiativa unui agent economic care dorește un parteneriat cu o entitate de cercetare, pentru valorificarea rezultatelor proprii sau valorificarea unor brevete, prin aplicarea în producție a tehnologiilor/produselor la care se referă, constituie căi de inovare cu potențial competitiv. Decizia conducerii firmei de a nu urma o cale de inovare duce la eliminarea firmei din competiție, iar pe de altă parte luând decizia de a „inova" poate să apară riscul unor cheltuieli substanțiale, fără posibilitatea de a fi recuperate în întregime.

Rezultă că inovarea este un proces complex, care necesită o analiză aprofundată a tipurilor de strategii inovatoare, a modului de abordare a dezvoltării de produse noi sau modernizate, a caracteristicilor produselor și a modului de utilizare a acestora, a tipului și specificului pieței căreia îi este destinat produsul și a poziției față de concurenți.

Strategii concurențiale

Tipurile de strategii concurențiale pentru care pot opta companiile sunt clasificate, în literatura de specialitate, pe baza unor criterii diferite. După C. Freeman, această clasificare este următoarea[10]:

- ***strategia ofensivă***, care urmărește obținerea supremației tehnologice și de piață, prin introducerea permanentă a unor noi produse;
- ***strategia defensivă***, care constă în lansarea pe piață a produselor noi imediat după inovatorul ofensiv, profitând de greșelile acestuia și de deschiderea unor noi piețe;
- ***strategia dependentă***, dezvoltată de firme-satelit, de către subcontractori;
- ***strategia tradițională***, care constă în crearea de produse cu modificări nesemnificative din punct de vedere tehnic, dar bazându-se pe adaptări cu specific local;
- ***strategia oportunistă,*** care nu se bazează nici pe rezultatele cercetării-dezvoltării de produs, nici pe un design complex, ci pe găsirea unei nișe de piață.

Existența mai multor strategii alternative oferă posibilitatea managerului să urmeze o combinație a acestora, favorabilă organizației pe care o conduce, și să ia decizii corecte de alocare a resurselor.

Adaptarea unui anumit tip de strategie de către firmă se face pe baza unei analize privind oportunitățile firmei și factorii favorizanți de care dispune: existența unei activități proprii de cercetare-dezvoltare de produs, posibilitatea aplicării unei proiectări creative bazate pe un design complex, de gradul de dezvoltare tehnologică și de capacitățile de producție, de poziția pe piață pe care o deține firma, de natura și specificul pieței, de ciclul de viață a produselor oferite de firmă etc.

În condițiile crizei actuale, se consideră ca fiind cele mai oportune strategiile concurențiale[11]. Pentru a-și devansa concurenții, o anumită întreprindere va trebui să cerceteze și să segmenteze piața, pentru a identifica aspectele și mijloacele de satisfacere a nevoilor respective; o segmentare pe categorii de clienți permite o diferențiere clară a ofertei.

Segmentarea pieței în funcție de preferințele/obiectivele clienților trebuie să dezvăluie, în cele mai mici detalii, nevoile clienților. De exemplu, raportul calitate/preț poate fi esențial pentru unii clienți, în timp ce prețul poate fi elementul determinant în luarea deciziei de cumpărare pentru alți clienți. Dar creșterile prețurilor fac, în general să scadă cererea, mărimea segmentului de piață, în acest caz, trebuie stabilită în funcție de politica de prețuri a întreprinderii. Calitatea produsului va fi percepută în mod diferit, după criterii subiective (prestigiu, satisfacția în utilizare, confort etc.) sau după criterii obiective (performanțe privind fiabilitatea și celelalte caracteristici tehnico-funcționale), dar și după apropierea de punctele de vânzare, existența pieselor de schimb, condițiile de plată etc.

---

[9] Pamfilie R., Procopie R., Bobe M., Cârceag M. *Inovația-viziune globală asupra produsului în mediul socio-economic.* Industria Textilă nr. 2/2009

[10] Freeman C. *The economics of Industrial Innovation. The third edition*, London and Washington, 1997

[11] Părăian E., Pascu E. *Designul și estetica mărfurilor*, Ed. Universitară, București, 2010

Rolul designului în perioade de criză

Un rol deosebit în satisfacerea cerințelor și preferințelor clienților diferitelor segmente de piață îl are proiectarea creativă, respectiv designul, instrument puternic de diferențiere a produselor în conformitate cu cerințele pieței.
Designul este considerat drept o parte esențială a procesului de inovare, el realizând o combinare creativă între elementele tehnico-științifice și cele artistico-estetice, implicând vizualizarea creativă a conceptelor, ideilor și a planurilor, contribuind astfel la concepția inițială a produselor/proceselor, proiectarea, introducerea în fabricație și activitatea de marketing a noului produs.
Designul industrial este o activitate creativă care determină caracteristicile de ordin formal ale produselor – caracteristicile estetice, în strânsă corelație cu cele funcționale, ergonomice și economice. Designul produselor poate fi, în prezent, o armă concurențială foarte puternică, contribuind la succesul pe piață al produselor și la satisfacerea cerințelor consumatorilor.
În condițiile crizei actuale, când adevăratele inovații sunt din ce în ce mai rare, supraviețuirea pe piață a unei firme, raportată la mediul concurențial, poate fi asigurată prin creativitatea designerilor în etapa de proiectare a produselor. Creativitatea specifică designerului constă tocmai în găsirea unor soluții de proiectare inovatoare sau de remodelare, pe baza cărora să se realizeze produse noi sau îmbunătățite, deoarece oricât de bine ar fi realizat un produs el trebuie cerut pe piață. Multe propuneri pot fi respinse, nu din cauza unor lipsuri intrinseci, ci a faptului că dezvoltarea lor ar duce la o deplasare a activității companiei într-o direcție nesigură, nedorită. Prin contrast, definirea riguroasă a piețelor și produselor de viitor stimulează o examinare sistematică a necesităților exprimate și potențiale ale consumatorilor, care pot fi satisfăcute prin produse noi sau îmbunătățite.
Procesul creativ de inovare poate avea efecte economice pozitive, dacă asigură înnoiri compatibile cu obiectivele companiei, în condiții de flexibilitate, care să permită modificări de strategie în situații excepționale.

CONCLUZII

Cercetarea pieței, stabilirea tipului de piață, orientarea spre client și diferențierea față de produsele concurenței sunt obiectivele primelor etape în activitatea de proiectare creativă.
Evaluarea posibilităților de realizare a capacității de producție, a materialelor utilizate și a procedeelor tehnologice aplicabile fac posibilă manifestarea creativității designerului. Datorită flexibilității și operativității sale, a capacității de a se plia nevoilor unor segmente largi de consumatori și chiar de a le anticipa, orice producător are nevoie imperativă de design, pentru a putea evolua și a fi competitiv pe piața internă și externă. Sunt numeroase exemple de companii al căror succes de piață se datorează designului produselor realizate de către acestea. Acest lucru trebuie înțeles de către organizațiile producătoare din țara noastră, în condițiile adoptării unui design complex, bazat pe o abordare multidisciplinară, folosind experiența lucrului în echipe multifuncționale, formate din specialiști în marketing, inginerie și design, aflați în relații funcționale bine consolidate, astfel încât produsele proiectate să fie definite prin specificații clare până în cele mai mici detalii. Acestea vor avea o rată a succesului mult mai mare față de produsele pentru care proiectarea nu a definit clar specificațiile de realizare a lor.

Lector universitar drd. ***Emilia Pascu***
Academia de Studii Economice – București

CRONICĂ

FILTECH 2011

Congresul internațional *FILTECH 2011* a avut loc în perioada 22–24 martie 2011, în orașul Wiesbaden, și a reunit pe toți cei implicați în sectoarele Filtrării și Separării sau în sectoare conexe acestora – cumpărători, comercianți, utilizatori, designeri, experți CD și, nu în ultimul rând, reprezentanți ai lumii academice.
Istoria dezvoltării FILTECH a continuat, devenind un eveniment european de un larg interes, dedicat în întregime tehnologiei filtrării și separării, și extinzându-și spațiul expozițional de la trei la cinci pavilioane, pentru a întâmpina expozanți și vizitatori din întreaga lume.
FILTECH 2011 a reunit peste 200 de companii inovatoare și lideri de piață ai industriei mondiale din domeniul separării și filtrării. Cu un procent de peste 50% vizitatori străini, FILTECH va purta o dată în plus distincția amplorii internaționale, fiind o platformă unică ce oferă posibilitatea de a afla noile tendințe în domeniu, de a culege informații și a genera afaceri, și, în același timp, o mare oportunitate de descoperire a noi piețe.
Pe parcusul celor trei zile ale congresului, au avut loc 180 de prezentări, care au oferit o reprezentativă trecere în revistă a celor mai noi descoperiri ale cercetării, a dezvoltărilor globale și a noilor abordări privind rezolvarea problemelor, din perspectiva metodelor de separare mecanică clasică a particulelor din lichide, a metodelor de filtrare cu membrane, a curățării în mediul gazos, a biotehnologiilor.
În plus față de descoperirile curente privind fundamentele definirii și simulării proceselor de separare, au fost prezentate noi metode și soluții instrumentale, ce includ descrierea testării filtrelor, măsurarea particulelor, metodele de caracterizare a membranelor și a altor componente periferice ce și-au dovedit utilitatea practică.

Comunicat de presă. FILTECH 2011,
Wiesbaden/Germania

O NOUĂ TEHNOLOGIE ÎN DOMENIUL TRICOTAJELOR

Australian Wool Innovation (AWI) a elaborat o nouă tehnologie în domeniul tricotajelor. „*Merino Retract*“ s-a bucurat de o primire foarte pozitivă pe piața articolelor tricotate.

Articolele de îmbrăcăminte confecționate din fire Merino Retrage au un aspect plăcut și un tușeu moale, de lână fiartă, fără a poseda, însă, niciuna dintre dezavantajele articolelor de îmbrăcăminte obișnuite, realizate din lână fiartă.

Produsele pot fi spălate în mașina de spălat și posedă excelente proprietăți de întindere, astfel încât să nu se șifoneze la ambalare.

Jimmy Jackson, managerul general pentru dezvoltarea și comercializarea produselor AWI, a subliniat că tehnologia Merino Retract s-a bucurat de un foarte mare interes, deoarece *„consumatorii de astăzi sunt în căutarea unor articole de îmbrăcăminte versatile, care să poată fi purtate în diferite situații și medii și care, în cele din urmă, scutesc consumatorii de timp pierdut, efort și bani“.*

Din acest motiv, noua tehnologie a fost implementată în colecția de toamnă/iarnă 2011/2012 a Merino Casual AWI.

Tehnologia Merino Retract și colecțiile Merino Casual AWI se adresează tendințelor globale spre un stil de îmbrăcăminte mai informal, casual.

Sursa: www.wool.com

NOI TIPURI DE FIBRĂ DIN VISCOZĂ

Compania ***Kelheim Fibres***, pe parcursul anului trecut, a lansat o largă gamă de fibre din viscoză, inclusiv tipurile de fibre superabsorbante *Dante, Bellini, Verdi* și *Bramante*, fibra *Poseidon*, cu proprietăți de schimbare de ioni, precum și *DeepDye* – o fibră cu capacitate sporită de absorbție a colorantului.

Aplicațiile posibile ale acestor noi fibre din viscoză sunt diverse și includ hârtia pentru hărți (Bellini), pansamentele (Verdi), filtrele pentru dedurizarea apei (Poseidon) și cartușele filtrante pentru purificarea apei reziduale din vopsitorii (DeepDye).

În colaborare cu ***Institute for Paper, Pulp and Fibre Tehnology,*** compania ***Kelheim*** a desfășurat cercetări extinse, la TU Graz, pentru a demonstra avantajele încorporării fibrelor de viscoză în hârtiile speciale. Acestea pot ajuta la controlul densității hârtiei, la îmbunătățirea porozității sau la modificarea proprietăților de îndoire a foii de hârtie. Fibrele de viscoză sporesc, de asemenea, rezistența la rupere a hârtiilor speciale.

Hârtiile în care sunt încorporate fibre de viscoză prezintă, în general, proprietăți mai bune de deshidratare și, în funcție de aditivii încorporați în fibre, au și proprietăți îmbunătățite de reținere a apei.

În anul 2010, compania ***Kelheim*** a inaugurat un nou centru tehnic in-house, cu stații pilot pentru testări oferite clienților.

Smart*textiles and nanotechnology, februarie 2011, p. 9*

Referenții articolelor publicate în acest număr al revistei INDUSTRIA TEXTILĂ/
Scientific reviewers for the papers published in this number:

Cerc. șt. gr. I prof. dr. ing./*Senior researcher prof. dr. eng.* EFTALEA CĂRPUȘ
Cerc. șt. gr. II dr. ing./*Senior researcher dr. eng.* IULIANA DUMITRESCU
Cerc. șt. dr. ing./*Senior researcher dr. eng.* SABINA OLARU
Cerc. șt. gr. III ing./*Senior researcher eng.* LILIOARA SURDU
Cerc. șt. gr. III dr. ing./*Senior researcher dr. eng.* ANGELA DOROGAN
Cerc. șt. gr. III dr. ing./*Senior researcher dr. eng.* ALINA POPESCU
Cercet. șt. drd. mat./*Senior researcher mat.* MIHAI STAN
Cerc. șt. drd. ing./*Senior researcher drd. eng.* ANA MARIA MOCIOIU
Cerc. șt. drd. ing./*Senior researcher eng.* ADRIAN SĂLIȘTEAN
Cerc. șt. drd. ing./*Senior researcher eng.* RĂZVAN SCARLAT
Ing./ *Eng.* RADU RĂDULESCU

Institutul Național de Cercetare-Dezvoltare pentru Textile și Pielărie
Str. Lucrețiu Pătrășcanu nr. 16, 030508 București/
The National Research & Development Institute for Textiles and Leather
16 Lucrețiu Pătrășcanu Street, 030508 Bucharest
e-mail: certex@ns.certex.ro

Revista „INDUSTRIA TEXTILĂ“, Editura CERTEX – Institutul Național de Cercetare-Dezvoltare pentru Textile și Pielărie – București

Redacția, administrația și casieria: București, str. Lucrețiu Pătrășcanu nr. 16, sector 3, Tel.: 021-340.42.00, 021-340.02.50/226, e-mail: certex@ns.certex.ro; Fax: +4021-340.55.15. Pentru abonamente, contactați redacția revistei. Instituțiile pot achita abonamentele în contul nostru de virament: RO25RNCB0074029214420001 B.C.R. sector 3, București.

Lucrare executată la **S. P. «BUCUREȘTII NOI»**, str. Hrisovului nr. 18A, sector 1, București, tel.: 667.64.28; 667.55.70; fax: 668.59.51